DISSERTATIONES SCHOLAE DOCTORALIS AD SANITATEM INVESTIGANDAM
UNIVERSITATIS HELSINKIENSIS

78/2018

MIKKO JALANKO

Alterations in Myocardial Function and Electrocardiology in Hypertrophic Cardiomyopathy

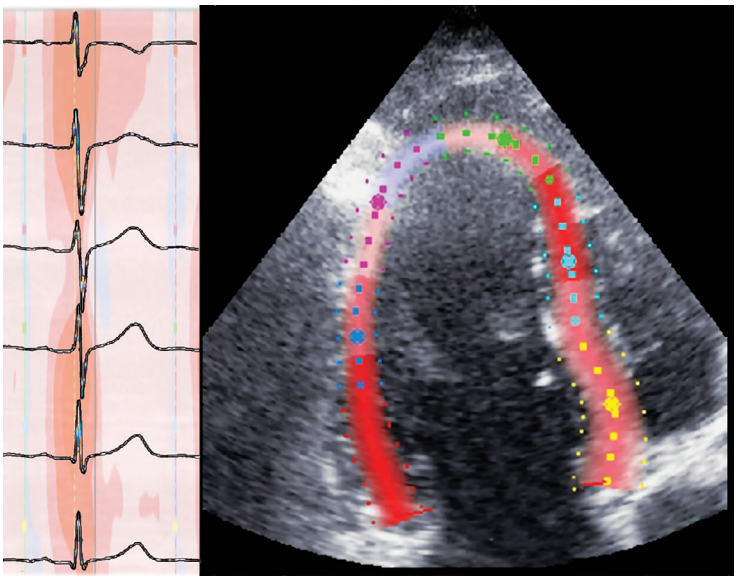

DIVISION OF CARDIOLOGY
HEART AND LUNG CENTER
HELSINKI UNIVERSITY HOSPITAL
FACULTY OF MEDICINE
DOCTORAL PROGRAMME IN CLINICAL RESEARCH
UNIVERSITY OF HELSINKI

Division of Cardiology, Heart and Lung Center
Helsinki University Hospital
and
Faculty of Medicine, University of Helsinki
Helsinki, Finland

ALTERATIONS IN MYOCARDIAL FUNCTION AND ELECTROCARDIOLOGY IN HYPERTROPHIC CARDIOMYOPATHY

Mikko Jalanko

ACADEMIC DISSERTATION

To be presented, with the permission of the Medical Faculty of the University of Helsinki, in a public examination in the Lecture Hall of the Comprehensive Cancer Center on 14.12.2018.

Helsinki 2018

Supervisors

Docent Mika Laine
Department of Cardiology
Heart and Lung Center, Helsinki University Hospital
and University of Helsinki
Helsinki, Finland

Docent Tiina Heliö
Department of Cardiology
Heart and Lung Center, Helsinki University Hospital
and University of Helsinki
Helsinki, Finland

Professor Johanna Kuusisto
Department of Medicine
Kuopio University Hospital
Kuopio, Finland

Reviewers

Docent Riikka Lautamäki
Heart Centre, Turku University Hospital
and the University of Turku
Turku, Finland

Associate Professor Antti Saraste
Heart Centre, Turku University Hospital
and the University of Turku
Turku, Finland

Opponent

Docent Paavo Uusimaa
Medical Director
Mehiläinen Länsi-Pohja Ltd.
Kemi, Finland
and University of Oulu
Oulu, Finland

ISBN 978-951-51-4683-0 (pbk.)
ISBN 978-951-51-4684-7 (PDF)
ISSN 2342-3161 (Print)
ISSN 2342-317X (Online)
Hansaprint

To my family

TABLE OF CONTENTS

List of original publications 8
Abbreviations 9
Abstract 10
1 Introduction 12
2 Review of the literature 14
2.1 Definition of hypertrophic cardiomyopathy 14
2.2 Epidemiology 14
2.3 Diagnosis 14
2.4 Genetics 14
2.4.1 Sarcomeric mutations 16
2.4.2 The genetics of HCM in Finland 16
2.4.3 From genotype to phenotype 17
2.5 Pathophysiology 18
2.5.1 Histological findings 18
2.5.2 Repolarization abnormalities 18
2.5.3 Altered Ca^{2+} handling 19
2.6 Ventricular arrhythmias 20
2.7 Metabolic changes in HCM 21
2.8 The 12-lead ECG in HCM 22
2.8.1 Terminal negativity of the P wave 22
2.8.2 Abnormal Q waves 22
2.8.3 Conduction disturbances and bundle branch block 23
2.8.4 The QRS complex 23
2.8.5 Conventional criteria for left ventricular hypertrophy 23
2.8.6 QT interval prolongation 24
2.8.7 ST depression and T wave inversion 25
2.9 24h ambulatory ECG 25
2.9.1 Median and maximal QTe 26
2.9.2 The QT/RR slope 27
2.9.3 T wave apex to T wave end 28
2.9.4 Atrial fibrillation 28
2.10 Echocardiography 28
2.10.1 Conventional echocardiography 28
2.10.2 Deformation of the left ventricle 29
2.10.3 Echocardiographic deformation imaging 30
2.10.4 Global and segmental longitudinal strain 31
2.10.5 Mechanical dispersion 34
2.10.6 Twist 34
2.11 Cardiac magnetic resonance imaging 35

2.11.1 Patterns of hypertrophy ... 35
2.11.2 Imaging fibrosis – late gadolinium enhancement ... 35
2.12 HCM and athlete's heart – differential diagnostics ... 36
2.13 Prognosis ... 36
2.14 Risk assessment of sudden cardiac death ... 37
2.15 Screening, clinical genetics and follow-up ... 38
3 Aims of the Study ... 39
4 Methods and materials ... 40
4.1 Patients ... 40
4.2 Laboratory assays ... 40
4.3 Genetic analysis ... 40
4.4 The 12-lead ECG ... 41
4.5 Ambulatory ECG ... 42
4.6 Echocardiography ... 43
4.6.1 2D strain echocardiography ... 43
4.6.2 Twist ... 43
4.7 Cardiac magnetic resonance imaging ... 44
4.8 Metabolomics ... 44
4.9 Statistical analysis ... 45
4.10 Ethical statement ... 46
5 Results ... 47
5.1 Imaging HCM (Study I) ... 47
5.1.1 Baseline ... 47
5.1.2 Global strain and mechanical dispersion ... 48
5.1.3 Segmental strain ... 48
5.1.4 Twist ... 49
5.1.5 Late gadolinium enhancement ... 51
5.1.6 Association of imaging to arrhythmias ... 52
5.2 ECG in HCM (Study II) ... 53
5.2.1 Overall ECG findings ... 53
5.2.2 ECG pathology correlates to disease severity ... 55
5.2.3 RV1 < RV2 > RV3 and septal remodeling ... 56
5.2.4 ECG criteria for diagnostics and screening ... 56
5.3 Repolarization abnormalities in HCM (Study III) ... 58
5.3.1 Baseline ... 58
5.3.2 Prolonged QTe ... 58
5.3.3 T wave peak to T wave end ... 58
5.3.4 Fibrosis associates to repolarization abnormalities ... 58
5.4 Metabolomic findings in HCM (Study IV) ... 59
6 Discussion ... 63
6.1 Main findings ... 63
6.2 Comparison with previous studies ... 63

6.2.1 Alterations in myocardial mechanics and association to arrhythmias 63
6.2.2 The abnormal ECG in HCM patients 64
6.2.3 Identifying G+/LVH- subjects with the ECG 65
6.2.4 Repolarization abnormalities 65
6.2.5 The metabolomic profile of HCM 66
6.3 Limitations 66
6.3.1 Study design, sample size and data collection 66
6.3.2 Generalizability 67
6.3.3 Methodological limitations 67
6.4 Clinical implications and future developments 68
6.4.1 Screening and diagnostics 68
6.4.2 Improving risk stratification of sudden cardiac death 68
7 Conclusions 70
Acknowledgements 72
References 74

LIST OF ORIGINAL PUBLICATIONS

This thesis is based on the following publications:

I Left ventricular mechanical dispersion is associated with nonsustained ventricular tachycardia in hypertrophic cardiomyopathy.
Jalanko M, Tarkiainen M, Sipola P, Jääskeläinen P, Lauerma K, Laine M, Nieminen MS, Laakso M, Heliö T, Kuusisto J.
Ann Med. 2016 Sep;48(6):417-427.

II Novel electrocardiographic features of mutation carriers for hypertrophic cardiomyopathy.
Jalanko M, Heliö T, Mustonen P, Kokkonen J, Huhtala H, Laine M, Jääskeläinen P, Tarkiainen M, Lauerma K, Sipola P, Laakso M, Kuusisto J, Nikus K.
Accepted for publication 15.7.2018 in J Electrocardiol. Published online 17.7.2018.

III Fibrosis and wall thickness affects ventricular repolarization dynamics in hypertrophic cardiomyopathy
Jalanko M, Väänänen H, Tarkiainen M, Sipola P, Jääskeläinen P, Lauerma K, Laitinen T, Laitinen T, Laine M, Heliö T, Kuusisto J, Viitasalo M.
Ann Noninvasive Electrocardiol. 2018 Nov;23(6):e12582.

IV The metabolome in Finnish carriers of the MYBPC3-Q1061X mutation for hypertrophic cardiomyopathy.
Jørgenrud B*, Jalanko M*, Heliö T, Jääskeläinen P, Laine M, Hilvo M, Nieminen MS, Laakso M, Hyötyläinen T, Orešič M, Kuusisto J.
PLoS One. 2015 Aug 12;10(8):e0134184

* The authors contributed equally to this work.

The publications are referred to in the text by their Roman numerals.

ABBREVIATIONS

2DSE	two-dimensional strain echocardiography
AF	atrial fibrillation
AP	action potential
CMRI	cardiac magnetic resonance imaging
DAD	delayed afterdepolarization
EAD	early afterdepolarization
EF	ejection fraction
FHSD	family history of sudden death
fQRS	fragmented QRS
G+/-	carrier (+) or noncarrier (-) of a pathological gene variant for HCM
GLS	global longitudinal strain
HCM	hypertrophic cardiomyopathy
I_{CaL}	L-type calcium current
I_{K1}	inwardly rectifying potassium current
I_{Kr}	rapid delayed rectifying potassium current
I_{Ks}	slow delayed rectifying potassium current
I_{Na}	sodium current
LGE	late gadolinium enhancement
LV	left ventricle
LVH+/-	left ventricular hypertrophy (+) or no hypertrophy (-)
MD	mechanical dispersion
LVOTO	left ventricular outflow tract obstruction
MWT	maximal wall thickness
NSVT	non-sustained ventricular tachycardia
PTF	P-terminal force
PWT	posterior wall thickness
QTe	time interval from onset of the QRS complex to the end of T wave
RV	right ventricle
SCD	sudden cardiac death
SWT	septal wall thickness
TDI	tissue Doppler imaging
VA	ventricular arrhythmia
VF	ventricular fibrillation
VT	ventricular tachycardia

ABSTRACT

Hypertrophic cardiomyopathy is the most common inherited cardiomyopathy with a highly variable phenotype. Penetrance of pathogenic variants is incomplete and age- and gender-related. The assessment of arrhythmogenic potential in HCM patients and identification of early signs of the disease in relatives of HCM patients is challenging. New tools are required to aid the clinician in diagnostics and the decision-making process of prophylactic implantable cardioverter defibrillator implantation. The aim of this thesis was to characterize the mechanical and electrical changes in the left ventricle of carriers of either the *MYBPC3*-Q1061X or *TPM1*-D175N mutation for hypertrophic cardiomyopathy and to identify novel imaging and electrocardiographic parameters with the potential to enhance sudden cardiac death risk stratification and follow-up.

A total of 140 subjects carrying a pathogenic variant for HCM were recruited for these studies from three centers in Finland, divided into two groups: those with left ventricular hypertrophy (G+/LVH+ n = 98) and those without hypertrophy (G+/LVH- n = 42).

We studied the association of ventricular arrhythmias on 24h ambulatory electrocardiograms to 2D strain echocardiographic global longitudinal strain (GLS) and mechanical dispersion in conjunction with cardiac magnetic resonance imaging (CMRI) with late gadolinium enhancement (LGE) in 31 G+/LVH+ HCM patients. GLS was reduced in HCM patients and correlated well to NT-proBNP and other markers of advanced disease. Mechanical dispersion was significantly increased in HCM patients with episodes of ventricular arrhythmia on ambulatory ECGs and was a better predictor of these episodes than GLS or LGE. Mechanical dispersion may be a useful marker of arrhythmogenic potential in HCM patients.

We evaluated a large array of established ECG parameters and novel electrocardiographic criteria of RV1<RV2>RV3 and septal remodeling in a cohort of 140 HCM mutation carriers with and without hypertrophy. An abnormal ECG was present in 97% of G+/LVH+ and 86% of G+/LVH- subjects. The major ECG criteria were 90% sensitive and 97% specific for differentiating G+/LVH+ HCM patients from control subjects. The combination criteria of RV1<RV2>RV3 + Q waves and septal remodeling identified G+/LVH- subjects with a 64% sensitivity and 97% specificity. The proposed novel ECG criteria may increase the efficacy of using electrocardiography in identification of G+/LVH- subjects.

Repolarization abnormalities are common in HCM and may contribute to the arrhythmic potential. A group of 46 HCM patients was assessed with a 24h ambulatory ECG with comprehensive repolarization analysis and these findings were associated to cardiac magnetic resonance and echocardiographic imaging. Rate dependent QTe interval was prolonged in HCM patients. Maximal wall thickness was associated with longer maximal QTe and median T wave peak to T wave end interval. HCM patients with late gadolinium enhancement on CMRI had a steeper QTe/RR slope compared to HCM patients without LGE and control subjects. In HCM multiple repolarization

abnormalities are present. The presence of LGE may independently affect the repolarization dynamics in HCM. This may contribute to ventricular arrhythmias in HCM patients with LGE.

The metabolome of carriers of the MYBPC3-Q1061X mutation was investigated with comprehensive laboratory assays. Concentrations of branched chain amino acids, triglycerides and ether phospholipids were increased in mutation carriers with hypertrophy as compared to controls and non-hypertrophic mutation carriers, and correlated with echocardiographic LVH and signs of diastolic and systolic dysfunction.

In conclusion, the pathophysiological changes of HCM affect myocardial mechanical and electrical properties in a multitude of ways. Some of these subtle changes can be identified in mutation carriers without hypertrophy and they might be useful in the screening and follow-up of HCM families. The mechanical and electrical alterations are intertwined and the echocardiographic measure of mechanical dispersion might be a marker of arrhythmic potential reflecting the changes in the myocardial structure and function. The presence of fibrosis in the myocardium alters the dynamics of ventricular repolarization. The use of novel electrocardiographic and echocardiographic techniques has increased the understanding of HCM pathophysiology and they could be of use in the clinical evaluation HCM.

1 INTRODUCTION

Hypertrophic cardiomyopathy (HCM) is the most common inherited cardiomyopathy, with a prevalence of approximately 0.2%. The first known description of HCM was by Henri Liouville dating back to 1869 (1). In 1958 Donald Teare published a small autopsy case series of young patients and coined the expression "Asymmetrical hypertrophy of the heart" (2). Since then the disease has become familiar to cardiologists as a genetically transmitted pathology with problems concerning the obstruction of the left ventricular outflow tract, exertional symptoms, ischemia, atrial fibrillation, and sudden death in the young.

After decades of investigation, the underlying pathophysiological process remains elusive and the road from genotype the phenotype is difficult to predict in individual patients. Modern imaging with two-dimensional echocardiographic strain and cardiac magnetic resonance imaging (CMRI) has expanded our knowledge of the disease but gaps remain. Various preclinical changes have been observed with electrocardiology and imaging but the results are varied and inconclusive at this time.

When a new HCM patient is identified it triggers a cascade of diagnostic measures in the family. A pathological gene variant is found in roughly 30-60% of probands aiding the diagnostic process of identifying mutation carriers in the same family. As the penetrance of HCM is age-related and incomplete the repeated use of imaging and electrocardiography in screening and follow-up is required. As an inexpensive method, the conventional 12-lead electrocardiogram is a valuable tool in the early diagnostic armamentarium but its sensitivity and specificity so far have been rather limited. The definition of ECG patterns and echocardiographic imaging parameters to identify early disease before the onset of hypertrophy would be of value in both the assessment of families with an identified pathological variant and those without.

HCM is one of the most common causes of sudden cardiac death in the young and athletes (3). The prediction of arrhythmic events is based on a number of risk factors that have been compiled into a risk calculator by the European Society of Cardiology (4,5). Although widely used, there remain gaps in evidence in the evaluation of sudden cardiac death risk in individual patients. Modern imaging has come forth with the quantification of fibrosis by CMRI late gadolinium enhancement and diagnosing segmental and global dysfunction more accurately with strain imaging. Finding the right parameters to detect susceptibility to arrhythmias is one of the themes in this thesis.

The pathological process in the myocardium of HCM patients results in repolarization abnormalities, that increase the risk for arrhythmias. Ambulatory ECG recording is a commonly used method of risk stratification, but there is relatively scarce data on the changes in repolarization in HCM.

The development of metabolomics to study the pathology of diseases has advanced rapidly. The methodology allows the analysis of a very large number of metabolites, for example amino acids and lipids, from tissue and blood samples. Metabolomic studies in other cardiomyopathies have expanded our knowledge of these conditions

and may aid in the identification of new biomarkers for diagnostics. There is limited data on the metabolomic changes in HCM.

Sixty years after Teare successfully described the cornerstone findings in HCM and outlined the familial pattern of inheritance in this disease we still face a number of diagnostic challenges and uncertainty about the pathophysiological process that results in asymmetrical hypertrophy. This thesis is about finding answers to some of these questions.

2 REVIEW OF THE LITERATURE

2.1 Definition of hypertrophic cardiomyopathy

Hypertrophic cardiomyopathy is defined as abnormal thickening of the ventricular wall, that is not explained by other cardiac pathology or abnormal loading conditions. The hypertrophy is characteristically asymmetric in nature. The definition of HCM encompasses therefore both hypertrophy due to pathological sarcomeric gene variants and other non-sarcomeric etiologies. The scope of this dissertation is limited to HCM attributable to gene mutations in the sarcomere.

2.2 Epidemiology

Hypertrophic cardiomyopathy is the most common inherited cardiomyopathy, with an approximate prevalence of 1/500 in the general population (6). It is the most common cardiomyopathy (61%) encountered in the outpatient clinic, excluding myocardial disease relating to coronary artery disease, hypertension, valvular disease and congenital heart disease (7). A significant number of subjects with HCM are not clinically diagnosed, according to a recent US-based survey (8).

2.3 Diagnosis

The conventional criteria for diagnosing hypertrophic cardiomyopathy is maximal wall thickness (MWT) of at least one segment of the left ventricle (LV) ≥ 15 mm by any imaging modality in the absence of abnormal loading conditions (for example aortic stenosis or hypertension) (4). In familial HCM, with a known proband (the first identified person in a family to fulfill diagnostic criteria for HCM) the diagnosis can be made with an MWT of ≥ 13 mm usually in conjunction with supporting ECG findings, laboratory tests, and possibly further imaging. The criteria published by McKenna et al. may be used to diagnose HCM in families with known probands (Table 1) (9). The diagnosis of HCM in a first degree relative can be made with

- One major criterion
- Two minor echocardiographic criteria
- One minor echocardiographic plus two minor electrocardiographic criteria.

2.4 Genetics

Mutations in the genes encoding the contractile apparatus of the myocyte – the sarcomere – are responsible for approximately 50% of cases of hypertrophic cardiomyopathy (Figure 1) (10-12). Pathological variants in non-sarcomeric genes and hypertrophic cardiomyopathy due to other etiologies constitute the rest of the known spectrum. Among the most important causes of non-sarcomeric HCM are storage diseases such as Pompe, Danon and Anderson-Fabry, mitochondrial diseases such as MELAS, malformation syndromes like Noonan and LEOPARD and amyloidosis (7).

Treatment of HCM due to non-sarcomeric etiology is targeted at the underlying cause and HCM risk stratification models cannot be applied to this patient population.

Major criteria
Echocardiography
Maximal wall thickness
≥ 13 mm anterior septum or posterior wall
≥ 15 mm posterior septum or free wall
Severe SAM
Electrocardiography
LVH and repolarization changes (Romhilt-Estes (13))
T-wave inversion in leads
I+aVL (≥ 3 mm, with QRS-R wave axis difference ≥ 30°)
V3-V6 (≥ 3 mm)
II + III + aVF (≥ 5 mm)
Abnormal Q wave (> 40ms or > 25% of R wave) in at least 2 leads
II, III, aVF(in absence of left anterior hemiblock)
V1-V4
I, aVI, V5-V6
Minor Criteria
Echocardiography
Maximal wall thickness
12 mm in anterior septum or posterior wall
14 mm posterior septum or free wall
Moderate SAM
Redundant MV leaflets
Electrocardiography
Complete BBB or (minor) interventricular conduction defect (in LV leads)
Minor repolarization changes in LV leads
Deep S in V2 (> 25 mm)
Unexplained chest pain, dyspnoea or syncope

Table 1 Criteria for diagnosing familial HCM, adapted from McKenna et al (9). BBB = bundle branch block, LVH = left ventricular hypertrophy, SAM = systolic anterior motion of the mitral valve anterior leaflet.

2.4.1 Sarcomeric mutations

Sarcomeric HCM is most commonly transmitted to offspring through dominant single gene mutations in an autosomal dominant pattern. To date over 1000 gene mutations in at least 13 different genes have been recorded (10). The predominant pathological variants resulting in hypertrophic cardiomyopathy in larger population studies are located in the myosing binding protein C (MYBPC3 40%), beta-myosin heavy chain (MYH7 40%), alpha-tropomyosin (TPM1 5%), and the troponins I (TNNI3 1-5%) and T (TNNT2 5%), summarized in Figure 1 and 2 (10,14). Other possible variants with lower prevalence and unclear significance are found in genes encoding alpha-actinin, alpha-actin, myozenin, myosin regulatory light chain (*MYL2*) and myosin essential light chain (*MYL3*). Patients with pathogenic sarcomeric mutations often in addition carry variants in titin, ion channel, and desmosomal genes, which may act as modifiers of the disease phenotype and progression (15). In approximately 5% of cases there is more than one pathological variant responsible for the disease, with usually a more severe phenotype as a result (15-17).

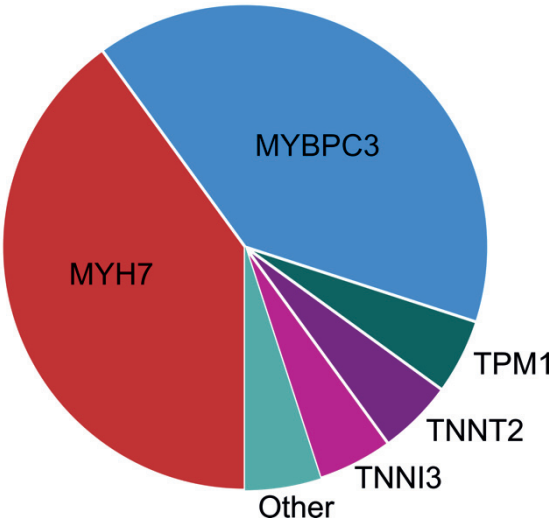

Figure 1 Distribution of gene mutations responsible for sarcomeric HCM according to published reports. MYH7 = beta-myosin heavy chain, MYBPC3 = myosin binding protein C, TPM1 = alpha-tropomyosin, TNNT2 = troponin T, TNNI3 = troponin I.

2.4.2 The genetics of HCM in Finland

The FinHCM-study, a multicenter trial of over 300 patients on the genetic background of HCM in Finland, originally discovered two pathogenic founder mutations in Finland - *MYBPC3*-Q1061X and *TPM*-D175N, that account for the majority of the identified mutations of HCM. The FinHCM study covered a large geographical area of central, eastern and western Finland. The myosin binding protein C mutation *MYBPC3*-Q1061X accounts for approximately 11% and MYBPC3 mutations in general for 16%, the alpha-tropomyosin mutation *TPM1*-D175N for 7% and the beta-myosin heavy chain mutation *MYH7*-R1053Q for 6% of HCM in the FinHCM study (18,19). A large proportion of HCM in Finland seems to be the result of just these three mutations, which is a typical finding relating to the common ancestry of the

Finnish people. This is known as the founder effect and it is also present in many other heritable diseases in Finland.

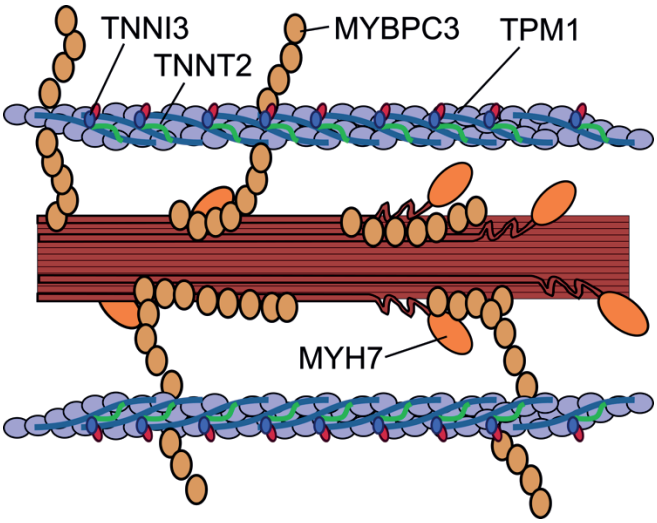

Figure 2 The sarcomere and the most common mutations involved in sarcomeric HCM.

2.4.3 From genotype to phenotype

Current understanding of the genotype to phenotype pathway has at least two possible mechanisms: 1) A missense mutation leads to a dysfunctional protein, a so called "poison peptide", which is incorporated in the sarcomere and results in change of function (20). Many pathogenic mutations in HCM, such as beta-myosin heavy chain variants, are of this type (11). 2) The other pathway leads to a truncated end-product that is not incorporated in the sarcomere. This results in haploinsufficiency: sarcomeres partly lacking the proteins in question. This pathway is typical of *MYBPC3*-mutations (21-23).

The penetrance of sarcomeric HCM mutations in general is relatively high, but there seems to be variation related to the specific mutation type with *MYBPC3* mutations exhibiting lower penetration ratios compared to, for example, MYH7 (10). The penetrance is age- and gender-related and especially *MYBPC3* mutations may manifest in older age (24,25). The phenotype resulting from sarcomeric mutations is also highly variable and is possibly mediated by modifying genetic factors and other variables (15). It has been suggested that some mutations in the beta-myosin heavy chains and the troponins carry a more significant risk for sudden cardiac death (SCD) than others, but these results are somewhat inconsistent (26-28). Thus the road from genotype to phenotype is very complex and for the clinician the variation in phenotype between individuals is more related to other factors than just the underlying pathological variant. In this literature review the expression G+/LVH+ constitutes

carriers of pathological gene variants for HCM with left ventricular hypertrophy (LVH+) and G+/LVH- subjects are pathological variant carriers without LVH.

2.5 Pathophysiology

2.5.1 Histological findings

The histopathological findings in HCM can be summarized as cellular hypertrophy, increased volume of the extracellular matrix, fibrosis, and disarray of the myocyte arrangement (2,29-31). There are abnormal intramural coronary arteries with narrow lumens due to thickening of the intimal and medial layers (32,33). The changes in microvasculature and thickening of the myocardial wall results in an abnormal perfusion demand and is the substrate for ischemia commonly encountered in HCM (34,35). Interstitial collagen expansion has been noted in pathological specimens of young HCM patients who died suddenly (36). The hypertrophy encountered in HCM is significantly different from the conventional concentric response of the LV due to pressure load for example from aortic stenosis or hypertension. The degree of hypertrophy is also usually more significant compared to myocardial changes relating to athlete's heart, which is later discussed in detail. In HCM the hypertrophy is predominantly asymmetrical, with a predilection for the septum and anterior wall (37). In some instances, the hypertrophy in HCM is confined to the apex or the inferolateral wall. The entity of concentric hypertrophy is also a possible finding in HCM patients but quite uncommon (1%). The pathophysiological process leading to asymmetric hypertrophy has been extensively studied but remains unclear.

2.5.2 Repolarization abnormalities

The action potential (AP), its constituent phases (0-4) and ion channels are presented in Figure 3A. The repolarization phase (2-3) is most commonly disturbed in hypertrophic cardiomyopathy, resulting from the interplay of ion channel pathology, calcium homeostasis and cellular level changes such as reduced T-tubule concentration (Figure 3B and Figure 4). The most common finding in single myocyte electrical patch clamp studies has been the prolongation of the AP (38,39). Multiple studies have found that the prolongation of the AP in HCM is accompanied by a higher occurrence of early after depolarizations (EAD), which are generally thought to be a primary trigger of ventricular tachycardia (38,40,41).

The prolongation of the AP results at least from (38,41):

1. increased I_{NaL}, as evidenced by the significant shortening of ADP by ranolazine, a selective blocker of I_{NaL}.
2. increase of L-type Ca2+ current density (I_{CaL})
3. selective downregulation of the inward rectifying current (I_{k1})
4. reduction in outward rectifying current (I_{Kr})

The interplay of many factors affecting the net repolarizing current outweighs the repolarization reserve and results in significantly prolonged APs prone to EADs.

Figure 3 A) The action potential and the relevant ion channels responsible. Phases of the AP: 0 = depolarization, 1 = early repolarization, 2 = slow repolarization, 3 = fast / terminal repolarization, 4 = diastolic membrane potential. B) In HCM, the repolarization is prolonged due to I_{Kr} reduction and increased I_{CaL} and I_{Na} making the phase 3 of AP prone to EADs. Altered Ca^{2+} handling and leaks lead to delayed after depolarizations (DAD).

2.5.3 Altered Ca^{2+} handling

The cellular level pathophysiologic changes relating to arrhythmogenesis in HCM are summarized in Figure 4. There is evidence of increased myofilament Ca^{2+} sensitization, increased intracellular Ca^{2+} concentration, and altered Ca^{2+} handling from multiple studies in animal models and extracted human myocytes (42-46). The delayed Ca^{2+} transient rise and decay in human and mouse models is at least partially due to a decrease in T-tubule density resulting from the disproportionate relation in the ratio of surface to volume growth (38,45). Ca^{2+} transients are also delayed locally in the T-tubule system and there is evidence from mouse models that part of the T-tubule system does not propagate the AP properly (45). This leads to prolonged kinetics of force development and relaxation. The contractile dysfunction does not seem to be dependent on the underlying mutation (44). Ca^{2+} leakage and uncontrolled release by the sarcoplasmic reticulum have been observed, recorded as spontaneous contractions (45). During diastole or stimulation pauses in mouse models, HCM myocytes exhibit abnormal Ca^{2+} sparks (45,47). HCM resulting from troponin T mutations has been associated with a higher incidence of lethal arrhythmias and this has been attributed to the increased Ca^{2+} sensitivity related to the mutation (39,48).

Alterations in Ca^{2+} transients and spontaneous Ca^{2+} sparks can lead to delayed afterdepolarizations (DAD) (38,45). In an iPS model of HCM due to a pathogenic variant in MYH7, patch-clamp studies of myocytes demonstrated DAD-like electrical activity and time-lapse videos recorded contractile arrhythmia in a significant number (12%) of observed cells (43). In an iPS model of the *MYBPC3*-Q1061X and *TMP1*-D175N pathological variants, altered Ca^{2+} transients and both EADs and DADs have been recorded on the cellular level (23).

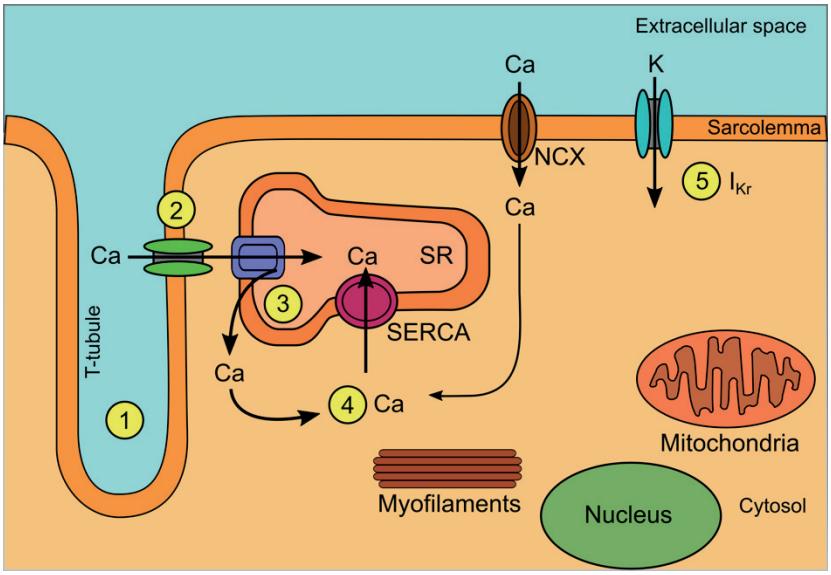

Figure 4 Cellular level pathophysiology of HCM: 1) Reduced T-tubule concentration. 2) Increased Ca^{2+} sensitivity and alteration in Ca^{2+} handling. 3) Abnormal Ca^{2+} release with Ca^{2+}-leak from the sarcoplasmic reticulum (SR) and diastolic sparks of Ca^{2+}. 4) Increase of cytosolic Ca^{2+}. 5) Reduction in I_{Kr} flow. NCX = Na-Ca exchanger, SERCA = Sarcoplasmic / endoplasmic reticulum Ca^{2+}-ATPase

2.6 Ventricular arrhythmias

The arrhythmia leading to SCD in HCM is ventricular tachycardia (VT) or ventricular fibrillation (VF). Malignant ventricular arrhythmias (VA) may be triggered with exercise, as is evident in the proportion of SCD in young athletes resulting from HCM (3,49). Arrhythmias during the resting hours are quite common as well, with approximately 20-27% of appropriate implantable cardioverter defibrillator (ICD) discharges happening during the night time (50,51). The individual assessment of risk for SCD is one of the major challenges in the diagnostics and follow-up of HCM patients.

The triggers giving rise to ventricular arrhythmias during bradycardia have been attributed to the perturbation of the repolarization phase of the action potential and manifestation of EADs (39,40,52). DADs are also present in cellular level studies of HCM and may play a part in the arrhythmias presenting with increased heart rates (38,39).

In addition to a trigger such as and EAD or a DAD, a clinically significant VA usually requires a myocardial substrate to perpetuate the arrhythmia. Ischemia due to microvascular changes and diminished perfusion reserve related to significant hypertrophy contribute to the arrhythmic potential. In hypertrophic cardiomyopathy

the heterogeneous composition of the myocardial wall, disarray of the myocytes, and patchy areas of fibrosis, provide a fertile field for the re-entry mechanism of VA (47,53).

2.7 Metabolic changes in HCM

In the adult heart the energy pool consists of adenosine triphosphate (ATP) and phosphocreatine (PCr). ATP is the primary fuel of contraction and ion pump function and PCr acts as a buffer and transport system for ATP (54). Cardiac work is dependent on efficient ATP generation by oxidative phosphorylation of free fatty acids (FFA) in the mitochondria (up to 90% of cardiac ATP). Approximately 10-30% of cardiac ATP is produced by the oxidation of lactate and glucose – although this increases after meals when levels of plasma glucose rise. In heart failure and hypertrophy FFA oxidation is impaired and ATP production is reduced (54). The failing heart uses more glucose and lactate as energy substrates.

The results of metabolism studies in HCM have not been entirely concordant (55). The underlying unifying concept in hypertrophic cardiomyopathy, regardless of mutation type, is the inefficient energy utilization of the myocyte (42). In a mouse model of HCM, a decrease in the free energy of ATP hydrolysis has been demonstrated with a reduction in contractile performance upon inotropic challenge (56). Impaired energy metabolism has been shown in vivo by a reduction in the PCr/ATP ratio on P-MRS spectroscopy, a marker of cellular energy status, in HCM gene mutation carriers with and without hypertrophy (57). A similar result has been shown in a HCM population with a single point mutation for HCM (Arg403Gln) (58). This study also demonstrated a significant reduction in creatinine kinase flux - a marker of reduced metabolic reserve. Flawed energetics in G+/LVH- subjects have also been documented with positron emission tomography (PET) imaging, demonstrating reduced myocardial external efficiency in the absence of flow abnormalities, indicating energy compromise to be an early finding in the pathophysiologic development of HCM (59). Giving perhexiline to improve myocardial carbohydrate utilization improved exercise capacity and corrected resting cardiac energetics in a pharmacological intervention study on HCM patients, further underlining the importance of impaired energy utilization (60).

Reduced free fatty acid uptake in the myocardium of HCM patients demonstrates the energy imbalance from another perspective and seems to precede changes in glucose metabolism (61). A Finnish study of patients with HCM attributable to the Asp175Asn mutation in the α-tropomyosin gene revealed, using PET imaging, increased myocardial oxidative metabolism and free fatty acid uptake in HCM patients with mild LVH. This decreased with advanced LV hypertrophy (62).

Metabolomics, the large-scale study of circulating metabolites for example from blood or tissue samples, and their association to cardiac and other diseases, has gained momentum in recent years (63). Metabolomics is a systems approach that aims to characterize complex metabolic networks in studied tissues or blood samples. The methodology yields a very large number of small metabolites, such as amino acids,

organic acids and lipids, extracted with high throughput gas and liquid chromatography coupled to mass spectrometry. It is sensitive to a large number of affecting factors, such as age, immune system status, diet and genetic variation (64-67). In cardiac disease the study of metabolomics might potentially identify new biomarkers (63). Current methodology allows for extensive quantification of a large amount of different metabolites (68). The application of metabolomics in the study of cardiomyopathies results in new data and is hypothesis generating (63). The use of metabolite clusters can increase the diagnostic accuracy in identifying patients with heart failure and preserved ejection fraction (69) and staging heart failure patients (70). In a HCM mouse model studying the effects of perhexiline, a metabolomic analysis of cardiac myocytes was performed, with indirect findings of reduced fatty acid oxidation and increased glucose metabolism (71).

2.8 The 12-lead ECG in HCM

A normal ECG in patients with HCM is uncommon. In most reports the ECG is pathological in approximately 95% of HCM patients. Commonly the findings constitute abnormal Q waves, ST segment abnormalities and patterns of left ventricular hypertrophy (72,73). Some reports also point to the possibility of ECG changes in G+/LVH- subjects – a finding of interest in the screening of HCM families (74,75). The sensitivity and specificity of these ECG findings in G+/LVH- subjects have been limited (74). A possible solution to increase diagnostic accuracy could be the use of multiple parameters in combination (76).

2.8.1 Terminal negativity of the P wave

Terminal negativity of the P wave in lead V1 or P-terminal force (PTF), determined usually as the negative portion the the P-wave in V1 being ≥ 0.04 mmsec, has been generally attributed to the dilatation of the left atrium. In a large population based study a PTF of ≥ 0.06 mms was independently associated with increased risk of death and atrial fibrillation (77). This would seem logical as left atrial dilatation can be considered a marker of the burden of many cardiac pathologies. The prevalence and significance of PTF in HCM has not been extensively studied, but has been a relatively common finding in some studies (72,74).

2.8.2 Abnormal Q waves

Abnormal Q waves are usually defined as ≥ 40 ms in duration, or ≥ 25% in depth of the following R wave, or ≥ 3 mm in depth, in at least two contiguous leads - except avR. They can be found in 30-50% of HCM patients (72,73,78-80). Q waves present quite early in the development of HCM in patients. Some reports indicate that they are present even before the development of hypertrophy (74,79,80). Q waves in HCM are narrow but deep and prominent. They occur most often in the inferior and lateral leads.

In HCM the mechanism behind Q waves is not clear. The asymmetrically hypertrophic left ventricle produces abnormal electrical activation with the prominent anterior septum canceling the forces from other areas of the LV and RV (73). In manifest HCM, fibrosis in the septum may result in loss of localized electrical forces, but even with modern CMR imaging only one study has found evidence of localized fibrosis associating to Q waves of the same area (81). These factors do not readily explain the Q waves seen in mutation carriers without hypertrophy for which there is no clear explanation at this point other than the possible effect of minor subclinical changes in the myocardial wall predating overt hypertrophy.

2.8.3 Conduction disturbances and bundle branch block

Minor conduction disturbances like left anterior hemi-block and intraventricular conduction delay (QRS 100-120 ms) are present in 20-30% of HCM patients (72). Right and left bundle branch blocks are relatively common in HCM, with a prevalence of approximately 5-10% depending on the cohort (72,73). They have been associated with septal fibrosis and indirectly related to syncope in HCM (73).

2.8.4 The QRS complex

Ventricular excitation waveforms (depolarization) form the QRS complex. Prolongation of the depolarizing phase in the myocardium results in widening of the QRS complex – a common and unspecific finding in many myocardial diseases. The uniformity of the depolarizing waveforms in the myocardium may be disrupted by pathological processes, resulting in additional notching of the QRS complex called fragmentation. The definition of fragmented QRS (fQRS) includes a QRS duration of ≤ 120 ms and various patterns of notching in the R and/or the S waves or the R' (a second upward deflection immediately following the downslope of the original R wave) with or without a Q wave (82). Common bundle branch blocks are exclusion criteria for fQRS. Fragmentation has been associated with fibrosis in the myocardium in cardiomyopathies (82,83) and may confer prognostic significance in ischemic cardiomyopathy probably relating to ventricular arrhythmias (84). In hypertrophic cardiomyopathy a connection between fragmentation of the QRS complex and malignant VAs has also been observed (85,86). Fragmentation may be one of the electrical results of the pathological myocardial process in HCM.

2.8.5 Conventional criteria for left ventricular hypertrophy

The application of the Sokolow-Lyon voltage criteria and Cornell's voltage product to assess LVH from ECG is ubiquitous in cardiology practice. In brief the Sokolow-Lyon voltage is positive when SV1 + RV5 or RV6 ≥ 3.5 mV (87) and Cornell's voltage product is positive when the QRS-duration (ms) x (RaVL [mV] + SV3 [mV] (+6 mV for women) ≥2440 (88). Their efficacy in the diagnostics of HCM has historically been suboptimal, with sensitivity being in the region of 30% and 40% respectively, even in recent publications (72,89,90). The Romhilt-Estes point score is a more complicated

system to assess hypertrophy (Table 2), with a better diagnostic yield of approximately 60% in HCM (72).

Romhilt-Estes point score	**Points**
Amplitude (positive if any of the following)	3
- largest R or S in limb leads ≥ 20 mm	
- S wave in V1 or V2 ≥ 30 mm	
- R wave in V5 or V6 ≥ 30 mm	
ST-T segment pattern (LV strain with ST-T vector opposite mean QRS vector)	3
Left atrial involvement	3
- V1 P-wave terminal negativity ≥ 1 mm + duration ≥ 40 ms	
Left axis deviation ≥ -30°	2
QRS duration ≥ 90 ms	1
Intrinsicoid deflection	1
- time from onset of QRS to peak of R wave ≥ 50 ms in V5 or V6	
Maximum total	13
Definite LVH	≥ 5
Probable LVH	4

Table 2 A point score system for diagnosing left ventricular hypertrophy, adapted from Romhilt and Estes (13).

2.8.6 QT interval prolongation

The time interval from the onset of the Q wave to the end of the T wave (QTe) is a measure of the duration of repolarization (91). In HCM the repolarization abnormalities on many levels result in prolongation of the QTe interval. As the QTe duration is dependent on heart rate, for standardization the QTe interval is often corrected for this. This is usually performed with the Bazett formula $QTc = QT \sqrt{RR}$ (92). This correction is the most common used in the literature, but even recently has been criticized for possibly overestimating the proportion of patients with pathological prolongation of the QT interval compared with the Fridericia and Framingham formulas (93). QTe prolongation has been independently associated with increased risk of sudden death. In the general population a QTc interval of ≥ 450 ms in men and ≥ 470 ms in women has been associated with a threefold risk of SCD (94).
The QTe prolongation in HCM is a complex interplay of different factors:

1. prolongation of the ADP on the cellular level (38)
2. delay of repolarization due to hypertrophy (95)
3. dispersion of repolarization due to asymmetric hypertrophy and myocardial wall pathology (96)

The QTe interval may be a relatively good measure of the pathologic process inherent in HCM. In a cohort of nearly 500 HCM patients the measured QTc on a resting 12-lead electrocardiogram correlated mildly to maximal wall thickness on

echocardiography and the basal gradient in the LVOT (95). The prevalence of a pathologic QTc > 480 ms was 13% in HCM patients compared to < 1/200 in the general population. In another series a measured QTc of > 440 ms was associated with larger left atria, thicker MWT, slightly elevated E/E' and mechanical dyssynchrony (97). Late gadolinium enhancement in addition to conventional measures of advanced HCM pathology were more prevalent in HCM patients with prolonged QTc and increased temporal lability of repolarization as measured by QT variance index and normalized QT variance (98). In a prospective study of 195 HCM patients QTc prolongation and fragmented QRS in ≥ 3 territories of the resting 12-lead ECG were predictive of malignant ventricular arrhythmias (85). QTc may be prolonged already in mutation carriers without LVH (99,100)

Spatial QTe dispersion, the difference between the smallest and largest values of QTe duration from all leads in a 12-lead ECG, is also increased in HCM (101-104). The dispersion is a measure of the spatial heterogeneity of repolarization in the LV and has been associated with ventricular arrhythmias in ambulatory ECGs (103,105). The angiotensin converting enzyme genotype of two deletion alleles (DD) has been associated with the most dispersion of QT in HCM patients in a small observational series (104). The ACE DD genotype is related to increased collagen content in the myocardium. On the other hand, the use of QTe dispersion as a prognostic marker has been questioned in a larger population based study (106)

In a prospective study of 164 HCM patients with implanted ICDs, a prolonged QTc was the best independent predictor of ventricular arrhythmias after adjustment for gender and left ventricular maximal wall thickness (107). This points to the dysfunction in repolarization as one of the key factors in arrhythmia potential in HCM, although the analysis did not include CMRI imaging or modern echocardiographic deformation techniques.

2.8.7 ST depression and T wave inversion

A multitude of repolarization abnormalities can be found in the ST segment of hypertrophic cardiomyopathy patients. Hypertrophy itself alters the gradient producing T waves in the ventricle. Myocardial fibrosis results in currents resembling ischemia. ST-segment depression or T wave inversion can be seen in approximately 30% of HCM patients (72) and are associated with late gadolinium enhancement on cardiac MRI (LGE) and wall thickness (72,73,108). In a retrospective setting of 173 HCM patients followed for a mean of 4 years ST-segment depression in the high lateral leads (I, aVL) and syncope predicted SCD or appropriate ICD therapy (109). No advanced imaging modalities i.e. deformation echocardiography or CMRI were employed.

2.9 24h ambulatory ECG

The 24h ambulatory ECG is a commonly used tool in the evaluation of hypertrophic cardiomyopathy. Usual applications include assessment of heart rate in response to

daily activity, exercise, and medications, analysis of conduction disturbances and atrial arrhythmias, optimization of therapy for atrial fibrillation, and the assessment of ventricular arrhythmias in relation to SCD risk. Table 3 presents common findings of ambulatory ECGs in HCM patients compiled from five separate studies (110-114).

Holter findings	Percentage
SVT	6%
AF	5%
PVC > 200/24h	12%
NSVT	23%
Conduction abnormalities	23%
AV I block	17%
AV II block	3%
Sinus pause > 2 s	7%

Table 3 Common findings in ambulatory 24h ECG in a total of 1044 HCM patients (110-114). SVT = supraventricular tachycardia; AF = atrial fibrillation; PVC = premature ventricular contraction; NSVT = non-sustained ventricular tachycardia; AV = atrioventricular; NSVT = non-sustained ventricular tachycardia.

The presence of non-sustained ventricular tachycardia (NSVT), defined as ≥ 3 consecutive ventricular beats at a rate of ≥ 120/min, has been associated with higher incidence of SCD in multiple studies (111,112,115,116). It has a prevalence of about 20-30% in the general HCM-population. Patients with recorded NSVT-episodes demonstrated thicker ventricles, larger left atria and higher incidence of left ventricular outflow tract obstruction (LVOTO) indicating a more advanced disease state compared to patients without NSVT (111). The use of betablocker therapy does not have a major impact on the incidence of NSVT (117).

2.9.1 Median and maximal QTe

The QTe values measured from ambulatory ECG recordings are mostly reported in trials as median or mean values in patients. Repolarization is a dynamic process and the potential for arrhythmias may relate to abnormal lengthening of the QT interval as a temporal phenomenon. Therefore, the assessment of maximal QTe interval in ambulatory ECGs may more accurately reflect the potential for arrhythmias in different cardiomyopathies. Using maximal QTe values measured from ambulatory ECGs was more sensitive in differentiating LQT1 and LQT2 patients from control subjects than baseline QTc from the ECG (118).

2.9.2 The QT/RR slope

A tool to assess QT dynamicity is the QT/RR slope. A QT/RR plot is generated by plotting the QTe interval values and their respective preceding RR-intervals from an ambulatory ECG recording on the y- and x-axis, respectively. A straight line is fitted to the plot to derive the QT/RR slope (Figure 5). The slope is the measure of the lengthening of the QT interval in relation to increasing RR-intervals. It is a measure of the dynamicity of repolarization in relation to heart rate.

Several investigators have analyzed the QT/RR slope and its association to prognosis in other cardiomyopathies. A reasonable body of evidence exists linking steeper QT/RR slopes to malignant arrhythmias or sudden cardiac death in ischemic cardiomyopathy. In the GREPI study the steeper QT/RR slopes, measured up to two weeks from myocardial infarction, predicted SCD in 7 years of follow-up (119). Similarly, in the EMIAT study patients who had a myocardial infarction and later experienced cardiac death during 21 months of follow-up had steeper QT/RR slopes (120). In heart failure due to varied etiologies the steeper QT/RR slopes have associated more with overall mortality, and not specifically to arrhythmic events (121-123). In HCM patients the QT/RR slope has been found steeper compared to control subjects and associated to higher estimated risk for arrhythmia (124), although no analysis of the effect of wall thickness or other structural findings of HCM to repolarization was performed in that study.

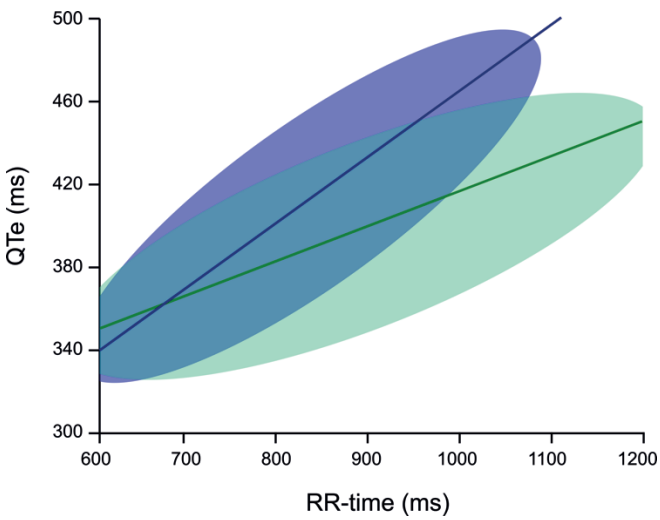

Figure 5 Schematic of measuring the QT/RR slope. A line is fitted to the QTe-RR point plot of the form y = ax + b, where a = slope and b = intercept. In green an example of a normal QTe/RR slope and in blue a steeper QTe/RR slope representing, for example, a patient with ischemic cardiomyopathy.

2.9.3 T wave apex to T wave end

The time period from T wave apex to end (TPE) is regarded as a measure of the global dispersion of repolarization in the LV (125,126). In a rabbit model of HCM the degree of left ventricular hypertrophy increased TPE and induced EADs that could initiate "R on T" VT (127). Prolonged TPE in lead V5 of the ECG taken at rest has been associated with increased risk of SCD (128). The finding was true also in subjects with normal QTc or not measurable QT due to a prolonged QRS. In a small sample of HCM patients TPE was prolonged and associated with SCD or VT (129).

2.9.4 Atrial fibrillation

Atrial fibrillation (AF) is the most common arrhythmia in HCM and a clinically significant problem due to the high incidence of thromboembolic complications and exercise tolerance reduction. Left ventricular outflow tract obstruction, mitral insufficiency, and diastolic dysfunction all elevate left atrial pressure and predispose to AF. An active search for AF should be undertaken in HCM patients, especially if the left atrium is enlarged (4). In pooled data of HCM patients the prevalence of AF was 22%, with a clear increase related to aging (130). The incidence of thromboembolic complications in HCM patients is markedly higher compared to the general population and the conventional risk calculators for stroke prediction work suboptimally in HCM. Therefore the guidelines advocate permanent anticoagulation in HCM patients with paroxysmal or permanent AF (4). The 24h ambulatory ECG is an inexpensive tool to hunt for AF. The incidence of AF in ambulatory monitoring in nonselected HCM populations is approximately 5% (Table 3). Atrial fibrillation is paroxysmal in two thirds and permanent in one third of HCM patients with AF (131). HCM patients with AF tend to be symptomatic and a more active approach to rhythm control in clinical management has been advocated in the form of a lower threshold for initiation of antiarrhythmic therapy, including amiodarone (4).

2.10 Echocardiography

2.10.1 Conventional echocardiography

Echocardiography is the single most versatile tool in assessing hypertrophic cardiomyopathy. In most cases, the diagnosis can be made by demonstration of significant hypertrophy of the LV wall and ruling out other possible causes such as abnormal loading conditions from aortic stenosis. The distribution of hypertrophy can readily be assessed with echocardiography further confirming the usually asymmetric nature of the disease. In a small minority of subjects where HCM is suspected, the limited acoustic windows make the diagnostics challenging and according to reports echocardiography misses the diagnosis of HCM in approximately 6% of cases (132). This is true especially in confined apical HCM (133).

Left ventricular dimensions are usually normal in HCM, but the LV lumen may be reduced due to significant hypertrophy. LV systolic function by conventional ejection fraction assessment is usually normal or hyperdynamic. Left atrial volumes can be enlarged due to diastolic dysfunction, mitral insufficiency and increased pressure from outflow tract obstruction. Diastolic dysfunction is a common finding in HCM. It is a result of the pathological process in the myocardial wall and can be further exacerbated by pressure load from outflow tract obstruction. Conventional tissue Doppler velocities of mitral valve annular motion in early diastole (Em, the beginning of ventricular filling) and late diastole (Am, during the atrial contraction) are usually reduced and filling pressure estimates elevated (increased E/Em). The mitral valve should be carefully assessed in HCM. The papillary muscles and the anterior leaflet of the mitral valve can be elongated and morphologically abnormal (134,135). Mild to moderate mitral insufficiency is quite common. Assessment of systolic anterior motion of the mitral valve (SAM) is important in assessing the possibility of outflow tract obstruction. Left ventricular outflow tract obstruction should be sought after at rest or with provocation, especially in symptomatic individuals. LVOTO is defined as an instantaneous Doppler peak gradient of ≥ 30 mmHg measured at rest or with provocation (for example the Valsalva maneuver or standing) or exercise and it carries prognostic value (136). The inherent problems with the assessment of LV systolic function by LVEF, such as interobserver variation, assessment of function indirectly through volume change, and relative insensitivity, has lead to the development of deformation imaging, which more comprehensively assesses the motion of the chamber.

2.10.2 Deformation of the left ventricle

The myocardial wall is composed of myocytes organized as lamina of typically four cells thick and separated by cleavage planes (137). The lamina are arranged in a helical fiber geometry which is left-handed in the epicardium and gradually changes to a right-handed helix in the endocardium for optimal energetics (138) (Figure 6). On the principle of larger radius for torque, the contraction of the left-handed helix dominates the systolic deformation resulting in a counterclockwise twisting motion as seen from the apex (139). During the cardiac cycle the wall of the left ventricle deforms by longitudinal and circumferential shortening, radial thickening and twisting along the long axis (140,141). This wringing motion is released in diastole almost like a spring coil. The three-dimensional nature of the mechanical cardiac cycle interconnects the phases of systole and diastole, making them dependent on each other (142,143). As can be readily observed from the anatomic arrangement, the process of asymmetric hypertrophy in HCM affects the systo-diastolic properties of the three-dimensionally contracting left ventricle significantly and the distribution of hypertrophy has a marked effect on the mechanics of LV function (144-147).

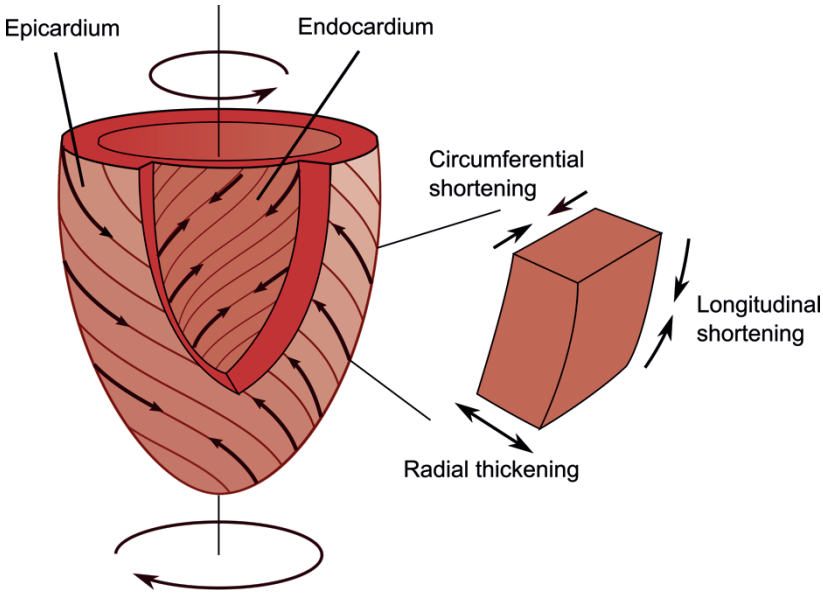

Figure 6 The organization of the myocardial wall of the left ventricle and motion during systole. The myocardial wall contracts with longitudinal and circumferential shortening and radial thickening during systole. The epicardial layer contracts with a left-handed helical arrangement of myocytes and the endocardium in a right-handed helix. The net rotation in the epicardium is counterclockwise and in the endocardium it is clockwise.

2.10.3 Echocardiographic deformation imaging

Previously the use of echocardiography to quantify myocardial function was characterized by problems of subjectivity, inter- and intraobserver variability, and the analysis of wall motion based on visual analysis. The need for noninvasive quantitative methods to analyze myocardial function has led to the development of two- and three-dimensional strain and strain rate imaging. Strain is a complex construct, but simplified to one dimension it is the lengthening or shortening of an object. Strain rate is the velocity of change of strain i.e. the velocity of deformation. Deformation of the myocardium measured with strain imaging is inherently relatively free of tethering effects and the overall translation of the heart in the chest cavity, making it a valuable tool as a sensitive marker of local and global dysfunction in a variety of disease states (148).

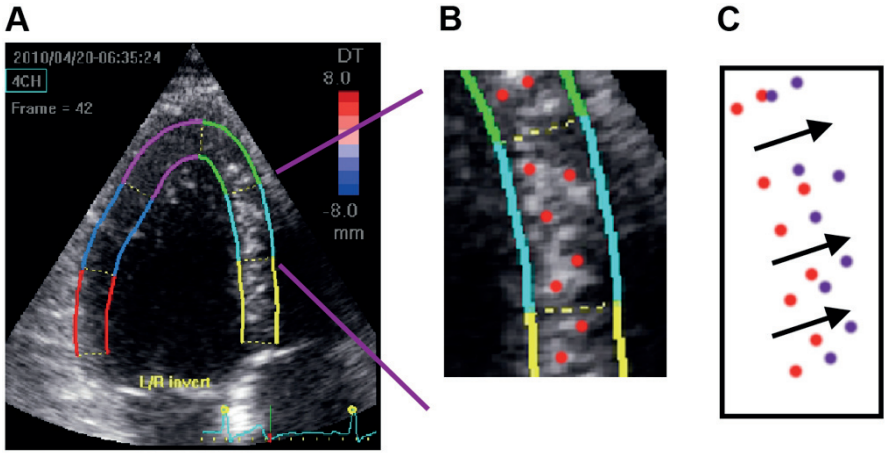

Figure 7 Speckle tracking principle. A) The myocardial wall endocardial and epicardial borders are identified. B) The algorithm identifies acoustic speckles in the ultrasound data. C) The temporal change of location of the speckles (arrows, red to violet) is quantified as movement which is measured as strain in 2D.

Strain imaging has been previously used with MRI tagging methods, invasive sonomicrometry crystals and tissue Doppler echocardiography (TDI). The TDI technique is highly dependent on angle of capture along the scanline - even more so than usual Doppler methods and can only measure deformation in one dimension (149). To overcome these issues, the method of speckle tracking echocardiography was developed (150). The methodology has been described previously (150,151). In brief, the software tracks natural acoustic markers known as "speckles" in normal 2D echocardiography images from frame to frame (Figure 7 and 8). The deformation of these speckles constitutes 2D strain. The benefits are angle independence and the ability to measure strain in two or three dimensions using echocardiography. 2D strain echocardiography (2DSE) with speckle tracking requires high image quality and tracking suffers from dropouts and artifacts. 2DSE has been validated both in vitro with tissue-mimicking gelatin blocks (151) and in vivo in animal models by sonomicrometry (152) and in humans compared to MRI tagging and tissue doppler strain (152,153).

2.10.4 Global and segmental longitudinal strain

Since the advent of 2DSE the use of longitudinal strain has been most widespread due to its relative ease in application and robustness of results. Global longitudinal strain (GLS) is usually defined as the mean value of all segmental longitudinal strains in the LV. 2DSE was early on applied in HCM patients with results of diminished global longitudinal strain and reduction of segmental strain in hypertrophied segments of the

LV compared to healthy subjects (154). These results have since been replicated in various HCM populations and Table 4 summarizes the results of some of these studies mainly focused on assessment of the global LV systolic function in a pooled data of 750 HCM patients (145,154-159). GLS is usually reduced in HCM compared to control subjects and the degree of reduction associates do the degree of hypertrophy (157). One of the marked findings in these studies was, that although to the naked eye the function of the LV was normal or near normal and the measured LVEF values matched those of the control population, there was a clear reduction in segmental strain values even in nonhypertrophied segments, implying reduced function in seemingly normal myocardium.

2D strain echocardiography is available from practically all vendors of ultrasound equipment in some form or another. GLS overcomes many of the problems concerning conventional LVEF measurements (160). Concern over the intervendor variability has been an issue that recently was investigated (161). Global longitudinal strain proved to be a robust measure of LV function and had better interobserver variability than conventional four-chamber LVEF (relative mean error 7.8% vs 13.1% for one vendor). The correlation between different vendors was high and the largest absolute GLS difference between vendors was 3.7%. For segmental strain the differences between vendors was higher and therefore should be serially assessed with the same software (162).

Strain imaging quantifies the pathological process in the myocardium of HCM patients in many ways and the segmental values are effected by both hypertrophy and fibrosis (163). Saito et al. (164) studied 48 HCM patients with GLS and CMRI. LGE was present in 75% of patients and these patients had higher LV mass index and lower absolute GLS compared to HCM patients without LGE (-11.8% vs -15.0%). Studies by DiSalvo et al. and Almaas et al. both found that septal segmental strain predicts NSVT on holter (165,166). The predictive value of strain was superior to septal LGE and correlated better to the presence of fibrosis in histopathological specimens of the septum in a small population of HCM patients undergoing myectomy (166).

GLS has also been associated to prognosis in HCM in a study of 119 HCM patients with a follow-up of 19 months. A reduced GLS of > -15% and exercise LVOT gradient > 50 mmHg were independent predictors of adverse cardiac events (167). Debonnaire et al. studied 92 patients prospectively with echo before ICD implantation (159). GLS > -14% and left atrial volume index > 34 ml/m^2 were independent predictors of ICD therapy. In a follow-up of 4.7 years 23% of patients received ICD therapy.

In a larger cohort of 400 HCM patients followed for a median of 3.1 years a reduction in GLS ≥ - 16% was an independent predictor of worse outcome (168). In the group with a GLS of ≥ - 10% a total of 33% met the composite end-point of ventricular tachycardia or fibrillation, death / cardiac transplantation or heart failure. In a similar setting of 427 HCM patients, with a follow-up of 6.7 yrs., both GLS ≥ -15% and left atrial volume index > 34 ml/m^2 independently indicated worse survival (169).

		HCM patients									Control subjects					
Study	**Method**	***n***	**Age (yrs)**	**Female (%)**	**MWT (mm)**	**LVEF (%)**	**NYHA**	**LVOTO**	**GLS**	**SD**	***n***	**Age (yrs)**	**Female (%)**	**LVEF (%)**	**GLS**	**SD**
Serri et al. 2006 JACC (154)	2D-STE	26	47 ± 18	27%	NA	69%	NA	NA	-15.5	6.3	45	42 ± 14	47%	67%	-20.6	6.1
Carasso et al. J Am Soc Echocargiogr 2008 (155)	VVI	72	43 ± 14	31%	20 ±6	68%	II	64%	-15.5	5.5	32	49 ± 18	50%	66%	-21.5	4.0
Urbano-Moral et al. Circ Cardiovasc Imaging 2014 (156)	3D-STE	59	46 ± 17	36%	20	59%	I - II	54%	-14.0	3.0	30	42 ± 10	40%	58%	-17.0	2.0
Haland et al. Open Heart 2017 (157)	2D-STE	180	41 ± 14	42%	19 ± 4	51%	II	NA	-16.4	3,7	80	54 ± 15	56%	61%	-22.3	3.7
Paraskevaidis et al. Am Heart J 2009 (158)	2D-STE	50	51 ± 18	42%	20 ± 4	71%	I - II	60%	-14.0	4.0						
Debonnaire et al. Int J Cardiovasc Img 2014 (159)	2D-STE	92	50 ± 14	32%	24 ± 5	70%	NA	NA	-13.3	3.5						
Reant et al. Int J Cardiovasc Img 2014 (145)	2D-STE	271	49 ± 16	29%	20 ± 5	68%	II	24%	-16.4	3.7						
Total		750	46	34%		66%			-15.6	3.9	187	48	50%	63%	-20.9	4.1

Table 4 Global longitudinal strain studies summary. VVI = velocity vector imaging.

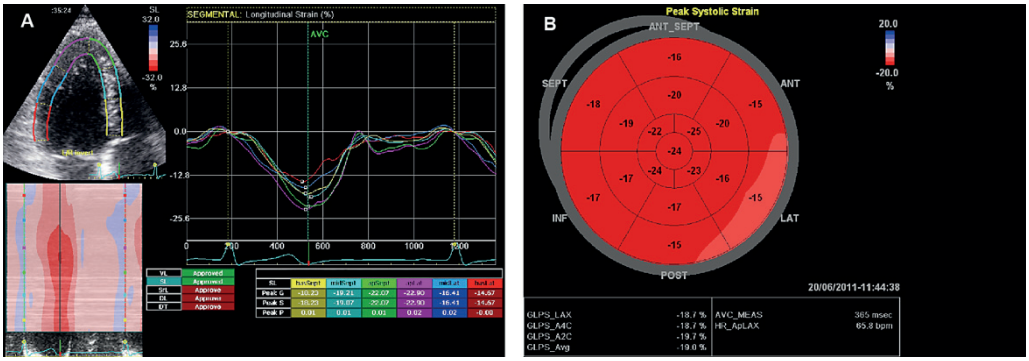

Figure 8 Example of measuring strain. A) Apical four-chamber view of segmental strains. B) Combined segmental strains from all apical views (A4C, A2C, A3C) in a bull's eye plot and global strain measurements.

2.10.5 Mechanical dispersion

2DSE enables the measurement of timing of mechanical events of the cardiac cycle. Of interest in many cardiomyopathies is the presence of asynchrony in systolic contraction. Marked dyssynchrony, from example a left bundle branch block, reduces the pump function of the LV. With 2DSE the segmental timing of contraction and its delays can be quantified. The dyssynchrony can be measured as the standard deviation of the timing of peak longitudinal strain happening around aortic valve closure. This measure has been termed mechanical dispersion (MD). In post-myocardial infarction patients and DCM subjects (lamin A/C mutation) MD was a significant predictor of arrhythmic events and more effective than GLS or LVEF (170-173).

2.10.6 Twist

The helical wrap of myocytes around the LV produces a twisting motion. This torsion of the LV may link the systolic contraction period to the diastolic forces in a spring coil like preservation of mechanical force. The twisting motion of the LV aids in the production of vortices of blood flow in both systole and diastole (174). For 2DSE measurement purposes the LV is viewed from the apex and twist is quantified as the net difference between basal and apical rotation (Figure 9) (175). Torsion is defined as twist standardized to the distance between the 2D imaging planes of the apex and base. During systole the apex rotates counterclockwise and there is a brief counterclockwise rotation of the base at the beginning of systole followed by a clockwise motion. Apical rotation is much larger in degrees and is the defining factor in the absolute measure of peak systolic twist. During diastole the apex and base reverse rotational direction to return to baseline at the end of diastole (Figure 9) (139,176). In HCM the absolute twist values are preserved but there is a delay in the completion of twist in systole and a corresponding delay in untwist during early diastole linking systolic and diastolic

function on the mechanical level (143,177). Age and female gender were associated with increased torsion in a CMRI tagging study of nearly 1500 subjects in a community based population study (178).

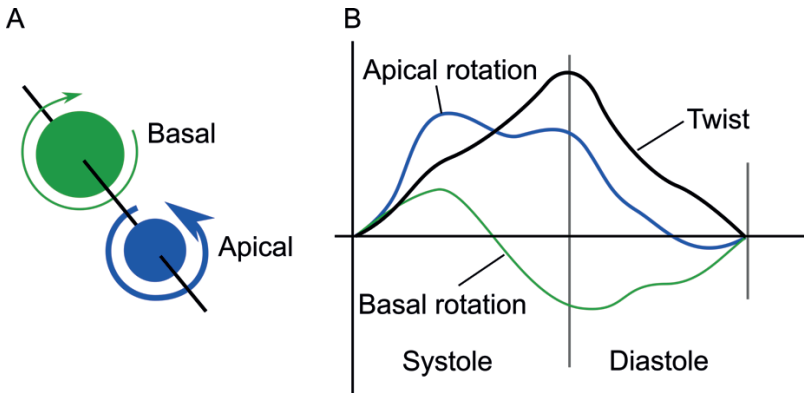

Figure 9 Measuring twist. A) The basal level rotates in clockwise direction and the apical level in counterclockwise direction as seen from the apex. B) The representative twist curves from the apical (blue) and basal (green) level and the resulting net twist (black). It is notable, that the majority of absolute twist degrees in systole is contributed by the larger rotation (in degrees) at the apical level.

2.11 Cardiac magnetic resonance imaging

2.11.1 Patterns of hypertrophy

In the last two decades, cardiac magnetic resonance imaging has moved from an academic curiosity to a cornerstone in the diagnostics of cardiomyopathies. In hypertrophic cardiomyopathy it is extensively used in the confirmation of diagnosis in ambiguous cases and in risk stratification. The hypertrophy in HCM can be very confined and its full characterization in some cases is not possible with echocardiography (132,179). CMRI has expanded our knowledge of the helical patterns and structure of hypertrophy (144). It is advocated as an initial diagnostic tool in a recent position paper on multimodality imaging in HCM (180). The main diagnostic value of CMRI in risk stratification is the reliable assessment of maximal wall thickness especially in patients with suboptimal echocardiographic windows and quantification of fibrosis with late gadolinium enhancement.

2.11.2 Imaging fibrosis – late gadolinium enhancement

Gadolinum is an organic chelate compound and administered intravenously concentrates in the extracellular space in myocardium. Focal enlarged areas of extracellular space concentrate gadolinium to an extent visible in CMR imaging. These focal areas represent scar or replacement fibrosis in HCM and can be quantified

relative to the mass or volume of the total LV myocardium (181,182). Imaging fibrosis with CMR-LGE is extensively used in phenotypic characterization and risk assessment in HCM (183). With current methods the prevalence of LGE in unselected HCM patient cohorts ranges from 30 to 68% (179,184,185). There is a correlation between increased hypertrophy and the amount of LGE (179,186).

Patients with LGE more frequently have NSVT on holter (184,186) and the extent of LGE correlates with a higher risk for adverse events (187,188). In a cohort of 424 HCM patients studied by Rubinshtein et al. a predictive effect for LGE was found for adverse events although the absolute number of events was small (186). In the largest CMRI study population to date of 1293 HCM patients, the extent of LGE associated independently to increased risk for SCD. The proposed cutoff of LGE ≥ 15% of LV mass carried a twofold increase in SCD risk in patients otherwise classified as low risk (189). These results have been confirmed in a pooled meta-analysis of LGE studies with a total HCM patient population of 2993 and a median follow-up of 3 years (185).

2.12 HCM and athlete's heart – differential diagnostics

The risk for lethal arrhythmias in young athletes with HCM is significant and current guidelines prohibit patients' participation in competitive sports (4). Professional level endurance sports may result in compensatory dilatation of the LV and concentric mild hypertrophy of usually ≤ 15 mm. ECG changes are also quite common in professional athletes. These changes can be identical to those in HCM. Therefore, the clinical differentiation between benign athlete's heart and HCM can be difficult.

Recently a position paper by the European Heart Rhythm Association on preparticipation screening has elaborated on the issue and is a good guide to the clinician (190). Family history and abnormal arrhythmias can be an important clue. Naturally, genetic testing is indicated if the pathogenic variant in the family is identified. Echocardiographically the hypertrophy in HCM is usually asymmetric compared to the concentric LVH of athlete's heart. The diastolic function in athlete's heart is usually normal with tissue Doppler evaluation, whereas in HCM the hypertrophied myocardial segments exhibit reduced diastolic velocities. In difficult cases the use of 2D strain echocardiography can aid – with usually reduced strain in the hypertrophied segments and possibly reduced GLS (191). CMR findings of asymmetric, localized hypertrophy and presence of LGE also strongly favor HCM. Deconditioning should result in regression of hypertrophy in athletes.

2.13 Prognosis

The clinical course of hypertrophic cardiomyopathy is highly variable due to multiple factors such as mutation type and modifying factors, onset of symptoms, degree of outflow tract obstruction and susceptibility to arrhythmias. In the unselected HCM population, the annual mortality rate is approximately 1%, which is close to the general population in Western societies (30). Elderly patients were largely omitted from the

early studies of HCM in the 1980s and 1990s. In recent large scale studies the mean age of patients is still around 50 years. As the demographics of many developed nations are shifting in balance towards an increasing number of elderly citizens, so too will the age balance of HCM change. This may affect clinical decision making in the future regarding medical and especially ICD therapy.

In the clinical spectrum of HCM one can appreciate certain subgroups of patients:

- Younger patients with high risk of SCD.
- Patients with significant obstruction of the LVOT requiring surgical or percutaneous intervention.
- Patients with debilitating symptoms, such as exertional dyspnea and chest pain, and who develop congestive heart failure with preserved EF.
- Patients with problematic atrial fibrillation and thromboembolic events.
- A smaller set of patients who progress to the burnt out phase of HCM.
- The expanding population of G+/LVH- subjects and the continuum from healthy mutation carrier to manifest HCM.

A targeted approach to these subgroups is needed to correctly address the problems of this relatively common inherited cardiomyopathy.

2.14 Risk assessment of sudden cardiac death

Hypertrophic cardiomyopathy is one of the most common causes of sudden cardiac death in the young and young athletes (3,192,193). The risk of SCD in general in HCM is more pronounced in the young (194). Current guidelines from the European Society of Cardiology delineate a comprehensive risk assessment of sarcomeric HCM resulting in an annual SCD risk given by an algorithm (4). The model is based on a large retrospective cohort study of SCD in HCM patients (5). The individual risk factors in the final model are age, maximal wall thickness, family history of sudden death, left ventricular outflow tract gradient, left atrial diameter, unexplained syncope, and NSVT recorded on ambulatory ECG.

As the risk for SCD is more pronounced in the young, the age of the patient has an inverse association to the risk (5,195). Maximal wall thickness correlates with increased risk for SCD in a non-linear fashion (5). Family history of sudden death confers an independent risk for SCD and according to one study the finding of multiple sudden deaths in the family increases this risk significantly (196). Although exercise testing is not included in the final risk calculator, it is still an integral part of the risk assessment in HCM patients. It is used to evaluate the manifestation of arrhythmias during exercise and to assess an abnormal blood pressure response, i.e. a drop in systolic blood pressure during exercise or failure to increase systolic blood pressure during exercise.

The guidelines from ESC date back to 2014 and since then significant progress in imaging of HCM has been made. Especially the findings of GLS and LGE associating independently to prognosis and arrhythmias may in the future influence the risk assessment of HCM patients (197). Another small but important subset of patients

missing from the risk model are those with apical aneurysm formation, which confers a higher risk for arrhythmic events and thromboembolic complications (198).

On the basis of previous findings, the risk stratification of individual patients and decision to implant an ICD requires sound clinical judgment. Implantation of ICDs carries approximately a 2% risk for access site complications (pneumothorax, haematoma) and a device infection rate of 1.5% according to a meta-analysis with a mean follow-up time of 18 months (199). With current programming algorithms the rate of inappropriate therapy is in the range of 16-21% in follow-up periods ranging from 10 to 46 months (200,201). These factors should be taken into account when discussing ICD therapy with HCM patients, who often are young and have a very long period of device therapy ahead of them.

2.15 Screening, clinical genetics and follow-up

Sarcomeric HCM is often genetically transmitted to offspring and therefore it is justified to evaluate family members of known HCM probands. Both the ACC/AHA and ESC guidelines have comprehensive instructions for the screening process (4,202). As HCM is the most common inherited cardiomyopathy the number of individuals that require screening is substantial.

Genetic testing is recommended for probands (4). Usually this is done by applying a pre-defined panel of the most common pathological variants responsible for HCM. The search may be expanded with larger scale whole exome sequencing in selected rare cases, but this is usually not indicated and often yields a number of variants of unknown significance. When a pathological variant is found in a family, a process of cascade screening starting from first degree relatives is applied.

In families without an identified pathogenic mutation, the first degree relatives of probands need to be clinically screened at regular time intervals. This consumes resources and the cost-effectiveness of the approach advocated by the guidelines has not been readily established. Therefore, it would be of value to find effective markers of early disease presentation to guide the screening process in G- families and assist in the evaluation of families with a known pathological variant (G+/LVH- subjects). A number of small scale studies have been performed to this effect in the G+/LVH- subjects with varied results.

Early studies on the subject found reduced diastolic TDI velocities in G+/LVH- individuals (203-205). With the advent of 2DSE there have been reports of reduced segmental strain (206,207) and diastolic abnormalities (208) in gene mutation carriers without hypertrophy. Recently a delay and decrease in untwisting has also been observed in G+/LVH- subjects (209). The problem with these studies on G+/LVH- subjects has been one of replication and somewhat contradictory findings. It is possible that mutation type plays a role in the preclinical phases of the disease. The effectiveness of 2DSE and TDI imaging in differentiating G+/LVH- subjects from healthy noncarriers requires further study.

3 AIMS OF THE STUDY

In general, the objective was to assess the mechanical and electrical alterations in the myocardium of carriers of pathogenic gene variants for HCM with modern imaging and repolarization analysis, evaluate the use of standard 12-lead ECG in the assessment of G+/LVH- subjects and study the metabolome in HCM.

More specifically the aims of this study were:

I. Investigate the association of global longitudinal strain, mechanical dispersion, and late gadolinium enhancement in HCM patients to recorded ventricular arrhythmias in 24h ambulatory ECGs.

II. Explore the distribution of ECG parameters in HCM mutation carriers and evaluate the diagnostic value of the ECG for detecting G+/LVH- subjects and to correlate the ECG findings with comprehensive imaging data.

III. Quantify the repolarization abnormalities in hypertrophic cardiomyopathy using ambulatory ECG recordings and elaborate their association to imaging in HCM.

IV. Investigate the metabolomic profile of carriers of the *MYBPC3*-Q1061X mutation and its association to echocardiographic findings.

4 METHODS AND MATERIALS

4.1 Patients

Genotyped families carrying either the *MYBPC3*-Q1061X or *TPM1*-D175N pathogenic variant for HCM were recruited from the Helsinki, Kuopio and Jyväskylä hospital districts between 2000 – 2012. Mutation carriers (G+) with documented maximum wall thickness ≥ 13 mm on echocardiography (LVH+) were classified as G+/LVH+ and nonhypertrophic individuals as G+/LVH-. The control population subjects were noncarriers of either of the variants from the same families (studies I, II, IV) and unrelated noncarriers (study III), without hypertrophy and structurally normal hearts on echocardiography.

In study I prospectively recruited 31 G+/LVH+ patients with the *MYBPC3*-Q1061X variant were divided into HCM/NSVT+ (n = 11) and HCM/NSVT- (n = 20) groups depending on the presence of NSVT on 24h ambulatory ECG and a control group of 20 noncarriers from the same families from the Helsinki and Kuopio University Hospital districts. The phenotypic status was confirmed with CMRI.

In study II the groups consisted of carriers of either the *MYBPC3*-Q1061X or *TPM1*-D175N variant recruited retrospectively from all three districts, with a total of G+/LVH+ n = 98, G+/LVH- n = 42 and control group n = 40 subjects.

Study III patient groups were prospectively recruited carriers of *MYBPC3*-Q1061X or *TPM1*-D175N mutations forming the patient group G+/LVH+ (n = 46). The control group subjects (n = 35) were noncarriers from the same families. Six G+/LVH+ patients were excluded from the original 52 screened due to non-sinus rhythm or bundle branch block.

In study IV patients from families with the *MYBPC3*-Q1061X mutation were recruited prospectively, the study groups were G+/LVH+ n = 34, G+/LVH- n = 19, and the control group n = 20.

4.2 Laboratory assays

Conventional blood samples were collected in a fasting state (12 hours) and immediately centrifuged at 3200 G for 10 minutes at 4°C. Plasma was separated and stored at -70°C (Kuopio) and -80°C (Helsinki). The plasma concentrations of NT-proBNP were determined with immunoassays utilizing antisera directed to NT-proBNP, as described previously (210).

4.3 Genetic analysis

All genetic analyses were performed at the University of Eastern Finland. The initial identification of the *TPM1*-D175N and *MYBPC3*-Q1061X mutations and technical aspects of the analyses have been described previously (19,211). In brief, extracted DNA from peripheral blood leukocytes was amplified with polymerase chain reaction. Genotyping of the *TPM1*-D175N and *MYBPC3*-Q1061X mutations was performed

using either the TaqMan Allelic Discrimination Assay (ABI PRISM 7000 Sequence Detection System, PE Applied Biosystems, Foster City, CA, USA) or direct sequencing (ABI PRISM 3100 Genetic Analyzer, PE Applied Biosystems, Foster City, CA, USA).

4.4 The 12-lead ECG

All standard 12-lead ECGs were recorded with 50 mm/s speed and measured manually. Conventional ECG parameters of heart rate, QRS duration, maximal QT interval and corrected QT (with the Bazett formula) were assessed for studies I and III.

In study II the ECGs were further analyzed by an array of previously described parameters by one investigator blinded to the clinical data:

1. R and S wave amplitude from all 12 standard ECG leads
2. ST segment depression or elevation, with a minimum of 0.5 mm change from the baseline drawn between consecutive PR segments
3. Negative T wave, at least 1 mm below the isoelectric line.
4. Pathological Q waves: any Q wave ≥ 40 ms in duration, or ≥ 3 mm deep, or qR-ratio ≥ 0.25, in ≥ 2 parallel leads except lead aVR (73)
5. Absence of normal Q wave in V5-V6 (212)
6. Highest R wave in the precordial leads outside of leads V4-V6 (213)
7. Left ventricular hypertrophy (LVH) according to the Sokolow-Lyon criteria,
8. LVH according to the Cornell voltage-duration product (defined as QRS-duration (ms) x (RaVL [mm] + SV3 [mm] ≥ 2440), for women +6 mm)
9. QRS duration >100 ms
10. RI+SIII > 25 mm (214)
11. RI+SIII-RIII-SI > 17 mm (215)
12. S > R V4 (216)
13. Romhilt-Estes point score ≥ 4 suggesting LVH (13)
14. P-terminal force (negative portion of the P wave in lead V1 ≥ -0.04 mmsec)
15. ST segment depression ≥ 0.5 mm in ≥ 2 parallel leads
16. T wave inversion ≥ 1 mm in ≥ 2 parallel leads, except for leads aVR and V1
17. Frontal plane left, right or superior axis deviation
18. Fragmented QRS (82)
19. Poor R wave progression (PRWP) (217)
20. Reverse R wave progression in leads V1-V3 (217)
21. Rhythm other than sinus
22. Prolonged PR interval ≥ 200 ms.
23. Prolonged QTc interval ≥ 440 ms.

In study II the McKenna major ECG criteria were assessed in the diagnostics of HCM (9). Composite ECG criteria were analyzed to aid in clinical identification of G+/LVH+ and LVH- subjects (II).

Two novel ECG parameters were also measured and analyzed in study II based on clinical practice findings and previously published ECG examples of HCM. The

RV1<RV2>RV3 sign defined as the abnormal distribution of R wave amplitudes in leads V1-V3, with R wave in V2 being largest.

The other ECG parameter was a composite labeled septal remodeling. We have shown this to have discriminatory power in the assessment of LMNA mutation carriers with and without the phenotype of dilated cardiomyopathy (218). Septal remodeling was positive with at least one of the following findings in the leads V1-V3:

1. pathological Q waves in ≥ 2 parallel leads
2. QRS fragmentation in ≥ 2 leads
3. PRWP accompanied by QRS fragmentation
4. disorderly distributed R-wave amplitudes, either RV2 > RV3 or RV1 > RV2

4.5 Ambulatory ECG

Data from digitally recorded 24-hour ambulatory ECGs from Marquette commercial AECG systems were collected and post-processed with a custom software built in collaboration with Aalto University. All data was processed and measured from the modified precordial lead V5. Data processing and algorithms for determining QRS trigger points, onset and offset of QRS and T wave apex and end have been described previously (118). Overall quality of the recording was assessed visually using all the available channels.

T wave apex was identified as the peak of the parabola fitted to the highest amplitude change after the QRS. The time instant when the steepest tangent after the T wave apex intersected the baseline was defined as T wave end.

Data was edited by excluding non-sinus beats, beats with low amplitude T waves (-0.1 - 0.1 mV) and beats where either the T wave apex or end was not identified by the algorithm. All beats with a noise level > 0.02 mV and beats with an RR interval change from the preceding beat of > 30% were excluded. Visual confirmation of the data was performed by plotting time interval values of Q - T apex (QTa), QTe and TPE against the preceding respective RR intervals and using linear limits set manually to remove outliers. To assess the rate dependence of QTe intervals, we calculated heart rate adapted values of median QTe interval using periods of stable heart rate for 60 seconds (beat-to-beat RR interval variation ≤ 10% in RR steps of 10 ms) as described previously (118).

QTe-RR and TPE-RR plots were obtained by plotting time intervals of QTe and TPE (y-axis) against their preceding RR intervals (x-axis). Median and maximum QTe and TPE interval values were measured at 100 ms RR intervals from 600 – 1200 ms. Three separate measurements of maximal value were taken to minimize outliers, with a requisite of variance of no more than 5% between the measured data points and visual confirmation of data quality and stability of at least 5 consecutive beats around the measured beats. QTe/RR slope was measured using data from the QTe-RR plots between RR intervals from 600 to 1200 ms.

4.6 Echocardiography

All echocardiographic measurements in studies I, III and IV were performed according to planned study protocol by experienced cardiologists (MJ, PJ, JK) using Vivid 7 and 9 ultrasound equipment (GE Vingmed, Norway). This data was collected for post-processing and measured centrally with dedicated EchoPac software (GE Vingmed, version 10.0.1, Norway) by one observer (MJ) blinded to clinical and genetic data. In study II approximately 30% of the echocardiographic data performed by experienced cardiologists was collected retrospectively from patient data records and not measured centrally.

All anatomical and functional measurements were performed using accepted guidelines (219). Maximal wall thickness in the LV was measured using 2D short axis imaging, except with apical hypertrophy the use of apical 2D views was accepted. LV ejection fraction was calculated using the biplane Simpson's method. Left ventricular outflow tract obstruction was defined as a resting gradient of ≥ 30 mmHg measured with a continuous wave Doppler from the apical windows through the LVOT with pulsed wave Doppler used for differentiating the level of obstruction. Tissue Doppler measurements were performed using pulsed wave Doppler at the mitral valve annulus level. TDI frame rate values of 150 - 250/s were considered acceptable.

4.6.1 2D strain echocardiography

2DSE measurements of segmental and global function were performed on echocardiographic loops (3 cycles) of adequate quality (50-70 frames per second) as described previously (150,154). Global longitudinal strain was measured as the average of all analyzed segments in each patient. Mechanical dispersion was measured as the standard deviation of time from R-wave to peak longitudinal strain in all 16 measured LV segments in each patient (170). 2DSE measurements were feasible in 87% of all segments recorded in study I.

4.6.2 Twist

2D short axis images from the basal and apical level were used to calculate twist. Twist and twisting velocity were calculated as the difference of apical to basal rotation and rotation rate respectively, measured from parasternal short axis views at the basal and apical levels with 2DSE (176). The cardiac cycle was normalized to systolic duration (time from R wave peak to aortic valve closure) to adjust for different heart rates comparing the apical and basal planes. The rotation curves were interpolated by the cubic spline method with 300 time points for the whole cycle. The measurements were performed using Matlab software (version R2010a, The MathWorks Inc., MA, USA). Peak twist, twisting velocity, untwisting velocity and their time points relative to systolic duration were measured. Recoil and recoil rate were calculated as: Recoil (%) = (Peak twist - Twist at mitral valve opening) / Peak twist and Recoil rate (%/s) = Recoil / Time from peak twist to mitral valve opening (220).

4.7 Cardiac magnetic resonance imaging

Cardiac magnetic resonance imaging was performed in both Kuopio and Helsinki University hospitals. A 1.5-T MR imaging unit (Magnetom Avanto; Siemens Medical Solutions, Erlangen, Germany) and a body-array coil were employed. After scout MR images were obtained, 8-mm sections with an ECG gated steady-state, free precession (SSFP) breath-hold cines in 3 standard long-axis planes (4-, 3-, and 2-chamber views) and sequential 8-mm short axis slices from atrium to apex, with an intersection gap of 20%, were acquired. The parameters used to perform cine MR imaging were as follows: 48/1.1 (repetition time ms / echo time ms), a 65° flip angle, a 192 x 256 matrix, and a 280 – 360-mm field of view. Contrast-enhanced MR imaging was performed after administration of gadoterate meglumine (Dotarem® 0.2 mmol/kg, injection rate 5 ml/sec) to generate sufficient contrast between the normal and abnormal myocardium. Delayed-enhancement images for detection of hyperenhancement were obtained 10 minutes after injection of contrast agent using segmented inversion recovery turbo fast-low angle shot (FLASH) sequence in short axis orientation and in two long axis orientations (4- and 2-chamber views). The imaging parameters were 700 / 1.08 ms (TR / TE), flip angle 50°, acquisition matrix 192 x 144 and 340 x 340 field of view. Slice thickness was 8 mm and intersection gap 20%. Inversion time was optimized to null the signal intensity of normal myocardium.

Two radiologists blinded to clinical and genetic data performed all of the anatomic measurements on MR images data by using dedicated software (Argus, Siemens, Erlangen, Germany), which was provided with the MR imaging system. The maximal end-diastolic wall thickness of the LV was measured in the short-axis orientation in each 17 segments according to American Heart Association (AHA) guidelines. However, the thickness of the true apex was measured on long-axis images. To evaluate LVEF, left ventricular end-diastolic volume (LVEDV), left ventricular end-systolic volume (LVESV) and left ventricular mass, the endo- and epicardium of the LV was manually traced at the end of diastole and systole, with the papillary muscles and the trabeculations excluded. LGE areas were traced with QMass® late-enhancement analysis software (QMass® 7.2, Medis Medical Imaging Systems, Netherlands) in short axis images and quantified segmentally as absolute and relative mass in a standard 16-segment model. A threshold of +6SD was used for detection of LGE.

4.8 Metabolomics

Peripheral blood samples were used to analyze the metabolomic profile with two analytical platforms at VTT Technical Research Centre of Finland (Espoo, Finland) described previously in study IV (221,222). Small, polar metabolites were profiled with two-dimensional gas chromatography coupled to time-of-flight mass spectrometry (GC×GC-TOFMS). This covered sugars, sterols, amino acids and various organic acids, including free fatty acids and ketoacids. The lipidomics platform used ultra

performance coupled to quadrupole time-of-flight mass spectrometry (UPLC-QTOFMS). The spectrum of molecular lipids such as phospholipids, triglycerides, sphingolipids and neutral lipids were analyzed. GC×GC-TOFMS raw data was processed with the Guineau software (221) and data from UPLC-QTOFMS with MZmine 2 (223).

In total 699 molecular lipids and 1603 small polar metabolites were detected, from which 238 lipids and 215 metabolites were identified in study IV. Identified metabolites and lipids found in at least 70% of the samples were used in the statistical analysis. The data were scaled with zero mean and unit variance to make the profiles comparable with each other. Bayesian model-based clustering was applied on the scaled data to group metabolites with similar profiles across all samples. Clustering was performed with the Mclust package in R (R Development Core Team (2014), R Foundation for Statistical Computing, Vienna, Austria) (224). Optimal model selection and data partitioning was determined accordingly by the clustering process.

4.9 Statistical analysis

Variables are presented as mean and standard deviation (SD) for normally distributed data, median and interquartile (IQR) range for non-parametric data, and count and percentage for categorical data. Differences between groups were analyzed with independent T-tests for two groups and one-way analysis of variance (ANOVA) and post-hoc pairwise tests using Bonferroni correction for > 2 groups for normally distributed data, Kruskal-Wallis test for nonparametric data with pairwise comparisons by Mann-Whitney U-test using Bonferroni correction, and Fisher's exact test for categorical data. In study I bivariate Spearman rank correlations of mechanical dispersion with echocardiographic and CMRI variables were performed in the HCM subjects. Significant predictors of NSVT on 24h ambulatory ECG were analyzed with binary logistic univariate regression. A multivariate logistic regression model with a forward stepwise likelihood ratio selection method to assess independent predictors of NSVT was built using the statistically significant variables from the univariate analysis. Receiver operating characteristics curves were used to assess the effectiveness of different variables from the regression analysis to discriminate HCM patients with and without NSVT. Area under the curve (AUC), sensitivity and specificity were calculated. The AUCs of different variables were compared with the U-statistic derived nonparametric (the DeLong) method in R using the package pROC (225). In study III we assessed the effect of different variables to the QTe/RR slope using multivariate linear regression. In study IV the analysis of covariance was used to adjust the ANOVA for age and gender. Individual metabolite levels were visualized using beanplots (226). In all statistical tests a two-way significance level of < 0.05 was considered significant. All statistical analyses were performed with SPSS IBM SPSS Version 21.0 (IBM Corp. Released 2012. IBM SPSS Statistics for Windows, Version 21.0. Armonk, NY: IBM Corp.) and R statistical software.

4.10 Ethical statement

The Ethics Committees of the Kuopio (25/99, 82/2001 and 96/2008) and Helsinki (307-13-03-01-2011) University Hospitals approved the study protocol. The study conforms to the principles outlined in the Declaration of Helsinki.

5 RESULTS

5.1 Imaging HCM (Study I)

5.1.1 Baseline

In study I we evaluated HCM patients (n = 31) and a group of control subjects (n = 20) for the association of 2DSE and CMRI findings to non-sustained ventricular tachycardias recorded on ambulatory 24h ECGs. The HCM patients had mild symptoms, with 90% being in New York Heart Association (NYHA) I-II functional class. Mean age was 49±11 years and 68% were male. Three patients were in permanent atrial fibrillation. Left ventricular end diastolic dimensions and LVEF values were normal and similar in HCM and control patients. Mean LVEF in HCM patients was 60 ± 10% with echocardiography and 63 ± 9% on CMRI. Maximal wall thickness was, by definition, larger in the HCM patients (21 ± 6 mm). The location of maximal wall thickness on echocardiography and CMRI was mostly in the septum and basal anterior segments, with one patient having maximal wall thickness in the inferobasal segment (Figure 10). Even though the thickest segments were in the septal apex in two patients, no isolated apical hypertrophy was present because these patients had hypertrophy extending to the basal septum as well. Mild mitral valve insufficiency (grade 1-2/4) was noted in 8 HCM patients. One patient had significant LVOT obstruction at rest.

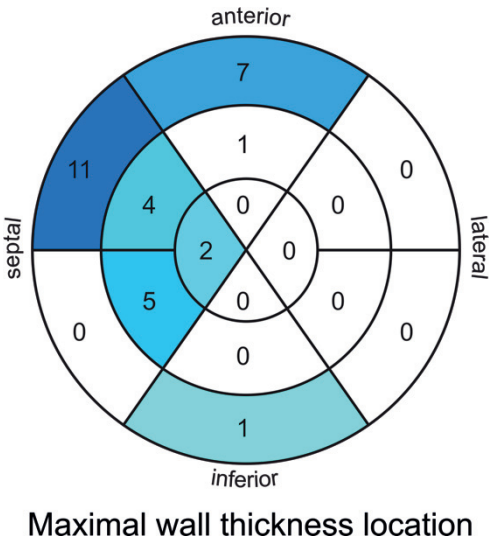

Figure 10 The distribution of maximal wall thickness measured with CMRI in HCM patients.

Diastolic function was reduced in HCM patients overall (Table 5). A marked reduction in septal Em was observed resulting in a lower mean Em (mean of septal and lateral Em values).

	Control	G+ / LVH +	p-value
MV E (m/s)	0.8 ± 0.1	0.7 ± 0.2	0.062
MV A (m/s)	0.6 ± 0.2	0.5 ± 0.2	0.630
MV DT	210 ± 56	213 ± 80	0.886
Mean Em	11.8 ± 3.8	8.7 ± 3.2	0.002*
E / Em	6.9 ± 1.8	8.5 ± 2.7	0.039*
Septal Em (cm/s)	11.3 ± 3.8	7.2 ± 3.4	< 0.001*
Lateral Em (cm/s)	12.2 ± 4.6	9.8 ± 3.9	0.046*

Table 5 Diastolic function parameters in HCM and control subjects. MV = mitral valve, DT = deceleration time, Em = early diastolic TDI PW velocity of mitral valve annulus.

5.1.2 Global strain and mechanical dispersion

Global strain was reduced in HCM patients compared to controls, even though systolic function assessed with conventional LVEF was similar. Mean GLS in HCM was -16.4 ± 4% in comparison to – 20.2 ± 2.4% in control subjects. GLS was a robust measure of the extent of HCM, with correlation to maximal wall thickness and increased NTproBNP (Figure 11). Mechanical dispersion was higher in HCM patients; 65 ± 34 compared to 41 ± 16 in the control group.

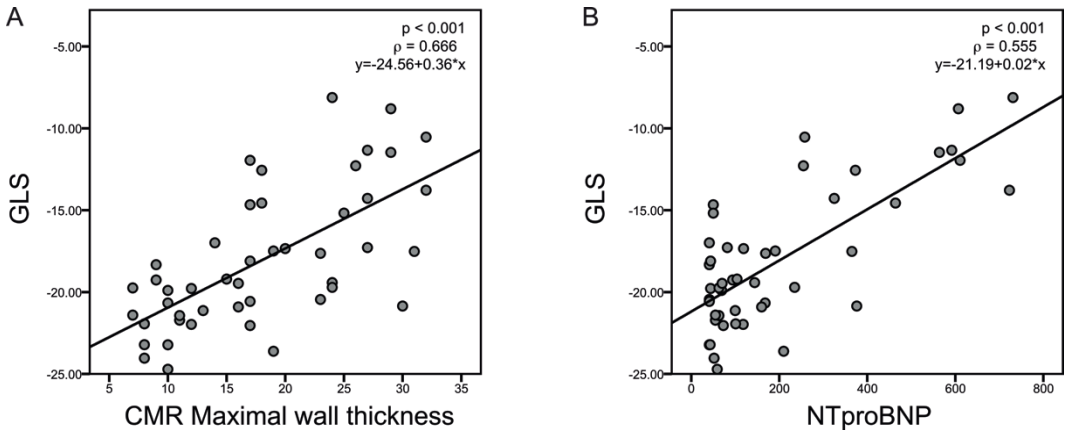

Figure 11 GLS correlation to A) Maximal wall thickness and B) NTproBNP.

5.1.3 Segmental strain

Left ventricular hypertrophy was most prominent in the anteroseptal area. Segmental strain values were most depressed in the basal septal and anterior wall segments coinciding with the location of hypertrophy (Figure 12). In control subjects the mean

segmental strain values were in the range of -18 – -25% whereas in the hypertrophied segments of HCM patients the mean values were -10 – -15%.

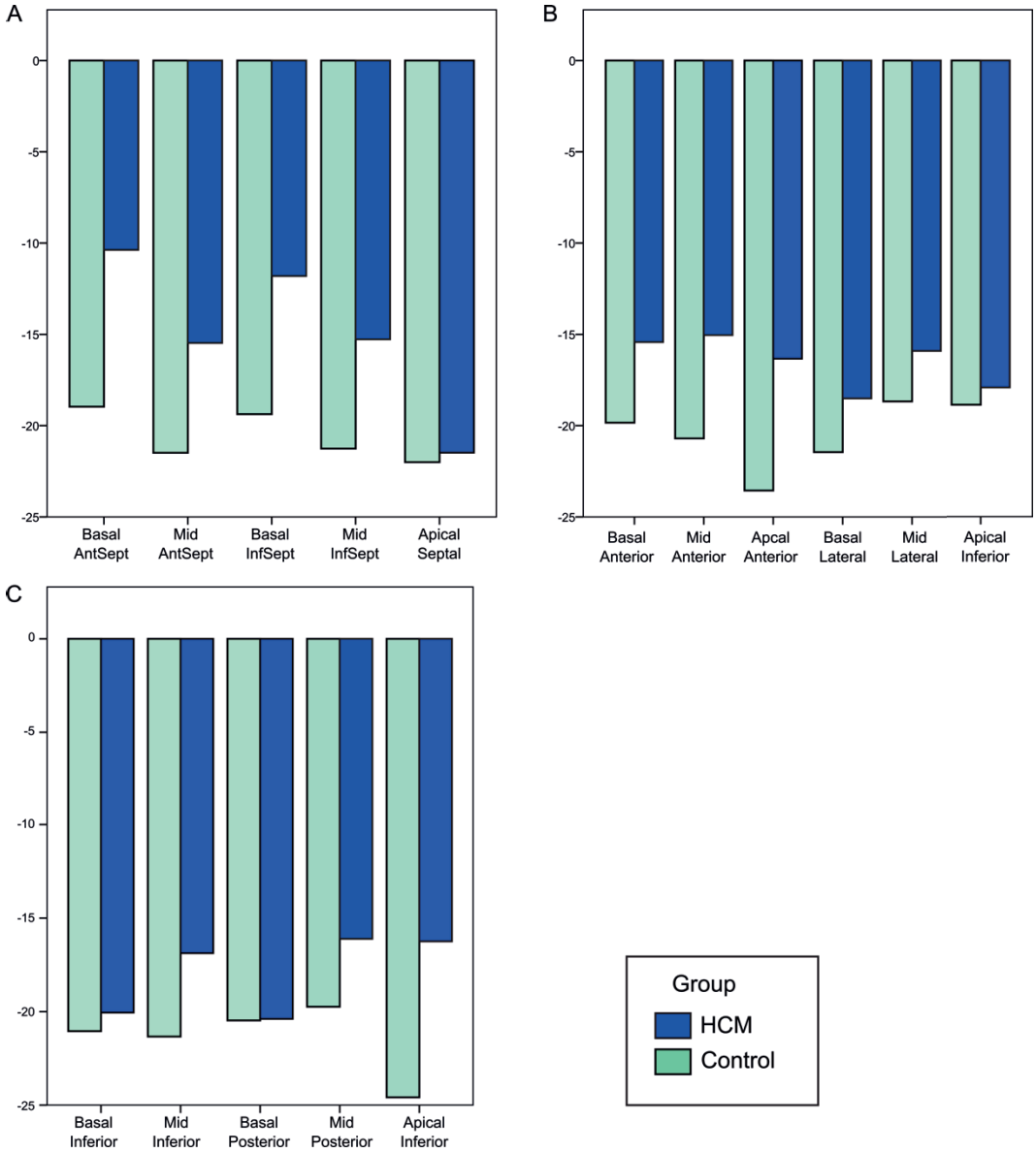

Figure 12 Segmental strains in HCM and control subjects grouped by location: A) Septal B) Anterolateral and C) Inferoposterior.

5.1.4 Twist

Twist was measured from rotations of the basal and apical 2D short axis images with 2DSE (unpublished results). Rotation at the basal level was briefly counterclockwise

followed by a clockwise motion to the peak of systole. The apical rotation was counterclockwise as viewed from the apex and was the dominant force in generating twist. Overall peak systolic twist and timing values were similar in HCM and control patients (Table 6 and Figure 13). Twisting rate, i.e. the speed of change of twist values was similar during systole but the curves separated during early diastole resulting in a delay of peak untwisting rate in HCM patients (marked with * in Figure 13).

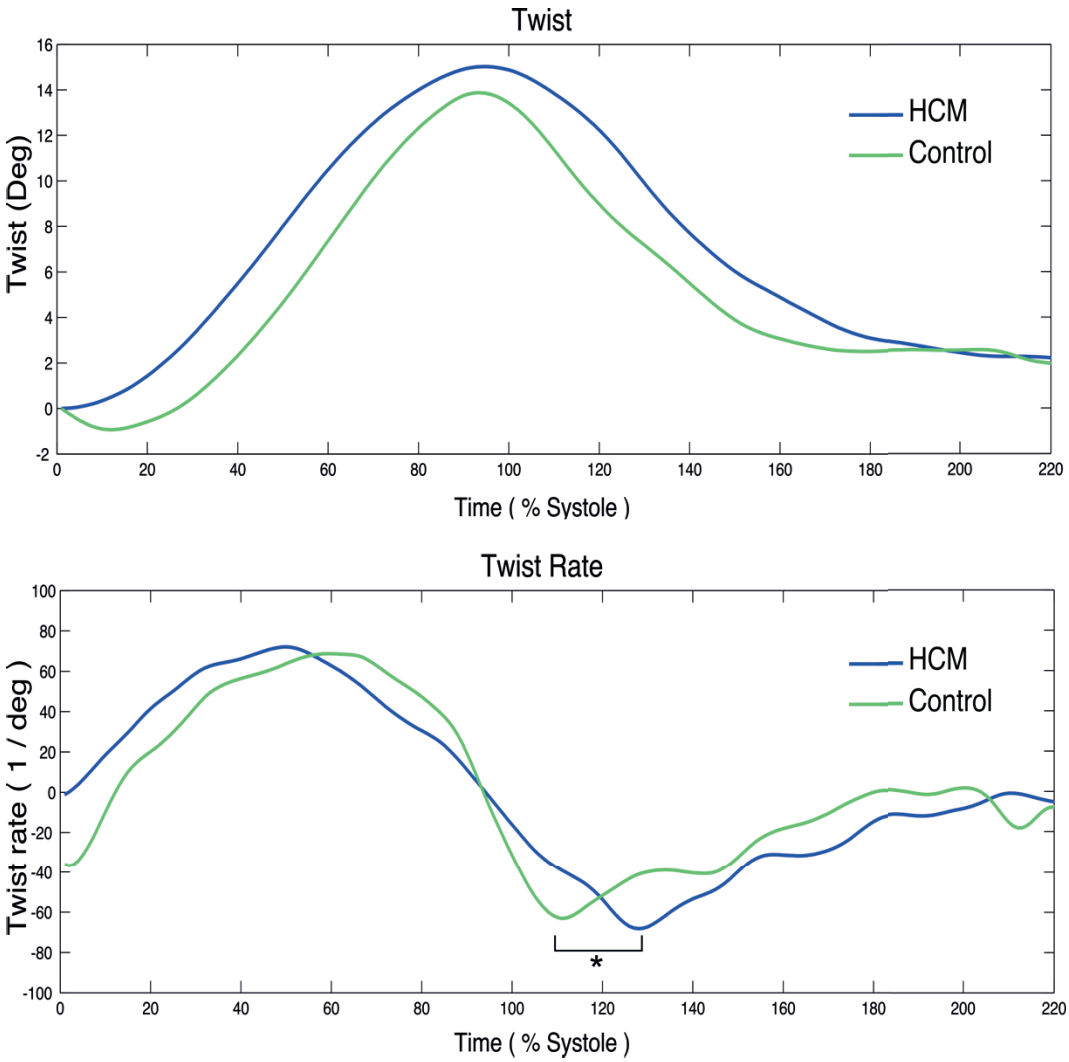

Figure 13 Twist and twist rate in HCM and control subjects. * $p < 0.05$ for difference between groups for time to peak untwist rate (unpublished results).

	Control	HCM	p -value
Peak Twist (deg)	14.5 ± 5.4	16.9 ± 9.4	NS
Peak twisting rate(deg/s)	96 ± 30	94 ± 40	NS
Time to peak twist (ms)	55 ± 19	55 ± 26	NS
Peak untwisting rate (deg/s)	-94 ± 39	-101 ± 59	NS
Time to peak untwisting rate (ms)	116 ± 11	137 ± 16	< 0.001
Recoil	32 ± 19	55 ± 41	NS
Recoil rate	1.3 ± 0.4	1.5 ± 0.7	NS

Table 6 Values of twist and twisting rate in HCM and control subjects (unpublished results).

5.1.5 Late gadolinium enhancement

Late gadolinium enhancement was found in 68% of HCM patients (21/31). No LGE was present in control subjects. HCM patients with LGE had similar maximal wall thickness (21 ± 5 mm), LV mass index (74 g/m^2) and LVEF (62 ± 10%) to HCM patients without LGE. The relative extent of LGE in the LV was 18 ± 16%. The location of maximum relative LGE on the segmental level followed the distribution of hypertrophy with largest values in the basal anteroseptal wall (Figure 14). An example of quantification of LGE is presented in Figure 15.

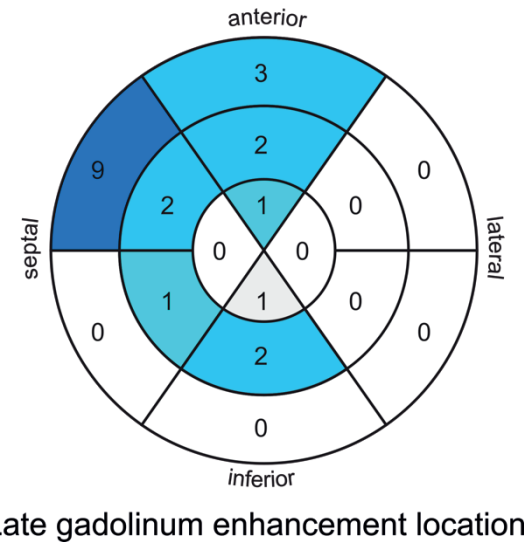

Figure 14 Location of maximal LGE in HCM patients.

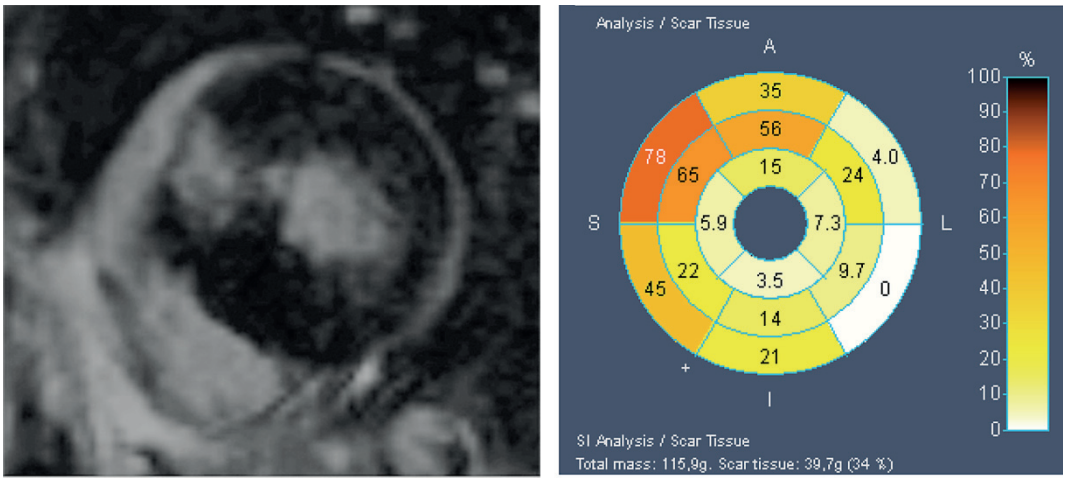

Figure 15 Example of quantifying LGE mass with dedicated software, giving the relative and absolute mass of the scar tissue and relative segmental extent from the cross-sectional CMR image.

5.1.6 Association of imaging to arrhythmias

In Study I there were 11 HCM patients with at least one recorded NSVT episode on 24h ambulatory ECG (HCM/NSVT+ group) and the remainder constituted the HCM/NSVT- group. The HCM/NSVT+ patients had a median of 2 (range 1-19) NSVT episodes at a maximum rate of 141 (120 – 192) bpm with a duration of 5 (3-13) beats. The imaging variables associated with NSVT episodes are summarized in Figure 16. Maximal wall thickness, global longitudinal strain and mechanical dispersion were significantly different between HCM+/NSVT+ and HCM/NSVT- groups. In addition, QRS duration was associated with NSVT. In univariate binary logistic regression analysis to differentiate between HCM/NSVT+ and HCM/NSVT- these four variables were statistically significant. Entered into a multivariate regression analysis only mechanical dispersion was independently associated with NSVT. The discriminatory power of MWT, GLS, QRS duration and MD were assessed with receiver operating characteristics curves. MD performed best, with an AUC = 0.81 and a relatively effective cutoff of MD = 72 ms yielding a sensitivity 0f 64% and specificity of 90% to identify HCM/NSVT+ from HCM/NSVT- patients.

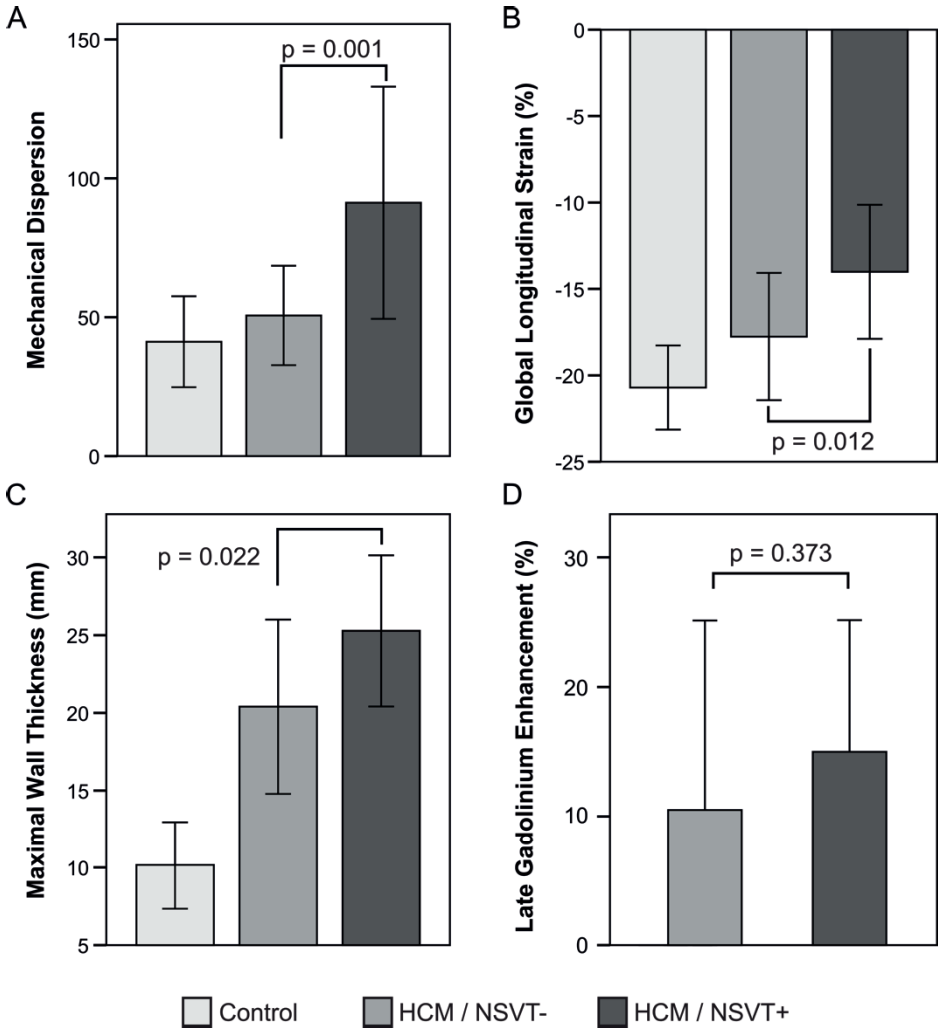

Figure 16 Imaging variables associated with NSVT episodes on 24h ambulatory ECG.

5.2 ECG in HCM (Study II)

5.2.1 Overall ECG findings

In study II we investigated the 12-lead ECG findings of 98 G+/LVH+, 42 G+/LVH- and 40 control subjects. Age and gender distribution were similar in the G+/LVH- and control groups. The G+/LVH+ patients were slightly older and more often male. G+/LVH- subjects were asymptomatic and 78% of the G+/LVH+ group were also in NYHA class I. LVEDD and LVEF were similar between study groups. The mean

maximal wall thickness in G+/LVH+ group was 18.7 ± 4.5 mm compared to 10.2 ± 1.1 mm in the control and 9.9 ± 1.4 mm in the G+/LVH- group ($p < 0.001$). Betablocker therapy was taken by 23% of the G+/LVH+ patients. Five percent of HCM (G+/LVH+) patients had left ventricular outflow obstruction at rest.

The 12-lead ECG findings of Study II are summarized in Table 7. A normal ECG in G+/LVH+ HCM patients was a rarity (3% G+/LVH+ vs 47% control group, $p < 0.001$). Common ECG findings in HCM patients were abnormal Q waves, repolarization abnormalities such as ST segment depression and T wave inversion and prolonged QT interval. Q waves were present usually in the inferior II, III and aVF leads (16%) and anterolateral V2-V6 leads (15%). Terminal negativity of the P-wave ≥ 0.04 mms (P-terminal force) was also common. The QRS complex was often fragmented and widened.

Identification of hypertrophy with conventional Sokolow-Lyon criteria or Cornell voltage product was suboptimal. The more complex Romhilt-Estes score was positive in 55% of HCM patients with echocardiographically verified LV hypertrophy. ECG criteria published by McKenna et al. used to identify possible HCM patients in families with identified probands were positive in 90% of HCM patients (9).

The majority (86%) of G+/LVH- subjects also exhibited ECG pathologies that reflect those found in G+/LVH+ patients. Q waves and novel ECG parameters of RV1<RV2>RV3 and septal remodeling were quite common in LVH- carriers of pathogenic variants and notably uncommon in the control group. Interestingly also the terminal negativity of the P wave and fragmented QRS were common findings in G+/LVH- subjects.

	Control (*n* = 30)	G+/LVH- (*n* = 42)	G+ / LVH+ (*n* = 98)	p-value
At least 1 ECG pathology	53%	86%	97%*†	<0.001
Novel ECG criteria				
RV1<RV2>RV3	3%	33%*	26%*	0.005
Septal remodeling	3%	45%*	49%*	<0.001
Q-waves and repolarization	0	33%*	82%*†	<0.001
Q wave	0	21%*	38%*	<0.001
ST depression	0	7%	51%*†	<0.001
T wave inversion	0	2%	44%*†	<0.001
Prolonged QTc	0	7%	18%*	0.006
Hypertrophy				
Sokolow-Lyon	10%	2%	15%	0.079
Cornell voltage product	0	7%	40%*†	<0.001
Romhilt-Estes score ≥4	3%	14%	55%*†	<0.001
Other ECG features				
P-terminal force	3%	17%	45%*†	<0.001
QRS >100 ms	0	5%	22%*†	<0.001
Fragmented QRS	27%	21%	46%†	0.011

Table 7 ECG findings in Study II. * = significant difference between indicated group and the control group. † = significant difference between G+/LVH+ and G+/LVH- groups.

5.2.2 ECG pathology correlates to disease severity

The median absolute number of ECG pathology in the G+/LVH+ patients was 5 (range 0-9). The number of identified ECG findings correlated with disease severity parameters, such as GLS, extent of LGE, MWT and NT-proBNP, in the imaging substudy (n = 65 mutation carriers, all $\rho > 0.55$ and $p < 0.001$ for bivariate Spearman rank correlation). The correlation of MWT to ECG pathology in all mutation carriers is presented in Figure 17.

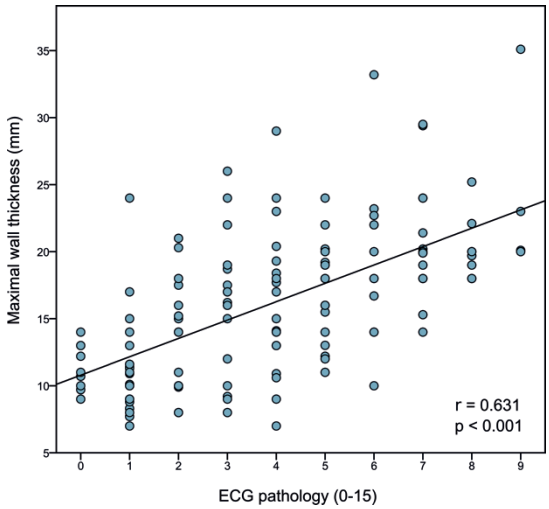

Figure 17 Spearman rank correlation of ECG pathology (0-15) to maximal wall thickness in all mutation carriers (n = 140).

5.2.3 RV1 < RV2 > RV3 and septal remodeling

Novel ECG criteria RV1<RV2>RV3 and septal remodeling were specific findings for mutation carriers. The RV1<RV2>RV3 finding was more prevalent in the G+/LVH- subjects and G+/LVH+ patients with milder left ventricular maximal wall thickness. In Figure 18 the distribution of novel ECG parameters and Q waves and repolarization abnormalities according to maximal wall thickness quartiles is summarized. In Figure 18 B an example of RV1<RV2>RV3 is presented. No local measurements of maximal wall thickness, distribution of hypertrophy, 2D strain or gadolinium late-enhancement correlated to the finding of RV1<RV2>RV3 or septal remodeling on ECG.

5.2.4 ECG criteria for diagnostics and screening

Using ECG criteria for screening of HCM requires both good sensitivity and specificity. The ECG major criteria (9), used in screening of relatives of HCM probands, exhibited both good sensitivity of 90% and specificity of 97% to discriminate between G+/LVH+ patients and control subjects, with a positive predictive value of 99%.

Notably the major ECG criteria were quite insensitive in discriminating between G+/LVH- subjects and the control group (sensitivity 36% and specificity 97%. The RV1<RV2>RV3 and septal remodeling findings had individually moderate sensitivity (33% and 45%, respectively). Used in combination with Q waves and repolarization abnormalities the sensitivities rose to acceptable levels for clinical practice (Table 8).

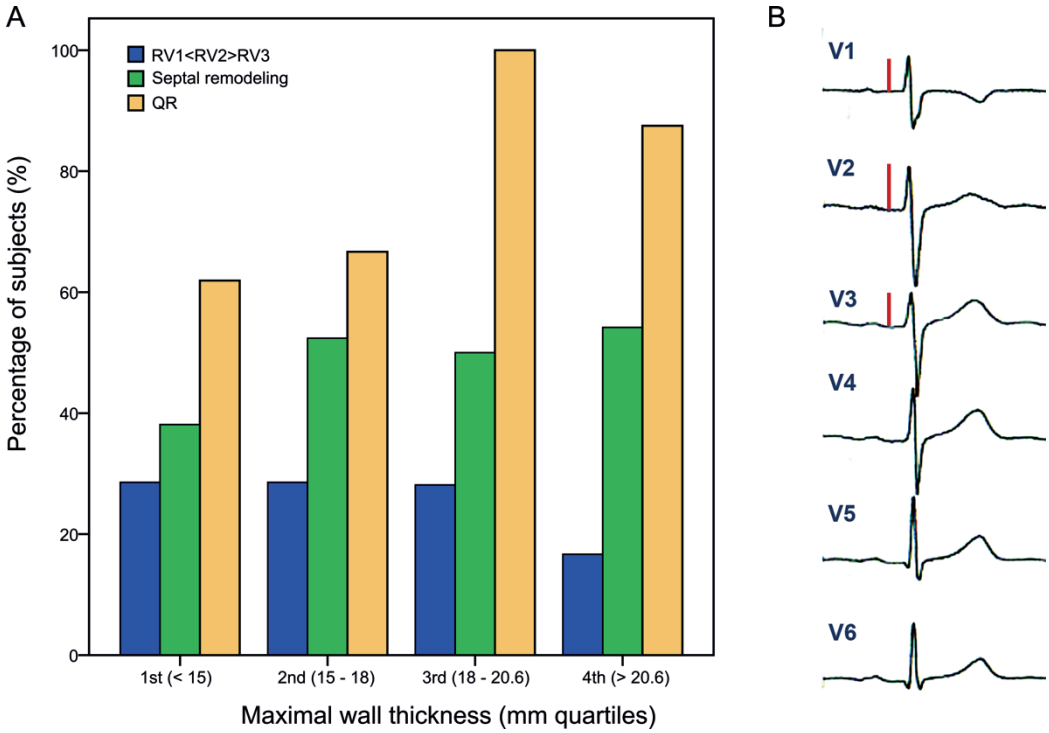

Figure 18 A. The distribution of RV1<RV2>RV3, septal remodeling and Q waves and repolarization abnormalities (QR) according to maximal wall thickness quartiles in HCM patients (n = 98). QR and septal remodeling prevalence increase with wall thickness whereas RV1<RV2>RV3 decreases. B. An example of RV1<RV2>RV3 in a young G+/LVH- female subject (18 years). Red lines indicate height of R wave in leads V1-V3 for illustration.

G+/LVH- (n=42)	Sensitivity (%)	Specificity (%)	PPV (%)	NPV (%)
Major criteria (≥1)	36 %	97 %	94 %	52 %
RV1<RV2>RV3 + QR	52 %	97 %	96 %	59 %
Septal remodeling + QR	64 %	97 %	96 %	66 %

Table 8 Combination criteria for discriminating between G+/LVH- and control groups. PPV = positive predictive value, NPV = negative predictive value. QR = Q waves and repolarization abnormalities.

5.3 Repolarization abnormalities in HCM (Study III)

5.3.1 Baseline

We studied the repolarization parameters of 46 HCM patients (G+/LVH+) carrying either the MYBPC3-Q1061X (52%) or the TPM1-D175N (48%) variant. The HCM patients and the control group (n = 35) were well balanced in baseline attributes such as age and gender. Mean maximal wall thickness on CMRI was 20.6 mm in the HCM group. LGE was present in 37% of HCM patients. There was no difference in heart rate or QRS duration on 12-lead ECG. The ambulatory ECG recordings were of adequate quality. Betablocker therapy was taken by 48% of HCM patients but we verified with a repeated measures ANOVA that this had no effect on the repolarization parameters (all tests $p > 0.5$). The mean heart rates in ambulatory ECG recordings were not different.

In HCM patients 26% had at least 1 NSVT episode on ambulatory ECG. No significant correlations of NSVT to measured repolarization parameters were found. The measured maximal QTe at 1000 ms RR interval (i.e. at a heart rate of 60 bpm) was 439 ms in HCM patients with NSVT episodes compared to 373 ms in HCM patients without NSVT.

5.3.2 Prolonged QTe

QTe interval was significantly prolonged in HCM patients. The heart rate adapted median QTe and maximum QTe results are summarized in Figure 19. Maximal wall thickness correlated to the maximum QTe interval. The effect of MWT on QTe was also assessed by comparing the maximum QTe values between HCM patients with mild hypertrophy (MWT < 20.6 mm) and moderate hypertrophy (MWT > 20.6 mm) which is summarized in Figure 19 B.

5.3.3 T wave peak to T wave end

Time interval from T wave peak to T wave end was not different between HCM patients in general and the control group, although a trend of increase in all TPE values in the HCM patients was observed. There was an effect of hypertrophy on TPE, which represents global dispersion of repolarization. HCM patients with MWT > 20.6 mm had significantly higher TPE values on the TPE-RR plot compare to HCM patients with milder hypertrophy.

5.3.4 Fibrosis associates to repolarization abnormalities

HCM patients with LGE had steeper QeT/RR slopes compared to HCM patients without LGE and control subjects. There was no difference in age, gender or maximal wall thickness between HCM patients with and without LGE. In multivariate linear regression LGE was the only independent predictor of QTe/RR slope.

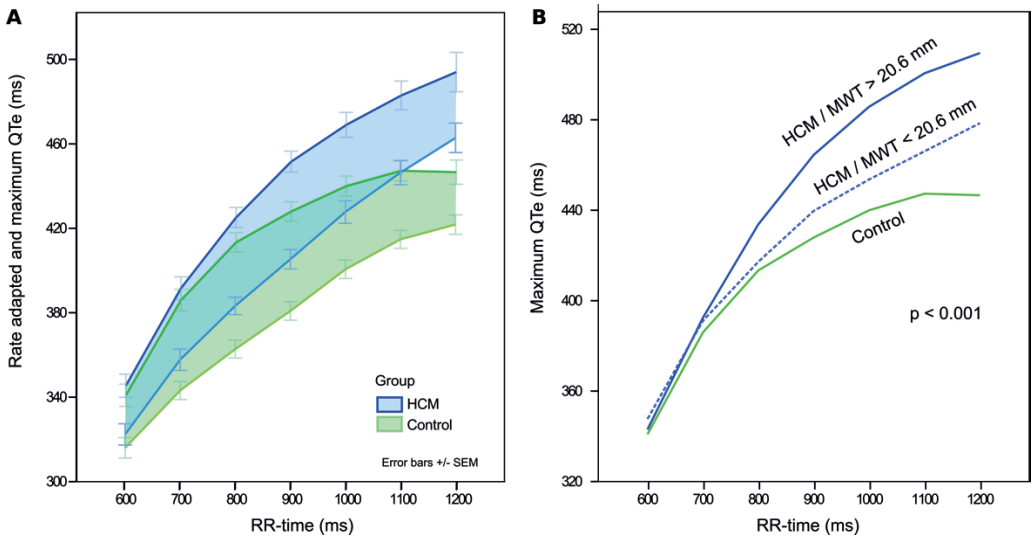

Figure 19 A) Rate adapted and maximum QTe in HCM (light blue and dark blue lines) and control subjects (light green and dark green lines). The area between the curves represent the difference between rate adapted and maximum QTe. B) Effect of maximal wall thickness (MWT) on maximal QTe interval values in HCM patients.

5.4 Metabolomic findings in HCM (Study IV)

In study IV we analyzed the metabolomic profile of *MYBPC3*-Q1061X mutation carriers to assess the possible changes of cardiac metabolism due to the mutation reflected in the peripheral blood metabolome. Blood samples were analyzed with comprehensive metabolomics profiling and resulted in a total of 86 polar metabolites and 238 molecular lipids identified and included in the analysis of data. The individual metabolites are co-regulated and interdependent and thus were analyzed with a Bayesian clustering method. The array of metabolites was grouped into seven lipid clusters (LC1-LC7) and four polar metabolite clusters (MC1-MC4). The lipid clusters were divided by the clustering method on the basis of structural and functional similarities. The metabolites clustered into one large cluster (MC1) and three smaller ones (MC2-4). The contents of clusters are summarized in Table 9.

Cluster	Size (*n*)	Description
LC1	46	Mainly PCs, but also PEs and TGs
LC2	86	Mainly PCs with ether-linkages and PEs, but also ChoEs, SMs, TGs
LC3	36	PUFA-containing PC and PE (plasmalogens) and PUFA-containing TGs
LC4	10	LysoPCs
LC5	21	Mainly saturated TGs and 1-3 double bonds, longer chains than LC6
LC6	19	Saturated TGs and TGs with 1-3 double bonds, shorter chains than LC3, LC5 and LC7
LC7	20	PUFA-containing TGs, long chains
MC1	69	Diverse
MC2	11	Carboxylic acids
MC3	4	Carboxylic acids
MC4	2	Branched-chain amino acids leucine and isoleucine

Table 9 Description of metabolite clusters. PC = phosphatidylcholine, PE = phosphatidylethanolamine, TG = triglyceride, PUFA = polyunsaturated fatty acid.

In Study IV the clusters were compared between G+/LVH+, G+/LVH- and control groups. Here we present the cluster analysis performed in two groups (unpublished data): Gene mutation carriers (pooled G+/LVH+ and G+/LVH- mutation carrier data, n = 53) and the control group (n = 20). In an analysis of covariance adjusted for age, gender, BMI, hypertension and diabetes the clusters MC4 and LC3 were significantly different between the mutation carrier and control groups (Figure 20). Cluster MC1 was also different but the difference in absolute values is rather small and deemed clinically not significant. The results of the two group analysis presented here are similar to the published results in study IV.

In addition to the cluster analysis we compared the difference of individual metabolite levels between G+/LVH+, G+/LVH- and control groups. The results followed the overall direction of the cluster analysis. Of the polar metabolites, valine, leucine, and ketoleucine had higher concentrations in the G/LVH+ group. A number of long-chain polyunsaturated triglycerides and two ether phospholipids were increased in the G+/LVH+ group.

In Spearman rank correlation of individual metabolites, we found some lysophospholipids, phospholipids and triglycerides correlating with increased MWT and LV mass and decreased measures of diastolic function such as TDI septal and lateral Em. The same was true, although with modest correlation coefficients, of the metabolite clusters MC4 and LC3 (Figure 21).

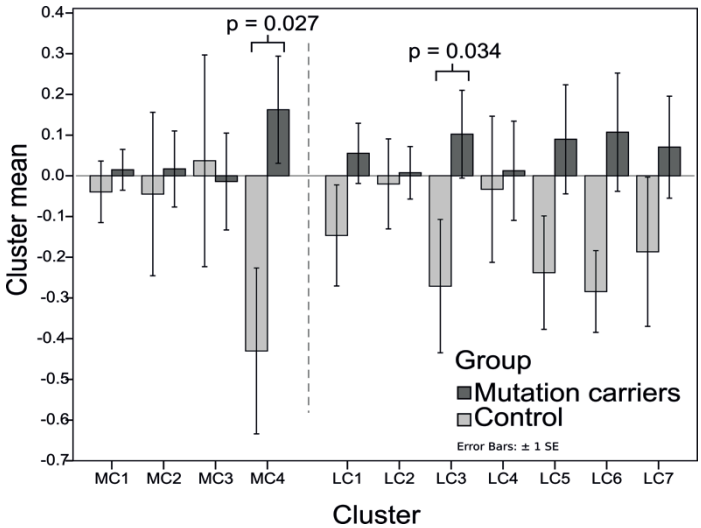

Figure 20 Metabolite clusters presented as mean values with error bars as ± SE. Significant differences between mean values of clusters MC4 and LC3. Groups are divided into mutation carriers (n = 53) and control subjects (n = 20).

Cluster	Control (*n*=20)	Mutation carriers (*n*=53)	p-value
MC1	-0.04 ± 0.34	0.01 ± 0.37	0.025
MC2	-0.04 ± 0.90	0.02 ± 0.68	0.211
MC3	0.04 ± 1.16	-0.01 ± 0.87	0.222
MC4	-0.43 ± 0.91	0.16 ± 0.96	0.027
LC1	-0.15 ± 0.55	0.06 ± 0.54	0.163
LC2	-0.02 ± 0.49	0.01 ± 0.47	0.803
LC3	-0.27 ± 0.73	0.10 ± 0.78	0.034
LC4	-0.03 ± 0.80	0.01 ± 0.89	0.253
LC5	-0.24 ± 0.62	0.09 ± 0.98	0.056
LC6	-0.28 ± 0.45	0.11 ±1.06	0.145
LC7	-0.19 ± 0.82	0.07 ± 0.91	0.067

Table 10 Analysis of metabolite clusters. P-value for analysis of covariance adjusted for age, gender, BMI, hypertension and diabetes.

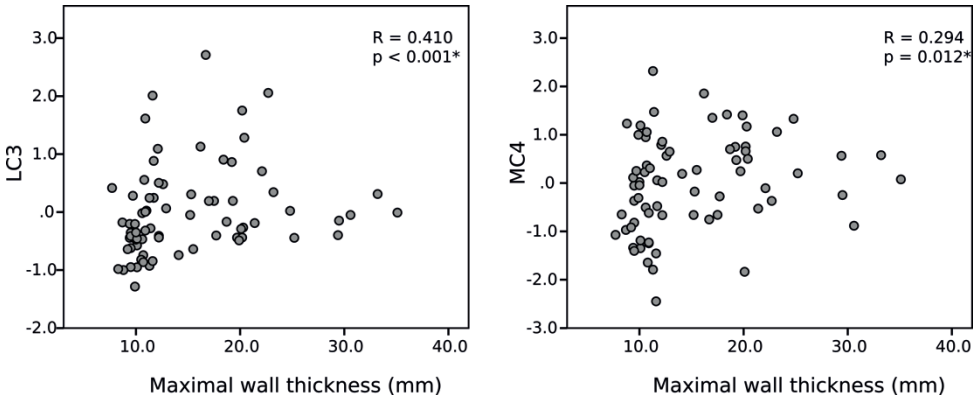

Figure 21 Correlation of mean metabolite cluster levels LC3 and MC4 with maximal wall thickness.

6 DISCUSSION

6.1 Main findings

The aim of this thesis was to investigate the alterations in myocardial mechanical and electrical function and metabolism associated with hypertrophic cardiomyopathy. We sought to assess the possible use of these findings in the diagnostics of suspected HCM patients and family members without hypertrophy and to develop more accurate tools for SCD risk assessment. Metabolomic profiling was employed to identify the subtle changes in HCM and enhance our knowledge of the pathophysiological process in HCM.

In Study I we demonstrated that 2D strain echocardiography is a powerful tool in the assessment of hypertrophic cardiomyopathy and mechanical dispersion is increased in HCM patients with NSVT episodes.

Conventional and novel ECG parameters were at the heart of Study II and the proposed new ECG criteria of RV1 < RV2 > RV3 and septal remodeling were quite specific in the identification of G+/LVH- subjects from nonhypertrophic control subjects. The use of ECG combination variables provided a reasonable sensitivity and specificity to help in this differentiation. Secondly we extrapolated on the idea of the degree of ECG pathology correlating to more advanced disease state in HCM and the possibility of temporal development of the ECG in HCM.

In Study III the repolarization abnormalities in HCM were comprehensively assessed and we found multiple alterations in repolarization in HCM patients and that fibrosis assessed with late gadolinium enhancement affects repolarization parameters in addition to hypertrophy.

Study IV presented results of metabolomic profiling in hypertrophic cardiomyopathy. We found a number of lipids and a few polar metabolites significantly different in HCM patients and they correlated with the degree of hypertrophy and diastolic dysfunction.

6.2 Comparison with previous studies

6.2.1 Alterations in myocardial mechanics and association to arrhythmias

Risk assessment of SCD in HCM is mainly based on variables not directly linked to the pathophysiological process in the myocardium, such as age, family history, unexplained syncope or presence of NSVT. These variables have been gathered from prospective and retrospective cohorts of HCM patients and are mostly indirect measures of the possibility of arrhythmia. Yet the substrate for lethal arrhythmias lies in the myocardial pathology itself with hypertrophy, disarray, fibrosis and increased perfusion demand being key players of arrhythmia vulnerability. Modern imaging with CMRI LGE and 2DSE enable us to quantify these changes in the myocardium.

2D echocardiographic strain imaging quantifies the local and global dysfunction in HCM accurately and robustly. Reduced longitudinal strain in the septum of HCM patients has been associated with the incidence of ventricular arrhythmias (165,166,227). In our study the global longitudinal strain and segmental strains in the septum and anterior wall were significantly reduced. The reduction in GLS associated to the presence of NSVT on ambulatory ECG. This is in line with the findings of a larger cohort of HCM patients studied by Debonnaire et al. where a reduction in GLS predicted ICD therapy (159).

The heterogeneity and local nature of changes in HCM have lead investigators to study the effect of dyssynchrony as a predictor of arrhythmia. Previously an association of intraventricular dyssynchrony, quantified with tissue Doppler imaging, to SCD in HCM patients was demonstrated (228). In ischemic and dilated cardiomyopathy and arrhythmogenic right ventricular dysplasia the mechanical dispersion measured with 2DSE has been an independent predictor of malignant arrhythmias (171,172,229,230). Mechanical dispersion associated to episodes of NSVT on ambulatory ECG in our study, possibly highlighting the importance of the asymmetrical nature of myocardial changes in HCM on myocardial mechanics and arrhythmic potential.

6.2.2 The abnormal ECG in HCM patients

The ECG is an inexpensive tool to screen for cardiomyopathies like HCM. We demonstrated that the major ECG criteria for HCM are an effective tool to identify G+/LVH+ patients in families with HCM. A multitude of repolarization abnormalities characterize the ECG phenotype of HCM patients. These changes reflect the disturbances of repolarization due to changes on the ion channel level and alterations in Ca^{2}+ handling as well as the structural changes of hypertrophy and fibrosis.

The origin of abnormal Q waves in HCM has been debated. The Q waves of HCM patients in this study were mostly located to the inferior and anterolateral wall of the LV. No correlations of the location of Q waves and late gadolinium enhancement were demonstrated in our study which corroborates the previous findings in larger CMRI cohorts of HCM patients (72,73). The G+/LVH- subjects also had Q waves on ECG but no LGE confirming that scar is not the only explanation for this rather common finding.

The suspicion of HCM based on the 12-lead ECG is raised by a combination of findings. Conventional criteria for LV hypertrophy (Sokolow-Lyon and Cornell voltage product) were rather insensitive for the identification of HCM in this study, as well as in previous reports, possibly due to the asymmetric nature of the hypertrophy. The use of the Romhilt-Estes point score was more effective but it is quite complicated to apply in clinical practice.

Terminal negativity of the P wave in lead V1 was common in both G+/LVH+ and G+/LVH- subjects. The mechanism for this is elusive as the G+/LVH- subjects had normal sized atria and diastolic function.

In general, for the practicing clinician our finding of increased HCM pathology, i.e. increased wall thickness, reduction in GLS and increase in LGE extent, correlating to absolute increase in the number of identified ECG pathology may provide additional information in the follow-up of these patients (72).

6.2.3 Identifying G+/LVH- subjects with the ECG

The ECG was abnormal in > 85% of G+/LVH- subjects. We demonstrated novel ECG criteria RV1<RV2>RV3 and septal remodeling to be quite specific for HCM mutation carriers. The RV1<RV2>RV3 sign was more prevalent in the young mutation carriers and in those with milder hypertrophy suggesting that the abnormal R wave distribution in V1-V3 leads may be an early sign of the disease which later is reduced due to increasing hypertrophy and other structural changes in the myocardial wall.

The proposed novel ECG criteria have an additive role in identifying G+/LVH- subjects when used in conjunction with other ECG criteria. Combining Q waves and repolarization disturbances and the RV1<RV2>RV3 results in an ECG criteria that can be used in clinical practice and yields a specificity of 52% and sensitivity of 97% for detection of G+/LVH- from control subjects.

6.2.4 Repolarization abnormalities

We demonstrated a number of changes in repolarization measurements in HCM patients. The rate adapted QTe is prolonged in HCM patients and increases relative to the control subjects at longer RR intervals of 1000 – 1200 ms. The median QTe was measured from stable heart rates to minimize the effect of sudden changes in RR intervals to the duration of repolarization. The prolongation of rate adapted QTe resembles that found in LQTS patients (118). The common denominator on the cellular level in both LQTS and HCM is the reduction in potassium current, especially I_{Kr}.

The interval from T wave apex to end on the surface ECG may be a measure of global dispersion as previously postulated (125,126). In this study median TPE was significantly prolonged in HCM patients with at least moderate hypertrophy (MWT > 20.6 mm). This may reflect the effect of increased hypertrophy and changes in the myocardium on the dispersion of global repolarization. Maximum QTe was also longer in these patients. In HCM the prolonged TPE has been associated with increased risk for arrhythmias (129).

In HCM patients with LGE we showed that the QTe/RR slope is steeper compared to HCM patients without LGE and control subjects. Overall QTe/RR slopes have been found steeper in higher risk HCM patients, but in a previous study the effect of wall thickness or other structural measurements on the steepness of the slope was not analyzed (124). The presence and especially the extent of LGE confers an independent risk for SCD (185). Some of this risk manifests from the arrhythmic substrate that fibrosis entails. It is also possible that LGE affects the repolarization

dynamics in general in HCM patients through the asymmetric changes in myocardial structure resulting in steeper QTe/RR slopes. This may add to the arrhythmic potential.

The risk for arrhythmias in HCM has usually been pronounced in exercise, as in the case of SCD in athletes with HCM. Yet in studies on the circadian distribution of ICD therapy approximately 20-27% of ventricular arrhythmias occur during rest (50,51). The repolarization abnormalities in our study increase with lower heart rates and may play a role in those malignant tachycardias that present during bradycardia in HCM patients.

6.2.5 The metabolomic profile of HCM

In our study on the metabolomic profile of HCM mutation carriers we found elevated levels of branched chain amino acids, phospholipids and several triglycerides. The levels of these metabolites correlated to imaging parameters of HCM disease progress such as hypertrophy and diastolic function. The decrease in glutamate and increase in threonine levels resemble the metabolomic changes found in DCM (231).

Myocardial energy utilization in HCM is impaired, as discussed in the literature review. Free fatty acid uptake is reduced and glucose metabolism is increased in HCM myocytes. Although speculative, the finding of elevated levels of circulating lipid metabolites, mostly TGs, in our study may indirectly reflect the changes in energy substrate utilization in HCM.

The increased levels of branched chain amino acids leucine and isoleucine in HCM mutation carriers mirror the findings in heart failure patients (232). In a metabolomic study of pressure overloaded mouse hearts an increase branched chain amino acids in explanted heart myocytes was observed (233). Branched chain amino acids enter the citric acid cycle via conversion to propionyl-CoA by the branched chain α-keto-acid dehydrogenase complex (BCKD). In hypertrophic and failing hearts the expression of PP2C, a phosphatase that dephosphorylates the BCKD, is reduced. This reduction has been shown to lead to elevated levels of branched chain amino acids in plasma in a murine model (234). The mammalian target of rapamycin mTOR is efficiently activated by branched chain amino acids and local elevations in concentration may lead to chronic induction of mTOR resulting in pro-hypertrophic effects via changes to insulin sensitivity (235).

6.3 Limitations

6.3.1 Study design, sample size and data collection

The design of studies I, III and IV were prospective and cross-sectional. The sample size of these studies is limited, which must be taken into account when assessing the statistical results. On the other hand, by restricting the number of studied pathological variants we have tried to minimize the possible effect of different genotypes on the results. In data collection we have not fully evaluated the conventional risk factors in

assessing SCD risk and missing data on family history and unexplained syncope have limited this approach.

Study II was retrospective in design, which poses inherent limitations and questions on the effect of possible confounding factors we may not have taken into account. The trial was designed to maximize available patients for analysis thus reflecting more the real life setting where patients are met. This may be also seen as a merit in the generalizability of results.

6.3.2 Generalizability

Most of the > 1000 mutations in HCM are limited to small patient groups, families or geographic areas. The effect of mutation type has been debated in HCM and for the most part the phenotype of individual patients is affected in large parts by the modifying factors and other yet poorly characterized factors that result in the very variable phenotypic expression of mutations. In HCM the difference between individuals is largely explained by these other factors than the causative mutation (236). Therefore, we advocate that the studies in this thesis represent pathophysiological changes mostly relating to HCM in general and the results are generalizable to HCM resultiing form *MYBPC3* and *TPM1* mutations as a whole.

6.3.3 Methodological limitations

Echocardiographic investigations were limited due to the natural limitations of available acoustic windows. No patients were excluded due to suboptimal visibility, which affects especially 2D strain echocardiography, where acoustic windows need to be of optimal quality. Yet it speaks firmly of the robustness of this newer technology that the segmental feasibility rate of strain measurements was nearly 90%.

The assessment of LGE on CMRI was not done with the same methodology and software in all patients in study III and therefore LGE was encoded as just visually present or absent. No reliable quantification of LGE was possible in study III, in contrast to study I where LGE measurements were performed with the same software platform from CMR images done with the same protocol.

24h ambulatory ECG data quality was somewhat suboptimal due to the long data collection period. Modern digital ECG recorders provide better quality data, which may help in the future if the initial findings of repolarization abnormalities are investigated further in a larger cohort.

Metabolomic platforms have the advantage of producing large amounts of data. The analysis of big data is challenging and certain guidelines must be followed. In study IV identification and acceptance of metabolites for analysis was performed according to generally agreed good practice and to minimize the possibility of type I error. Cluster analysis was used to assess data on a larger scale to find patterns and take the intercorrelatedness into account.

6.4 Clinical implications and future developments

6.4.1 Screening and diagnostics

We identified novel ECG criteria for the identification of G+/LVH- subjects. The 12-lead ECG is an inexpensive tool to apply in the screening of relatives of HCM probands. A chance finding of one of the more specific ECG pathologies in previously healthy subjects could prompt the search for HCM. The use of combination criteria like RV1<RV2>RV3 and Q waves and repolarization abnormalities could significantly enhance the predictive value of electrocardiography. The criteria are also relatively simple to use in clinical practice. In addition, a change in a HCM patient's ECG over time may be a marker of worsening disease state as our results imply. In general, the value of the 12-lead ECG in the diagnostics of HCM patients should not be forgotten.

The problem of screening is especially evident in HCM families without a known pathogenic variant. If screened individuals do not present with the HCM phenotype they have to be clinically assessed at regular intervals due to the age related penetrance of the disease. It would seem logical to combine an array of different imaging, electrocardiographic and laboratory parameters, such as NT-proBNP, in the screening process. This could aid in the allocation of resources and concentrate diagnostic efforts to individuals more at risk of developing the disease. In the future a trial to assess a combination of measurements that result in the best possible sensitivity and specificity to identify family members at risk of developing manifest HCM would be of value. It is also possible that current efforts to develop pharmacological therapies for HCM may result in drugs that significantly delay the development of pathological changes. At that point the identification of at risk individuals to target therapies would be of even greater importance.

6.4.2 Improving risk stratification of sudden cardiac death

The assessment of risk for SCD in HCM has always been difficult for the clinician. Prior to the 2014 ESC Guidelines the conventional risk factors missed approximately 30% of HCM patients who developed lethal arrhythmias (5). With the current risk factor calculator endorsed by the ESC the predictive power of overall risk assessment has probably increased, but is still not optimal (4,197). Novel parameters that quantify the arrhythmic potential in the structural changes of the myocardium may in the future aid in the risk assessment of individual patients.

Ultimately the risk assessment protocol aims to identify individuals who would benefit from an ICD. Recent larger scale CMRI studies and a meta-analysis pooling this data together have implicated that an LGE mass of ≥ 15% of the LV confers significant risk for SCD (185,189). The areas of LGE in the LV seem to be the localized substrate for ventricular arrhythmias (237). GLS has also been found to predict proper ICD therapy and outcomes (159,168,169). Our finding of the association of mechanical dispersion to recorded NSVT is a preliminary finding and, if confirmed in

a larger HCM patient cohort, may in the future be studied as an additional risk factor for arrhythmia. The recent findings from modern imaging techniques will most likely be incorporated in the risk assessment of HCM patients in the future.

7 CONCLUSIONS

1. Mechanical dispersion measured with 2DSE significantly correlates to episodes of NSVT on ambulatory ECGs of HCM patients and is an independent predictor for these arrhythmias. With further study the use mechanical dispersion might be of value in the SCD risk stratification of HCM.

2. The conventional 12-lead ECG is abnormal in 97% of G+/LVH+ and 86% of G+/LVH- subjects. Q waves and repolarization changes, QRS fragmentation, terminal negativity of the P wave in lead V1 and criteria for hypertrophy are common findings in ECGs of mutation carriers. The proposed novel ECG criteria of RV1<RV2>RV3 and septal remodeling are quite specific for mutation carriers and have additional value in the identification of G+/LVH- subjects. The RV1<RV2>RV3 sign is more prevalent in the young mutation carriers and in those with milder hypertrophy whereas repolarization abnormalities, signs of hypertrophy and PTF are more prevalent with increasing age and hypertrophy. The use of ECG in screening of HCM families can be a specific and cost-effective tool.

3. A number of repolarization abnormalities were found in the 24h ambulatory ECGs of HCM patients. Notably the rate adapted median QTe is prolonged in HCM patients and hypertrophy and fibrosis affect repolarization significantly. LGE independently associates to steeper QT/RR slopes in HCM patients. These abnormalities in ventricular repolarization may contribute to the arrhythmogenic potential in HCM.

4. A number of branched chain amino acids, triglycerides and phospholipids were elevated in HCM patients and their levels correlated to imaging variables related to HCM, such as hypertrophy and diastolic dysfunction.

ACKNOWLEDGEMENTS

This study was carried out at the Heart and Lung Center of the Helsinki University Hospital and the University of Helsinki during 2009-2018.

I begun this project with my supervisor docent Mika Laine some time ago. Mika has been an invaluable source of ideas, resources, and, perhaps most importantly, of encouragement. We have persevered and now we have crossed the finish line.

To my second supervisor docent Tiina Heliö I owe my deepest gratitude for her ideas and insight into the many faces of hypertrophic cardiomyopathy. Her resources have been of immense help in this project.

My third supervisor professor Johanna Kuusisto became a supervisor in name only recently, but has been the *de facto* driving force of the research into hypertrophic cardiomyopathy both in this project, as well as in Finland in general, from the start. Much of the groundwork for the ideas and data in this book are based on the extensive work she and others from Kuopio have done over the years.

I am grateful to the reviewers docent Riikka Lautamäki and associate professor Antti Saraste for their meticulous and efficient work.

During my forays into the wilderness that is the electrocardiogram, I have been guided by professor Kjell Nikus on many an occasion. I have had the utmost joy of working with him in our joint venture and owe a resounding thank you for all the hard work he has put into our ECG project.

My work began with modern echocardiography research, but over the years evolved into encompassing practically every aspect of the clinical study of HCM. I am grateful to professor Matti Viitasalo for his academic excellence in the repolarization project and steering it to a decisive and successful finish.

Alongside my echocardiographic and electrocardiographic research project, the work of my fellow colleague Mika Tarkiainen on MRI findings in HCM has continued. We have shared ideas, data, statistical tips, and collaborations in manuscripts. I am thankful for your comments and contribution in our joint work.

The project on the metabolome of HCM would not have been possible without the work of my Norwegian co-author Benedicte Jørgenrud and the team at VTT, to all of whom I extend my gratitude.

I am fortunate to have worked with Pertti Jääskeläinen on so many manuscripts. His comments and ideas have always been of great value and quick to appear. This project has benefited significantly from the expertise of cardiac MRI radiologists Petri Sipola and Kirsi Lauerma. I am thankful for the insight of professor Markku Laakso to this study. I am deeply in debt to Sini Weckström for keeping the HCM project in one piece and collecting all the relevant data under one roof. I am grateful to Jere Paavola for all the support in deciphering the inner workings of the repolarization analysis software. I am also indebted to the technical expertise of Heikki Väänänen, the mastermind behind the repolarization software.

To all the skillful and hardworking researchers and clinicians I have been blessed to work with, and have not singled out here, I owe my heartfelt gratitude to your

excellent contribution. In the words of Bilbo Baggins: "I don't know half of you half as well as I should like; and I like less than half of you half as well as you deserve."

The road to this stage in my research has been long and I would not have made it without the support of friends and family. My friends from the old Tapiola High School neighbourhood and from the early years of medical school have been of utmost importance to me. I hope our friendships will continue and grow stronger with the coming years.

My parents have always supported me in all the possible ways that loving parents can. In addition, I find your strong academic background and work ethic to have had a lasting effect on me from very early on. To my dear brother I wish all the best and thank you for your support. I would also like to thank, from the bottom of my heart, my mother-in-law Miia. She has been an integral part of our extended family since the birth of our first child. Her help with the kids has, on many occasions, enabled the continuation of this academic project.

Finally, I would not be here without the everlasting friendship and love of my wife Tuija. You are the rock on which I and our family stand on. Your support for my "hobby" has made this book and all the events leading to it possible. Most importantly we are now part of something greater than ourselves - embodied in our three beloved children Joonas, Sara and Emilia.

This study was supported financially by grants from the Aarne Koskelo Foundation, The Finnish Foundation for Cardiovascular Research, The Ida Montin Foundation, and The Finnish Medical Foundation. The congress presentation was supported by the Finnish Cardiac Society.

Helsinki, November 2018

Mikko Jalanko

REFERENCES

1. Liouville H. Rétrécissement cardiaque sous aortique. Gazette Med Paris. 1869 Jan 1;24:161–3.
2. Teare D. Asymmetrical hypertrophy of the heart in young adults. Br Heart J. 1958 Jan;20(1):1–8.
3. Maron BJ, Haas TS, Murphy CJ, Ahluwalia A, Rutten-Ramos S. Incidence and causes of sudden death in U.S. college athletes. J Am Coll Cardiol. 2014 Apr 29;63(16):1636–43.
4. Elliott PM, Anastasakis A, Borger MA, Borggrefe M, Cecchi F, Charron P, et al. 2014 ESC Guidelines on diagnosis and management of hypertrophic cardiomyopathy: The Task Force for the Diagnosis and Management of Hypertrophic Cardiomyopathy of the European Society of Cardiology (ESC). Eur Heart J. 2014 Aug 29;35(39):2733–79.
5. O'Mahony C, Jichi F, Pavlou M, Monserrat L, Anastasakis A, Rapezzi C, et al. A novel clinical risk prediction model for sudden cardiac death in hypertrophic cardiomyopathy (HCM risk-SCD). Eur Heart J. 2014 Aug 7;35(30):2010–20.
6. Maron BJ, Gardin JM, Flack JM, Gidding SS, Kurosaki TT, Bild DE. Prevalence of hypertrophic cardiomyopathy in a general population of young adults. Echocardiographic analysis of 4111 subjects in the CARDIA Study. Coronary Artery Risk Development in (Young) Adults. Circulation. 1995 Aug 15;92(4):785–9.
7. Elliott P, Charron P, Blanes JRG, Tavazzi L, Tendera M, Konté M, et al. European Cardiomyopathy Pilot Registry: EURObservational Research Programme of the European Society of Cardiology. Eur Heart J. 2016 Jan 7;37(2):164–73.
8. Maron MS, Hellawell JL, Lucove JC, Farzaneh-Far R, Olivotto I. Occurrence of Clinically Diagnosed Hypertrophic Cardiomyopathy in the United States. Am J Cardiol. 2016 May 15;117(10):1651–4.
9. McKenna WJ, Spirito P, Desnos M, Dubourg O, Komajda M. Experience from clinical genetics in hypertrophic cardiomyopathy: proposal for new diagnostic criteria in adult members of affected families. Heart. 1997 Feb;77(2):130–2.
10. Sabater-Molina M, Pérez-Sánchez I, Hernández Del Rincón JP, Gimeno JR. Genetics of hypertrophic cardiomyopathy: A review of current state. Clin Genet. 2017 Apr 3;93(1):3–14.
11. Maron BJ, Maron MS, Semsarian C. Genetics of Hypertrophic Cardiomyopathy After 20 Years. J Am Coll Cardiol. 2012 Jun 26;60(8):705–15.
12. Bos JM, Towbin JA, Ackerman MJ. Diagnostic, Prognostic, and Therapeutic Implications of Genetic Testing for Hypertrophic Cardiomyopathy. J Am Coll Cardiol. 2009 Jul 14;54(3):201–11.
13. Romhilt DW, Estes EH. A point-score system for the ECG diagnosis of left ventricular hypertrophy. Am Heart J. 1968 Jun;75(6):752–8.
14. Richard P, Charron P, Carrier L, Ledeuil C, Cheav T, Pichereau C, et al. Hypertrophic cardiomyopathy: distribution of disease genes, spectrum of mutations, and implications for a molecular diagnosis strategy. Circulation. 2003 Apr 21;107(17):2227–32.
15. Lopes LR, Syrris P, Guttmann OP, O'Mahony C, Tang HC, Dalageorgou C, et al. Novel genotype-phenotype associations demonstrated by high-throughput sequencing in patients with hypertrophic cardiomyopathy. Heart. 2015 Feb;101(4):294–301.

16. Ingles J, Doolan A, Chiu C, Seidman J, Seidman C, Semsarian C. Compound and double mutations in patients with hypertrophic cardiomyopathy: implications for genetic testing and counselling. J Med Genet. 2005 Oct;42(10):e59.

17. Kelly M, Semsarian C. Multiple mutations in genetic cardiovascular disease: a marker of disease severity? Circ Cardiovasc Genet. 2009 Apr;2(2):182–90.

18. Jääskeläinen P, Heliö T, Aalto-Setälä K, Kaartinen M, Ilveskoski E, Hämäläinen L, et al. A new common mutation in the cardiac beta-myosin heavy chain gene in Finnish patients with hypertrophic cardiomyopathy. Ann Med. 2014 Sep;46(6):424–9.

19. Jääskeläinen P, Heliö T, Aalto-Setälä K, Kaartinen M, Ilveskoski E, Hämäläinen L, et al. Two founder mutations in the alpha-tropomyosin and the cardiac myosin-binding protein C genes are common causes of hypertrophic cardiomyopathy in the Finnish population. Ann Med. 2013 Feb;45(1):85–90.

20. Rottbauer W, Gautel M, Zehelein J, Labeit S, Franz WM, Fischer C, et al. Novel splice donor site mutation in the cardiac myosin-binding protein-C gene in familial hypertrophic cardiomyopathy. Characterization Of cardiac transcript and protein. J Clin Invest. 1997 Jul 15;100(2):475–82.

21. Marston S, Copeland O, Jacques A, Livesey K, Tsang V, McKenna WJ, et al. Evidence from human myectomy samples that MYBPC3 mutations cause hypertrophic cardiomyopathy through haploinsufficiency. Circ Res. 2009 Jul 31;105(3):219–22.

22. Andersen PS, Havndrup O, Bundgaard H, Larsen LA, Vuust J, Pedersen AK, et al. Genetic and phenotypic characterization of mutations in myosin-binding protein C (MYBPC3) in 81 families with familial hypertrophic cardiomyopathy: total or partial haploinsufficiency. Eur J Hum Genet. 2004 Aug;12(8):673–7.

23. Ojala M, Prajapati C, Pölönen R-P, Rajala K, Pekkanen-Mattila M, Rasku J, et al. Mutation-Specific Phenotypes in hiPSC-Derived Cardiomyocytes Carrying Either Myosin-Binding Protein C or α-Tropomyosin Mutation for Hypertrophic Cardiomyopathy. Stem Cells Int. 2016;2016:1684792.

24. Niimura H, Bachinski LL, Sangwatanaroj S, Watkins H, Chudley AE, McKenna W, et al. Mutations in the gene for cardiac myosin-binding protein C and late-onset familial hypertrophic cardiomyopathy. New Engl J Med. 1998 Apr 30;338(18):1248–57.

25. Oliva-Sandoval MJ, Ruiz-Espejo F, Monserrat L, Hermida-Prieto M, Sabater M, Garcia-Molina E, et al. Insights into genotype-phenotype correlation in hypertrophic cardiomyopathy. Findings from 18 Spanish families with a single mutation in MYBPC3. Heart. 2010 Nov 18;96(24):1980–4.

26. Charron P, Dubourg O, Desnos M, Isnard R, Hagege A, Bonne G, et al. Genotype-phenotype correlations in familial hypertrophic cardiomyopathy. A comparison between mutations in the cardiac protein-C and the beta-myosin heavy chain genes. Eur Heart J. 1998 Jan;19(1):139–45.

27. Moolman JC, Corfield VA, Posen B, Ngumbela K, Seidman C, Brink PA, et al. Sudden death due to troponin T mutations. J Am Coll Cardiol. 1997 Mar 1;29(3):549–55.

28. Ackerman MJ, VanDriest SL, Ommen SR, Will ML, Nishimura RA, Tajik AJ, et al. Prevalence and age-dependence of malignant mutations in the beta-myosin heavy chain and troponin T genes in hypertrophic cardiomyopathy: a comprehensive outpatient perspective. J Am Coll Cardiol. 2002 Jun 19;39(12):2042–8.

29. Maron BJ, Roberts WC. Quantitative analysis of cardiac muscle cell disorganization in the ventricular septum of patients with hypertrophic cardiomyopathy. Circulation. 1979 Apr;59(4):689–706.

30. Maron BJ. Hypertrophic cardiomyopathy: a systematic review. JAMA. 2002 Mar 13;287(10):1308–20.

31. Tanaka A, Yuasa S, Mearini G, Egashira T, Seki T, Kodaira M, et al. Endothelin-1 induces myofibrillar disarray and contractile vector variability in hypertrophic cardiomyopathy-induced pluripotent stem cell-derived cardiomyocytes. J Am Heart Assoc. 2014 Nov 11;3(6):e001263.

32. Tanaka M, Fujiwara H, Onodera T, Wu DJ, Matsuda M, Hamashima Y, et al. Quantitative analysis of narrowings of intramyocardial small arteries in normal hearts, hypertensive hearts, and hearts with hypertrophic cardiomyopathy. Circulation. 1987 Jun;75(6):1130–9.

33. Maron BJ, Wolfson JK, Epstein SE, Roberts WC. Intramural ("small vessel") coronary artery disease in hypertrophic cardiomyopathy. J Am Coll Cardiol. 1986 Sep;8(3):545–57.

34. Cannon RO, Rosing DR, Maron BJ, Leon MB, Bonow RO, Watson RM, et al. Myocardial ischemia in patients with hypertrophic cardiomyopathy: contribution of inadequate vasodilator reserve and elevated left ventricular filling pressures. Circulation. 1985 Feb;71(2):234–43.

35. Basso C, Thiene G, Corrado D, Buja G, Melacini P, Nava A. Hypertrophic cardiomyopathy and sudden death in the young: pathologic evidence of myocardial ischemia. Hum Pathol. 2000 Aug;31(8):988–98.

36. Shirani J, Pick R, Roberts WC, Maron BJ. Morphology and significance of the left ventricular collagen network in young patients with hypertrophic cardiomyopathy and sudden cardiac death. J Am Coll Cardiol. 2000 Jan;35(1):36–44.

37. Klues HG, Schiffers A, Maron BJ. Phenotypic spectrum and patterns of left ventricular hypertrophy in hypertrophic cardiomyopathy: morphologic observations and significance as assessed by two-dimensional echocardiography in 600 patients. J Am Coll Cardiol. 1995 Dec;26(7):1699–708.

38. Coppini R, Ferrantini C, Yao L, Fan P, Del Lungo M, Stillitano F, et al. Late sodium current inhibition reverses electromechanical dysfunction in human hypertrophic cardiomyopathy. Circulation. 2013 Feb 5;127(5):575–84.

39. Landstrom AP, Dobrev D, Wehrens XHT. Calcium Signaling and Cardiac Arrhythmias. Circ Res. 2017 Jun 9;120(12):1969–93.

40. Clusin WT. Calcium and cardiac arrhythmias: DADs, EADs, and alternans. Crit Rev Clin Lab Sci. 2003 Jun;40(3):337–75.

41. Passini E, Mincholé A, Coppini R, Cerbai E, Rodriguez B, Severi S, et al. Mechanisms of pro-arrhythmic abnormalities in ventricular repolarisation and anti-arrhythmic therapies in human hypertrophic cardiomyopathy. J Mol Cell Cardiol. 2016 Jul;96:72–81.

42. Ashrafian H, McKenna WJ, Watkins H. Disease pathways and novel therapeutic targets in hypertrophic cardiomyopathy. Circ Res. 2011 Jun 24;109(1):86–96.

43. Lan F, Lee AS, Liang P, Sanchez-Freire V, Nguyen PK, Wang L, et al. Abnormal calcium handling properties underlie familial hypertrophic cardiomyopathy pathology in patient-specific induced pluripotent stem cells. Cell Stem Cell. 2013 Jan 3;12(1):101–13.

44. van Dijk SJ, Paalberends ER, Najafi A, Michels M, Sadayappan S, Carrier L, et al. Contractile dysfunction irrespective of the mutant protein in human hypertrophic cardiomyopathy with normal systolic function. Circ: Heart Fail. 2012 Jan;5(1):36–46.

45. Crocini C, Ferrantini C, Scardigli M, Coppini R, Mazzoni L, Lazzeri E, et al. Novel insights on the relationship between T-tubular defects and contractile dysfunction in a mouse model of hypertrophic cardiomyopathy. J Mol Cell Cardiol. 2016 Feb;91:42–51.

46. Helms AS, Alvarado FJ, Yob J, Tang VT, Pagani F, Russell MW, et al. Genotype-Dependent and -Independent Calcium Signaling Dysregulation in Human Hypertrophic Cardiomyopathy. Circulation. 2016 Nov 29;134(22):1738–48.

47. Rowlands C, Owen T, Lawal S, Cao S, Pandey S, Yang H-Y, et al. Age and strain related aberrant Ca 2+release is associated with sudden cardiac death in the ACTC E99K mouse model of hypertrophic cardiomyopathy. Am J Physiol Heart Circ Physiol. 2017 Sep 8;(313):H1213–26.

48. Fatkin D, McConnell BK, Mudd JO, Semsarian C, Moskowitz IG, Schoen FJ, et al. An abnormal Ca(2+) response in mutant sarcomere protein-mediated familial hypertrophic cardiomyopathy. J Clin Invest. 2000 Dec;106(11):1351–9.

49. Gimeno JR, Tomé-Esteban M, Lofiego C, Hurtado J, Pantazis A, Mist B, et al. Exercise-induced ventricular arrhythmias and risk of sudden cardiac death in patients with hypertrophic cardiomyopathy. Eur Heart J. 2009 Nov;30(21):2599–605.

50. Maron BJ, Semsarian C, Shen W-K, Link MS, Epstein AE, Estes NAM, et al. Circadian patterns in the occurrence of malignant ventricular tachyarrhythmias triggering defibrillator interventions in patients with hypertrophic cardiomyopathy. Heart Rhythm. 2009 May;6(5):599–602.

51. O'Mahony C, Lambiase PD, Rahman SM, Cardona M, Calcagnino M, Quarta G, et al. The relation of ventricular arrhythmia electrophysiological characteristics to cardiac phenotype and circadian patterns in hypertrophic cardiomyopathy. Europace. 2012 May;14(5):724–33.

52. Volders PG, Vos MA, Szabo B, Sipido KR, de Groot SH, Gorgels AP, et al. Progress in the understanding of cardiac early afterdepolarizations and torsades de pointes: time to revise current concepts. Cardiovasc Res. 2000 Jun;46(3):376–92.

53. Sakamoto N, Sato N, Oikawa K, Karim Talib A, Sugiyama E, Minoshima A, et al. Late gadolinium enhancement of cardiac magnetic resonance imaging indicates abnormalities of time-domain T-wave alternans in hypertrophic cardiomyopathy with ventricular tachycardia. Heart Rhythm. 2015 Aug;12(8):1747–55.

54. Doenst T, Nguyen TD, Abel ED. Cardiac metabolism in heart failure: implications beyond ATP production. Circ Res. 2013 Aug 30;113(6):709–24.

55. Vakrou S, Abraham MR. Hypertrophic cardiomyopathy: a heart in need of an energy bar? Front Physiol. 2014;5:309.

56. Javadpour MM, Tardiff JC, Pinz I, Ingwall JS. Decreased energetics in murine hearts bearing the R92Q mutation in cardiac troponin T. J Clin Invest. 2003 Sep;112(5):768–75.

57. Crilley JG, Boehm EA, Blair E, Rajagopalan B, Blamire AM, Styles P, et al. Hypertrophic cardiomyopathy due to sarcomeric gene mutations is characterized by impaired energy metabolism irrespective of the degree of hypertrophy. J Am Coll Cardiol. 2003 May 21;41(10):1776–82.

58. Abraham MR, Bottomley PA, Dimaano VL, Pinheiro A, Steinberg A, Traill TA, et al. Creatine kinase adenosine triphosphate and phosphocreatine energy supply in a single kindred of patients with hypertrophic cardiomyopathy. Am J Cardiol. 2013 Sep 15;112(6):861–6.

59. Timmer SAJ, Germans T, Brouwer WP, Lubberink M, van der Velden J, Wilde AAM, et al. Carriers of the hypertrophic cardiomyopathy MYBPC3 mutation are characterized by reduced

myocardial efficiency in the absence of hypertrophy and microvascular dysfunction. Eur J Heart Fail. 2011 Dec;13(12):1283–9.

60. Abozguia K, Elliott P, McKenna W, Phan TT, Nallur-Shivu G, Ahmed I, et al. Metabolic modulator perhexiline corrects energy deficiency and improves exercise capacity in symptomatic hypertrophic cardiomyopathy. Circulation. 2010 Oct 19;122(16):1562–9.

61. Tadamura E, Kudoh T, Hattori N, Inubushi M, Magata Y, Konishi J, et al. Impairment of BMIPP uptake precedes abnormalities in oxygen and glucose metabolism in hypertrophic cardiomyopathy. J Nucl Med. 1998 Mar;39(3):390–6.

62. Tuunanen H, Kuusisto J, Toikka J, Jääskeläinen P, Marjamäki P, Peuhkurinen K, et al. Myocardial perfusion, oxidative metabolism, and free fatty acid uptake in patients with hypertrophic cardiomyopathy attributable to the Asp175Asn mutation in the alpha-tropomyosin gene: a positron emission tomography study. J Nucl Cardiol. 2007 May;14(3):354–65.

63. Griffin JL, Atherton H, Shockcor J, Atzori L. Metabolomics as a tool for cardiac research. Nat Rev Cardiol. 2011 Nov;8(11):630–43.

64. Lenz EM, Bright J, Wilson ID, Hughes A, Morrisson J, Lindberg H, et al. Metabonomics, dietary influences and cultural differences: a 1H NMR-based study of urine samples obtained from healthy British and Swedish subjects. J Pharm Biomed Anal. 2004 Nov 19;36(4):841–9.

65. Oresic M. Metabolomics, a novel tool for studies of nutrition, metabolism and lipid dysfunction. Nutr Metab Cardiovasc Dis. 2009 Dec;19(11):816–24.

66. Illig T, Gieger C, Zhai G, Römisch-Margl W, Wang-Sattler R, Prehn C, et al. A genome-wide perspective of genetic variation in human metabolism. Nat Genet. 2010 Feb;42(2):137–41.

67. Nikkilä J, Sysi-Aho M, Ermolov A, Seppänen-Laakso T, Simell O, Kaski S, et al. Gender-dependent progression of systemic metabolic states in early childhood. Mol Syst Biol. 2008;4:197.

68. Maekawa K, Hirayama A, Iwata Y, Tajima Y, Nishimaki-Mogami T, Sugawara S, et al. Global metabolomic analysis of heart tissue in a hamster model for dilated cardiomyopathy. J Mol Cell Cardiol. 2013 Feb 20;59C:76–85.

69. Zordoky BN, Sung MM, Ezekowitz J, Mandal R, Han B, Bjorndahl TC, et al. Metabolomic fingerprint of heart failure with preserved ejection fraction. PLoS ONE. 2015;10(5):e0124844.

70. Deidda M, Piras C, Dessalvi CC, Locci E, Barberini L, Torri F, et al. Metabolomic approach to profile functional and metabolic changes in heart failure. J Transl Med. 2015 Sep 12;13:297.

71. Gehmlich K, Dodd MS, Allwood JW, Kelly M, Bellahcene M, Lad HV, et al. Changes in the cardiac metabolome caused by perhexiline treatment in a mouse model of hypertrophic cardiomyopathy. Mol Biosyst. 2015 Feb;11(2):564–73.

72. Delcrè SDL, Di Donna P, Leuzzi S, Miceli S, Bisi M, Scaglione M, et al. Relationship of ECG findings to phenotypic expression in patients with hypertrophic cardiomyopathy: a cardiac magnetic resonance study. Int J Cardiol. 2013 Aug 10;167(3):1038–45.

73. Dumont CA, Monserrat L, Soler R, Rodríguez E, Fernandez X, Peteiro J, et al. Interpretation of electrocardiographic abnormalities in hypertrophic cardiomyopathy with cardiac magnetic resonance. Eur Heart J. 2006 Jul;27(14):1725–31.

74. Lakdawala NK, Thune JJ, Maron BJ, Cirino AL, Havndrup O, Bundgaard H, et al. Electrocardiographic features of sarcomere mutation carriers with and without clinically overt hypertrophic cardiomyopathy. Am J Cardiol. 2011 Dec 1;108(11):1606–13.

75. Poutanen T, Tikanoja T, Jääskeläinen P, Jokinen E, Silvast A, Laakso M, et al. Diastolic dysfunction without left ventricular hypertrophy is an early finding in children with hypertrophic cardiomyopathy-causing mutations in the beta-myosin heavy chain, alpha-tropomyosin, and myosin-binding protein C genes. Am Heart J. 2006 Mar;151(3):725.e1–725.e9.

76. Potter SLP, Holmqvist F, Platonov PG, Steding K, Arheden H, Pahlm O, et al. Detection of hypertrophic cardiomyopathy is improved when using advanced rather than strictly conventional 12-lead electrocardiogram. J Electrocardiol. 2010 Nov;43(6):713–8.

77. Eranti A, Aro AL, Kerola T, Anttonen O, Rissanen HA, Tikkanen JT, et al. Prevalence and prognostic significance of abnormal P terminal force in lead V1 of the ECG in the general population. Circ Arrhythm Electrophysiol. 2014 Dec;7(6):1116–21.

78. Ryan MP, Cleland JG, French JA, Joshi J, Choudhury L, Chojnowska L, et al. The standard electrocardiogram as a screening test for hypertrophic cardiomyopathy. Am J Cardiol. 1995 Oct 1;76(10):689–94.

79. al-Mahdawi S, Chamberlain S, Chojnowska L, Michalak E, Nihoyannopoulos P, Ryan M, et al. The electrocardiogram is a more sensitive indicator than echocardiography of hypertrophic cardiomyopathy in families with a mutation in the MYH7 gene. Br Heart J. 1994 Aug;72(2):105–11.

80. Panza JA, Maron BJ. Relation of electrocardiographic abnormalities to evolving left ventricular hypertrophy in hypertrophic cardiomyopathy during childhood. Am J Cardiol. 1989 May 15;63(17):1258–65.

81. Papavassiliu T, Flüchter S, Haghi D, Süselbeck T, Wolpert C, Dinter D, et al. Extent of myocardial hyperenhancement on late gadolinium-enhanced cardiovascular magnetic resonance correlates with q waves in hypertrophic cardiomyopathy. J Cardiovasc Magn Reson. 2007;9(3):595–603.

82. Das MK, Khan B, Jacob S, Kumar A, Mahenthiran J. Significance of a fragmented QRS complex versus a Q wave in patients with coronary artery disease. Circulation. 2006 May 30;113(21):2495–501.

83. Basaran Y, Tigen K, Karaahmet T, Isiklar I, Cevik C, Gurel E, et al. Fragmented QRS complexes are associated with cardiac fibrosis and significant intraventricular systolic dyssynchrony in nonischemic dilated cardiomyopathy patients with a narrow QRS interval. Echocardiography. 2011 Jan;28(1):62–8.

84. Das MK, Suradi H, Maskoun W, Michael MA, Shen C, Peng J, et al. Fragmented wide QRS on a 12-lead ECG: a sign of myocardial scar and poor prognosis. Circ Arrhythm Electrophysiol. 2008 Oct;1(4):258–68.

85. Debonnaire P, Katsanos S, Joyce E, van den Brink OVW, Atsma DE, Schalij MJ, et al. QRS Fragmentation and QTc Duration Relate to Malignant Ventricular Tachyarrhythmias and Sudden Cardiac Death in Patients with Hypertrophic Cardiomyopathy. J Cardiovasc Electrophysiol. 2015 May;26(5):547–55.

86. Femenía F, Arce M, Van Grieken J, Trucco E, Mont L, Abello M, et al. Fragmented QRS as a predictor of arrhythmic events in patients with hypertrophic obstructive cardiomyopathy. J Interv Card Electrophysiol. 2013 Dec;38(3):159–65.

87. Sokolow M, Lyon TP. The ventricular complex in left ventricular hypertrophy as obtained by unipolar precordial and limb leads. Am Heart J. 1949 Feb;37(2):161–86.

88. Molloy TJ, Okin PM, Devereux RB, Kligfield P. Electrocardiographic detection of left ventricular hypertrophy by the simple QRS voltage-duration product. J Am Coll Cardiol. 1992 Nov 1;20(5):1180–6.

89. Konno T, Shimizu M, Ino H, Fujino N, Hayashi K, Uchiyama K, et al. Differences in diagnostic value of four electrocardiographic voltage criteria for hypertrophic cardiomyopathy in a genotyped population. Am J Cardiol. 2005 Nov 1;96(9):1308–12.

90. Montgomery JV, Harris KM, Casey SA, Zenovich AG, Maron BJ. Relation of electrocardiographic patterns to phenotypic expression and clinical outcome in hypertrophic cardiomyopathy. Am J Cardiol. 2005 Jul 15;96(2):270–5.

91. Lepeschkin E, Surawicz B. The measurement of the Q-T interval of the electrocardiogram. Circulation. 1952 Sep;6(3):378–88.

92. Bazett HC. An analysis of the time-relations of the electrocardiograms. Heart. 1920 Jan 1;(7):353–70.

93. Vandenberk B, Vandael E, Robyns T, Vandenberghe J, Garweg C, Foulon V, et al. Which QT Correction Formulae to Use for QT Monitoring? J Am Heart Assoc. 2016 Jun 17;5(6).

94. Straus SMJM, Kors JA, De Bruin ML, van der Hooft CS, Hofman A, Heeringa J, et al. Prolonged QTc interval and risk of sudden cardiac death in a population of older adults. J Am Coll Cardiol. 2006 Jan 17;47(2):362–7.

95. Johnson JN, Grifoni C, Bos JM, Saber-Ayad M, Ommen SR, Nistri S, et al. Prevalence and clinical correlates of QT prolongation in patients with hypertrophic cardiomyopathy. Eur Heart J. 2011 May;32(9):1114–20.

96. Sakata K, Shimizu M, Ino H, Yamaguchi M, Terai H, Hayashi K, et al. QT dispersion and left ventricular morphology in patients with hypertrophic cardiomyopathy. Heart. 2003 Aug;89(8):882–6.

97. Badran HM, Elnoamany MF, Soltan G, Ezat M, Elsedi M, Abdelfatah RA, et al. Relationship of mechanical dyssynchrony to QT interval prolongation in hypertrophic cardiomyopathy. Eur Heart J Cardiovasc Imaging. 2012 May;13(5):423–32.

98. Magrì D, De Cecco CN, Piccirillo G, Mastromarino V, Serdoz A, Muscogiuri G, et al. Myocardial repolarization dispersion and late gadolinium enhancement in patients with hypertrophic cardiomyopathy. Circ J. 2014;78(5):1216–23.

99. Jouven X, Hagege A, Charron P, Carrier L, Dubourg O, Langlard JM, et al. Relation between QT duration and maximal wall thickness in familial hypertrophic cardiomyopathy. Heart. 2002 Aug;88(2):153–7.

100. Uchiyama K, Hayashi K, Fujino N, Konno T, Sakamoto Y, Sakata K, et al. Impact of QT variables on clinical outcome of genotyped hypertrophic cardiomyopathy. Ann Noninvasive Electrocardiol. 2009 Jan;14(1):65–71.

101. Zaidi M, Robert A, Fesler R, Derwael C, Brohet C. Dispersion of ventricular repolarization in hypertrophic cardiomyopathy. J Electrocardiol. 1996;29 Suppl:89–94.

102. Dritsas A, Sbarouni E, Gilligan D, Nihoyannopoulos P, Oakley CM. QT-interval abnormalities in hypertrophic cardiomyopathy. Clin Cardiol. 1992 Oct;15(10):739–42.

103. Buja G, Miorelli M, Turrini P, Melacini P, Nava A. Comparison of QT dispersion in hypertrophic cardiomyopathy between patients with and without ventricular arrhythmias and sudden death. Am J Cardiol. 1993 Oct 15;72(12):973–6.

104. Kaya CT, Gurlek A, Altin T, Kilickap M, Karabulut HG, Turhan S, et al. The relationship between angiotensin converting enzyme gene I/D polymorphism and QT dispersion in patients with hypertrophic cardiomyopathy. J Renin-Angiotensin-Aldosterone Syst. 2010 Sep;11(3):192–7.

105. Magrì D, Piccirillo G, Ricotta A, De Cecco CN, Mastromarino V, Serdoz A, et al. Spatial QT Dispersion Predicts Nonsustained Ventricular Tachycardia and Correlates with Confined Systodiastolic Dysfunction in Hypertrophic Cardiomyopathy. Cardiology. 2015;131(2):122–9.

106. Maron BJ, Leyhe MJ, Casey SA, Gohman TE, Lawler CM, Crow RS, et al. Assessment of QT dispersion as a prognostic marker for sudden death in a regional nonreferred hypertrophic cardiomyopathy cohort. Am J Cardiol. 2001 Jan 1;87(1):114–5.

107. Gray B, Ingles J, Medi C, Semsarian C. Prolongation of the QTc interval predicts appropriate implantable cardioverter-defibrillator therapies in hypertrophic cardiomyopathy. JACC Heart Fail. 2013 Apr;1(2):149–55.

108. Chen X, Zhao S, Zhao T, Lu M, Yin G, Jiang S. T-wave inversions related to left ventricular basal hypertrophy and myocardial fibrosis in non-apical hypertrophic cardiomyopathy: A cardiovascular magnetic resonance imaging study. Eur J Radiol. 2014;83:297–302.

109. Haghjoo M, Mohammadzadeh S, Taherpour M, Faghfurian B, Fazelifar AF, Alizadeh A, et al. ST-segment depression as a risk factor in hypertrophic cardiomyopathy. Europace. 2009 May;11(5):643–9.

110. Adabag AS, Casey SA, Kuskowski MA, Zenovich AG, Maron BJ. Spectrum and prognostic significance of arrhythmias on ambulatory Holter electrocardiogram in hypertrophic cardiomyopathy. J Am Coll Cardiol. 2005 Mar 1;45(5):697–704.

111. Monserrat L, Elliott PM, Gimeno JR, Sharma S, Penas-Lado M, McKenna WJ. Non-sustained ventricular tachycardia in hypertrophic cardiomyopathy: an independent marker of sudden death risk in young patients. J Am Coll Cardiol. 2003 Sep 3;42(5):873–9.

112. Maron BJ, Savage DD, Wolfson JK, Epstein SE. Prognostic significance of 24 hour ambulatory electrocardiographic monitoring in patients with hypertrophic cardiomyopathy: A prospective study. Am J Cardiol. Excerpta Medica; 1981 Aug;48(2):252–7.

113. Spirito P, Rapezzi C, Autore C, Bruzzi P, Bellone P, Ortolani P, et al. Prognosis of asymptomatic patients with hypertrophic cardiomyopathy and nonsustained ventricular tachycardia. Circulation. American Heart Association, Inc; 1994 Dec 1;90(6):2743–7.

114. Savage DD, Seides SF, Maron BJ, Myers DJ, Epstein SE. Prevalence of arrhythmias during 24-hour electrocardiographic monitoring and exercise testing in patients with obstructive and nonobstructive hypertrophic cardiomyopathy. Circulation. 1979 May;59(5):866–75.

115. Elliott PM, Gimeno JR, Tomé MT, Shah J, Ward D, Thaman R, et al. Left ventricular outflow tract obstruction and sudden death risk in patients with hypertrophic cardiomyopathy. Eur Heart J. 2006 Aug;27(16):1933–41.

116. D'Andrea A, Caso P, Romano S, Scarafile R, Riegler L, Salerno G, et al. Different effects of cardiac resynchronization therapy on left atrial function in patients with either idiopathic or ischaemic dilated cardiomyopathy: a two-dimensional speckle strain study. Eur Heart J. 2007 Oct 17;28(22):2738–48.

117. McKenna WJ, Chetty S, Oakley CM, Goodwin JF. Arrhythmia in hypertrophic cardiomyopathy: Exercise and 48 hour ambulatory electrocardiographic assessment with and without beta adrenergic blocking therapy. Am J Cardiol. 1980 Jan;45(1):1–5.

118. Viitasalo M, Oikarinen L, Väänänen H, Swan H, Piippo K, Kontula K, et al. Differentiation between LQT1 and LQT2 patients and unaffected subjects using 24-hour electrocardiographic recordings. Am J Cardiol. 2002 Mar 15;89(6):679–85.

119. Chevalier P, Burri H, Adeleine P, Kirkorian G, Lopez M, Leizorovicz A, et al. QT dynamicity and sudden death after myocardial infarction: results of a long-term follow-up study. J Cardiovasc Electrophysiol. 2003 Mar;14(3):227–33.

120. Milliez P, Leenhardt A, Maisonblanche P, Vicaut E, Badilini F, Siliste C, et al. Usefulness of ventricular repolarization dynamicity in predicting arrhythmic deaths in patients with ischemic cardiomyopathy (from the European Myocardial Infarct Amiodarone Trial). Am J Cardiol. 2005 Apr 1;95(7):821–6.

121. Cygankiewicz I, Zareba W, Vazquez R, Almendral J, Bayes-Genis A, Fiol M, et al. Prognostic value of QT/RR slope in predicting mortality in patients with congestive heart failure. J Cardiovasc Electrophysiol. 2008 Oct;19(10):1066–72.

122. Pathak A, Curnier D, Fourcade J, Roncalli J, Stein PK, Hermant P, et al. QT dynamicity: a prognostic factor for sudden cardiac death in chronic heart failure. Eur J Heart Fail. 2005 Mar 2;7(2):269–75.

123. Watanabe E, Arakawa T, Uchiyama T, Tong M, Yasui K, Takeuchi H, et al. Prognostic significance of circadian variability of RR and QT intervals and QT dynamicity in patients with chronic heart failure. Heart Rhythm. 2007 Aug;4(8):999–1005.

124. Quinteiro RA, Biagetti MO, Fernandez A, Borzone FR, Gargano A, Casabe HJ. Can QT/RR relationship differentiate between low- and high-risk patients with hypertrophic cardiomyopathy? Ann Noninvasive Electrocardiol. 2015 Jul;20(4):386–93.

125. Gupta P, Patel C, Patel H, Narayanaswamy S, Malhotra B, Green JT, et al. T(p-e)/QT ratio as an index of arrhythmogenesis. J Electrocardiol. 2008 Nov;41(6):567–74.

126. Opthof T, Coronel R, Wilms-Schopman FJG, Plotnikov AN, Shlapakova IN, Danilo P, et al. Dispersion of repolarization in canine ventricle and the electrocardiographic T wave: Tp-e interval does not reflect transmural dispersion. Heart Rhythm. 2007 Mar;4(3):341–8.

127. Yan GX, Rials SJ, Wu Y, Liu T, Xu X, Marinchak RA, et al. Ventricular hypertrophy amplifies transmural repolarization dispersion and induces early afterdepolarization. Am J Physiol Heart Circ Physiol. 2001 Nov;281(5):H1968–75.

128. Panikkath R, Reinier K, Uy-Evanado A, Teodorescu C, Hattenhauer J, Mariani R, et al. Prolonged Tpeak-to-tend interval on the resting ECG is associated with increased risk of sudden cardiac death. Circ Arrhythm Electrophysiol. 2011 Aug;4(4):441–7.

129. Shimizu M, Ino H, Okeie K, Yamaguchi M, Nagata M, Hayashi K, et al. T-peak to T-end interval may be a better predictor of high-risk patients with hypertrophic cardiomyopathy associated with a cardiac troponin I mutation than QT dispersion. Clin Cardiol. 2002 Jul;25(7):335–9.

130. Guttmann OP, Rahman MS, O'Mahony C, Anastasakis A, Elliott PM. Atrial fibrillation and thromboembolism in patients with hypertrophic cardiomyopathy: systematic review. Heart. 2014 Mar;100(6):465–72.

131. Vaidya K, Semsarian C, Chan KH. Atrial Fibrillation in Hypertrophic Cardiomyopathy. Heart Lung Circ. 2017 Sep;26(9):975–82.

132. Rickers C, Wilke NM, Jerosch-Herold M, Casey SA, Panse P, Panse N, et al. Utility of cardiac magnetic resonance imaging in the diagnosis of hypertrophic cardiomyopathy. Circulation. 2005 Aug 9;112(6):855–61.

133. Moon JCC, Fisher NG, McKenna WJ, Pennell DJ. Detection of apical hypertrophic cardiomyopathy by cardiovascular magnetic resonance in patients with non-diagnostic echocardiography. Heart. 2004 Jun;90(6):645–9.

134. Kwon DH, Setser RM, Thamilarasan M, Popovic ZV, Smedira NG, Schoenhagen P, et al. Abnormal papillary muscle morphology is independently associated with increased left ventricular outflow tract obstruction in hypertrophic cardiomyopathy. Heart. 2007 Aug 9;94(10):1295–301.

135. Klues HG, Maron BJ, Dollar AL, Roberts WC. Diversity of structural mitral valve alterations in hypertrophic cardiomyopathy. Circulation. 1992 May;85(5):1651–60.

136. Maron MS, Olivotto I, Betocchi S, Casey SA, Lesser JR, Losi MA, et al. Effect of left ventricular outflow tract obstruction on clinical outcome in hypertrophic cardiomyopathy. N Engl J Med. 2003 Jan 23;348(4):295–303.

137. Sengupta PP, Korinek J, Belohlavek M, Narula J, Vannan MA, Jahangir A, et al. Left Ventricular Structure and Function. J Am Coll Cardiol. 2006 Nov;48(10):1988–2001.

138. Vendelin M, Bovendeerd PHM, Engelbrecht J, Arts T. Optimizing ventricular fibers: uniform strain or stress, but not ATP consumption, leads to high efficiency. Am J Physiol Heart Circ Physiol. 2002 Sep;283(3):H1072–81.

139. Sengupta PP, Tajik AJ, Chandrasekaran K, Khandheria BK. Twist mechanics of the left ventricle: principles and application. JACC Cardiovasc Imaging. 2008 May;1(3):366–76.

140. Chen J, Liu W, Zhang H, Lacy L, Yang X, Song S-K, et al. Regional ventricular wall thickening reflects changes in cardiac fiber and sheet structure during contraction: quantification with diffusion tensor MRI. Am J Physiol Heart Circ Physiol. 2005 Nov;289(5):H1898–907.

141. Costa KD, Takayama Y, McCulloch AD, Covell JW. Laminar fiber architecture and three-dimensional systolic mechanics in canine ventricular myocardium. Am J Physiol. 1999 Feb;276(2 Pt 2):H595–607.

142. Pasipoularides A. LV twisting and untwisting in HCM: ejection begets filling. Diastolic functional aspects of HCM. Am Heart J. 2011 Nov;162(5):798–810.

143. Pacileo G, Baldini L, Limongelli G, Di Salvo G, Iacomino M, Capogrosso C, et al. Prolonged left ventricular twist in cardiomyopathies: a potential link between systolic and diastolic dysfunction. Eur J Echocardiogr. 2011 Nov 15;12(11):841–9.

144. Florian A, Masci PG, De Buck S, Aquaro GD, Claus P, Todiere G, et al. Geometric Assessment of Asymmetric Septal Hypertrophic Cardiomyopathy by CMR. JACC Cardiovasc Imaging. Journal of the American College of Cardiology; 2012 Jul;5(7):702–11.

145. Reant P, Donal E, Schnell F, Reynaud A, Daudin M, Pillois X, et al. Clinical and imaging description of the Maron subtypes of hypertrophic cardiomyopathy. Int J Cardiovasc Imaging. 2014 Nov 25.

146. Geske JB, Bos JM, Gersh BJ, Ommen SR, Eidem BW, Ackerman MJ. Deformation patterns in genotyped patients with hypertrophic cardiomyopathy. Eur Heart J Cardiovasc Imaging. 2014 Apr;15(4):456–65.

147. Yang H, Carasso S, Woo A, Jamorski M, Nikonova A, Wigle ED, et al. Hypertrophy pattern and regional myocardial mechanics are related in septal and apical hypertrophic cardiomyopathy. J Am Soc Echocardiogr. 2010 Oct;23(10):1081–9.

148. D'hooge J. Regional Strain and Strain Rate Measurements by Cardiac Ultrasound: Principles, Implementation and Limitations. Eur J Echocardiogr. 2000 Sep;1(3):154–70.

149. Urheim S, Edvardsen T, Torp H, Angelsen B, Smiseth OA. Myocardial strain by Doppler echocardiography. Validation of a new method to quantify regional myocardial function. Circulation. 2000 Sep 5;102(10):1158–64.

150. Leitman M, Lysyansky P, Sidenko S, Shir V, Peleg E, Binenbaum M, et al. Two-dimensional strain–a novel software for real-time quantitative echocardiographic assessment of myocardial function. J Am Soc Echocardiogr. 2004 Oct;17(10):1021–9.

151. Korinek J, Wang J, Sengupta PP, Miyazaki C, Kjaergaard J, McMahon E, et al. Two-Dimensional Strain–A Doppler-Independent Ultrasound Method for Quantitation of Regional Deformation: Validation In Vitro and In Vivo. J Am Soc Echocardiogr. 2005 Dec;18(12):1247–53.

152. Amundsen BH, Helle-Valle T, Edvardsen T, Torp H, Crosby J, Lyseggen E, et al. Noninvasive Myocardial Strain Measurement by Speckle Tracking Echocardiography. J Am Coll Cardiol. 2006 Feb;47(4):789–93.

153. Cho G-Y, Chan J, Leano R, Strudwick M, Marwick TH. Comparison of two-dimensional speckle and tissue velocity based strain and validation with harmonic phase magnetic resonance imaging. Am J Cardiol. 2006 Jun 1;97(11):1661–6.

154. Serri K, Reant P, Lafitte M, Berhouet M, Le Bouffos V, Roudaut R, et al. Global and Regional Myocardial Function Quantification by Two-Dimensional Strain. J Am Coll Cardiol. 2006 Mar;47(6):1175–81.

155. Carasso S, Yang H, Woo A, Vannan MA, Jamorski M, Wigle ED, et al. Systolic Myocardial Mechanics in Hypertrophic Cardiomyopathy: Novel Concepts and Implications for Clinical Status. J Am Soc Echocardiogr. 2008 Jun;21(6):675–83.

156. Urbano-Moral JA, Rowin EJ, Maron MS, Crean A, Pandian NG. Investigation of global and regional myocardial mechanics with 3-dimensional speckle tracking echocardiography and relations to hypertrophy and fibrosis in hypertrophic cardiomyopathy. Circ Cardiovasc Imaging. 2014 Jan;7(1):11–9.

157. Haland TF, Hasselberg NE, Almaas VM, Dejgaard LA, Saberniak J, Leren IS, et al. The systolic paradox in hypertrophic cardiomyopathy. Open Heart. 2017;4(1):e000571.

158. Paraskevaidis IA, Farmakis D, Papadopoulos C, Ikonomidis I, Parissis J, Rigopoulos A, et al. Two-dimensional strain analysis in patients with hypertrophic cardiomyopathy and normal systolic function: a 12-month follow-up study. Am Heart J. 2009 Sep;158(3):444–50.

159. Debonnaire P, Thijssen J, Leong DP, Joyce E, Katsanos S, Hoogslag GE, et al. Global longitudinal strain and left atrial volume index improve prediction of appropriate implantable cardioverter defibrillator therapy in hypertrophic cardiomyopathy patients. Int J Cardiovasc Imaging. 2014 Mar;30(3):549–58.

160. Maciver DH. A new method for quantification of left ventricular systolic function using a corrected ejection fraction. Eur J Echocardiogr. 2011 Mar;12(3):228–34.

161. Farsalinos KE, Daraban AM, Ünlü S, Thomas JD, Badano LP, Voigt J-U. Head-to-Head Comparison of Global Longitudinal Strain Measurements among Nine Different Vendors: The EACVI/ASE Inter-Vendor Comparison Study. J Am Soc Echocardiogr. 2015 Oct;28(10):1171–1181–e2.

162. Mirea O, Pagourelias ED, Duchenne J, Bogaert J, Thomas JD, Badano LP, et al. Intervendor Differences in the Accuracy of Detecting Regional Functional Abnormalities: A Report From the EACVI-ASE Strain Standardization Task Force. JACC Cardiovasc Imaging. 2018 Jan;11(1):25–34.

163. Popović ZB, Kwon DH, Mishra M, Buakhamsri A, Greenberg NL, Thamilarasan M, et al. Association Between Regional Ventricular Function and Myocardial Fibrosis in Hypertrophic Cardiomyopathy Assessed by Speckle Tracking Echocardiography and Delayed Hyperenhancement Magnetic Resonance Imaging. J Am Soc Echocardiogr. 2008 Dec 1;21(12):1299–305.

164. Saito M, Okayama H, Yoshii T, Higashi H, Morioka H, Hiasa G, et al. Clinical significance of global two-dimensional strain as a surrogate parameter of myocardial fibrosis and cardiac events in patients with hypertrophic cardiomyopathy. Eur Heart J Cardiovasc Imaging. 2012 Jul;13(7):617–23.

165. Di Salvo G, Pacileo G, Limongelli G, Baldini L, Rea A, Verrengia M, et al. Non Sustained Ventricular Tachycardia in Hypertrophic Cardiomyopathy and New Ultrasonic Derived Parameters. J Am Soc Echocardiogr. 2010 Jun 1;23(6):581–90.

166. Almaas VM, Haugaa KH, Strøm EH, Scott H, Smith H-J, Dahl CP, et al. Noninvasive assessment of myocardial fibrosis in patients with obstructive hypertrophic cardiomyopathy. Heart. 2013 Dec 24;(100):631–8.

167. Reant P, Reynaud A, Pillois X, Dijos M, Arsac F, Touche C, et al. Comparison of resting and exercise echocardiographic parameters as indicators of outcomes in hypertrophic cardiomyopathy. J Am Soc Echocardiogr. 2015 Feb;28(2):194–203.

168. Liu H, Pozios I, Haileselassie B, Nowbar A, Sorensen LL, Phillip S, et al. Role of Global Longitudinal Strain in Predicting Outcomes in Hypertrophic Cardiomyopathy. Am J Cardiol. 2017 Aug 15;120(4):670–5.

169. Hiemstra YL, Debonnaire P, Bootsma M, van Zwet EW, Delgado V, Schalij MJ, et al. Global Longitudinal Strain and Left Atrial Volume Index Provide Incremental Prognostic Value in Patients With Hypertrophic Cardiomyopathy. Circ Cardiovasc Imaging. 2017 Jul;10(7).

170. Haugaa KH, Smedsrud MK, Steen T, Kongsgaard E, Loennechen JP, Skjaerpe T, et al. Mechanical Dispersion Assessed by Myocardial Strain in Patients After Myocardial Infarction for Risk Prediction of Ventricular Arrhythmia. JACC Cardiovasc Imaging. 2010 Mar 1;3(3):247–56.

171. Haugaa KH, Hasselberg NE, Edvardsen T. Mechanical Dispersion by Strain Echocardiography: A Predictor of Ventricular Arrhythmias in Subjects With Lamin A/C Mutations. JACC Cardiovasc Imaging. 2015 Jan;8(1):104–6.

172. Haugaa KH, Goebel B, Dahlslett T, Meyer K, Jung C, Lauten A, et al. Risk assessment of ventricular arrhythmias in patients with nonischemic dilated cardiomyopathy by strain echocardiography. J Am Soc Echocardiogr. 2012 Jun;25(6):667–73.

173. Ersbøll M, Valeur N, Andersen MJ, Mogensen UM, Vinther M, Svendsen JH, et al. Early echocardiographic deformation analysis for the prediction of sudden cardiac death and life-threatening arrhythmias after myocardial infarction. JACC Cardiovasc Imaging. 2013 Aug;6(8):851–60.

174. Sengupta PP, Krishnamoorthy VK, Korinek J, Narula J, Vannan MA, Lester SJ, et al. Left Ventricular Form and Function Revisited: Applied Translational Science to Cardiovascular Ultrasound Imaging. J Am Soc Echocardiogr. 2007 May;20(5):539–51.

175. Helle-Valle T. New Noninvasive Method for Assessment of Left Ventricular Rotation: Speckle Tracking Echocardiography. Circulation. 2005 Nov 15;112(20):3149–56.

176. Burns AT, McDonald IG, Thomas JD, Macisaac A, Prior D. Doin' the twist: new tools for an old concept of myocardial function. Heart. 2008 Feb 28;94(8):978–83.

177. Moral JAU, Godinez JAA, Maron MS, Malik R, Eagan JE, Patel AR, et al. Left Ventricular Twist Mechanics in Hypertrophic Cardiomyopathy Assessed by Three-Dimensional Speckle Tracking Echocardiography. Am J Cardiol. 2011 Dec 15;108(12):1788–95.

178. Yoneyama K, Gjesdal O, Choi E-Y, Wu CO, Hundley WG, Gomes AS, et al. Age, sex, and hypertension-related remodeling influences left ventricular torsion assessed by tagged cardiac magnetic resonance in asymptomatic individuals: the multi-ethnic study of atherosclerosis. Circulation. 2012 Nov 20;126(21):2481–90.

179. Maron MS, Maron BJ, Harrigan C, Buros J, Gibson CM, Olivotto I, et al. Hypertrophic Cardiomyopathy Phenotype Revisited After 50 Years With Cardiovascular Magnetic Resonance. J Am Coll Cardiol. 2009 Jul 14;54(3):220–8.

180. Cardim N, Galderisi M, Edvardsen T, Plein S, Popescu BA, D'Andrea A, et al. Role of multimodality cardiac imaging in the management of patients with hypertrophic cardiomyopathy: an expert consensus of the European Association of Cardiovascular Imaging Endorsed by the Saudi Heart Association. Eur Heart J Cardiovasc Imaging. 2015 Mar;16(3):280.

181. Moravsky G, Ofek E, Rakowski H, Butany J, Williams L, Ralph-Edwards A, et al. Myocardial fibrosis in hypertrophic cardiomyopathy: accurate reflection of histopathological findings by CMR. JACC Cardiovasc Imaging. 2013 May;6(5):587–96.

182. Moon JCC, Reed E, Sheppard MN, Elkington AG, Ho SY, Burke M, et al. The histologic basis of late gadolinium enhancement cardiovascular magnetic resonance in hypertrophic cardiomyopathy. J Am Coll Cardiol. 2004 Jun 16;43(12):2260–4.

183. Moon JCC, McKenna WJ, McCrohon JA, Elliott PM, Smith GC, Pennell DJ. Toward clinical risk assessment in hypertrophic cardiomyopathy with gadolinium cardiovascular magnetic resonance. J Am Coll Cardiol. 2003 May 7;41(9):1561–7.

184. Adabag AS, Maron BJ, Appelbaum E, Harrigan CJ, Buros JL, Gibson CM, et al. Occurrence and Frequency of Arrhythmias in Hypertrophic Cardiomyopathy in Relation to Delayed Enhancement on Cardiovascular Magnetic Resonance. J Am Coll Cardiol. 2008 Apr;51(14):1369–74.

185. Weng Z, Yao J, Chan RH, He J, Yang X, Zhou Y, et al. Prognostic Value of LGE-CMR in HCM: A Meta-Analysis. JACC Cardiovasc Imaging. 2016 Dec;9(12):1392–402.

186. Rubinshtein R, Glockner JF, Ommen SR, Araoz PA, Ackerman MJ, Sorajja P, et al. Characteristics and clinical significance of late gadolinium enhancement by contrast-enhanced magnetic resonance imaging in patients with hypertrophic cardiomyopathy. Circ Heart Fail. 2010 Jan;3(1):51–8.

187. Fluechter S, Kuschyk J, Wolpert C, Doesch C, Veltmann C, Haghi D, et al. Extent of late gadolinium enhancement detected by cardiovascular magnetic resonance correlates with the inducibility of ventricular tachyarrhythmia in hypertrophic cardiomyopathy. J Cardiovasc Magn Reson. 2010;12:30.

188. O'Hanlon R, Grasso A, Roughton M, Moon JC, Clark S, Wage R, et al. Prognostic significance of myocardial fibrosis in hypertrophic cardiomyopathy. J Am Coll Cardiol. 2010 Sep 7;56(11):867–74.

189. Chan RH, Maron BJ, Olivotto I, Pencina MJ, Assenza GE, Haas T, et al. Prognostic value of quantitative contrast-enhanced cardiovascular magnetic resonance for the evaluation of sudden death risk in patients with hypertrophic cardiomyopathy. Circulation. 2014 Aug 5;130(6):484–95.

190. Mont L, Pelliccia A, Sharma S, Biffi A, Borjesson M, Terradellas JB, et al. Pre-participation cardiovascular evaluation for athletic participants to prevent sudden death: Position paper from the EHRA and the EACPR, branches of the ESC. Endorsed by APHRS, HRS, and SOLAECE. Europace. Europace; 2017 Jan;19(1):139–63.

191. Richand V, Lafitte S, Reant P, Serri K, Lafitte M, Brette S, et al. An ultrasound speckle tracking (two-dimensional strain) analysis of myocardial deformation in professional soccer players compared with healthy subjects and hypertrophic cardiomyopathy. Am J Cardiol. 2007 Jul 1;100(1):128–32.

192. Maron BJ, Doerer JJ, Haas TS, Tierney DM, Mueller FO. Sudden deaths in young competitive athletes: analysis of 1866 deaths in the United States, 1980-2006. Circulation. 2009 Mar 3;119(8):1085–92.

193. Maron BJ, Olivotto I, Spirito P, Casey SA, Bellone P, Gohman TE, et al. Epidemiology of hypertrophic cardiomyopathy-related death: revisited in a large non-referral-based patient population. Circulation. 2000 Aug 22;102(8):858–64.

194. Maron BJ, Rowin EJ, Casey SA, Garberich RF, Maron MS. What Do Patients With Hypertrophic Cardiomyopathy Die from? Am J Cardiol. 2016 Feb 1;117(3):434–5.

195. Spirito P, Autore C, Rapezzi C, Bernabò P, Badagliacca R, Maron MS, et al. Syncope and risk of sudden death in hypertrophic cardiomyopathy. Circulation. 2009 Apr 7;119(13):1703–10.

196. Dimitrow PP, Chojnowska L, Rudziński T, Piotrowski W, Ziólkowska L, Wojtarowicz A, et al. Sudden death in hypertrophic cardiomyopathy: old risk factors re-assessed in a new model of maximalized follow-up. Eur Heart J. 2010 Dec;31(24):3084–93.

197. Maron MS, Rowin EJ, Maron BJ. How to Image Hypertrophic Cardiomyopathy. Circ Cardiovasc Imaging. 2017 Jul;10(7).

198. Rowin EJ, Maron BJ, Haas TS, Garberich RF, Wang W, Link MS, et al. Hypertrophic Cardiomyopathy With Left Ventricular Apical Aneurysm: Implications for Risk Stratification and Management. J Am Coll Cardiol. 2017 Feb 21;69(7):761–73.

199. Ezzat VA, Lee V, Ahsan S, Chow AW, Segal O, Rowland E, et al. A systematic review of ICD complications in randomised controlled trials versus registries: is our "real-world" data an underestimation? Open Heart. 2015;2(1):e000198.

200. Kutyifa V, Zareba W, Moss AJ. ICD programming to reduce shocks and improve outcomes. Current cardiology reports. 2014;16(6):496.

201. Olde Nordkamp LRA, Postema PG, Knops RE, van Dijk N, Limpens J, Wilde AAM, et al. Implantable cardioverter-defibrillator harm in young patients with inherited arrhythmia

syndromes: A systematic review and meta-analysis of inappropriate shocks and complications. Heart Rhythm. 2016 Feb;13(2):443–54.

202. Gersh BJ, Maron BJ, Bonow RO, Dearani JA, Fifer MA, Link MS, et al. 2011 ACCF/AHA guideline for the diagnosis and treatment of hypertrophic cardiomyopathy: a report of the American College of Cardiology Foundation/American Heart Association Task Force on Practice Guidelines. Circulation. 2011 Dec 13;124(24):e783–831.

203. Nagueh SF, Bachinski LL, Meyer D, Hill R, Zoghbi WA, Tam JW, et al. Tissue Doppler imaging consistently detects myocardial abnormalities in patients with hypertrophic cardiomyopathy and provides a novel means for an early diagnosis before and independently of hypertrophy. Circulation. 2001 Jul 10;104(2):128–30.

204. Cardim N, Perrot A, Ferreira T, Pereira A, Osterziel KJ, Reis RP, et al. Usefulness of Doppler myocardial imaging for identification of mutation carriers of familial hypertrophic cardiomyopathy. Am J Cardiol. 2002 Jul 15;90(2):128–32.

205. Ho CY, Carlsen C, Thune JJ, Havndrup O, Bundgaard H, Farrohi F, et al. Echocardiographic Strain Imaging to Assess Early and Late Consequences of Sarcomere Mutations in Hypertrophic Cardiomyopathy. Circ: Cardiovasc Gen. 2009 Aug 18;2(4):314–21.

206. De S, Borowski AG, Wang H, Nye L, Xin B, Thomas JD, et al. Subclinical echocardiographic abnormalities in phenotype-negative carriers of myosin-binding protein C3 gene mutation for hypertrophic cardiomyopathy. Am Heart J. Mosby, Inc; 2011 Aug 1;162(2):262–3.

207. Yiu KH, Atsma DE, Delgado V, Ng ACT, Witkowski TG, Ewe SH, et al. Myocardial Structural Alteration and Systolic Dysfunction in Preclinical Hypertrophic Cardiomyopathy Mutation Carriers. Biondi-Zoccai G, editor. PLoS ONE. 2012 May 4;7(5):e36115.

208. Kauer F, van Dalen BM, Michels M, Soliman OII, Vletter WB, van Slegtenhorst M, et al. Diastolic abnormalities in normal phenotype hypertrophic cardiomyopathy gene carriers: a study using speckle tracking echocardiography. Echocardiography. 2013 May;30(5):558–63.

209. Kauer F, van Dalen BM, Michels M, Schinkel AFL, Vletter WB, van Slegtenhorst M, et al. Delayed and decreased LV untwist and unstrain rate in mutation carriers for hypertrophic cardiomyopathy. Eur Heart J Cardiovasc Imaging. 2017 Apr 1;18(4):383–9.

210. Ala-Kopsala M, Ruskoaho H, Leppäluoto J, Seres L, Skoumal R, Toth M, et al. Single assay for amino-terminal fragments of cardiac A- and B-type natriuretic peptides. Clin Chem. 2005 Apr;51(4):708–18.

211. Jääskeläinen P, Kuusisto J, Miettinen R, Kärkkäinen P, Kärkkäinen S, Heikkinen S, et al. Mutations in the cardiac myosin-binding protein C gene are the predominant cause of familial hypertrophic cardiomyopathy in eastern Finland. J Mol Med. 2002 Jul;80(7):412–22.

212. Xiao HB, Gibson DG. Absent septal q wave on electrocardiogram: a forgotten marker of myocardial disease. Int J Cardiol. 1996 Jan;53(1):1–4.

213. Surawicz B, Knilans T. Chou's electrocardiography in clinical practice: adult and pediatric. 2008.

214. Gubner R. Electrocardiographic criteria of left ventricular hypertrophy. Arch Intern Med (Chic). American Medical Association; 1943 Aug 1;72(2):196–209.

215. Lewis T. Observations upon ventricular hypertrophy with special reference to preponderance of one or the other chamber. Heart. 1914 Jan 1;5:367–402.

216. Ostman-Smith I, Wisten A, Nylander E, Bratt E-L, Granelli AD-W, Oulhaj A, et al. Electrocardiographic amplitudes: a new risk factor for sudden death in hypertrophic cardiomyopathy. Eur Heart J. 2010 Feb;31(4):439–49.

217. Zema MJ, Kligfield P. Electrocardiographic poor R wave progression. I: correlation with the Frank vectorcardiogram. J Electrocardiol. 1979 Jan;12(1):3–10.

218. Ollila L, Nikus K, Holmström M, Jalanko M, Jurkko R, Kaartinen M, et al. Clinical disease presentation and ECG characteristics of LMNA mutation carriers. Open Heart. 2017;4(1):e000474.

219. Lang RM, Bierig M, Devereux RB, Flachskampf FA, Foster E, Pellikka PA, et al. Recommendations for chamber quantification: a report from the American Society of Echocardiography's Guidelines and Standards Committee and the Chamber Quantification Writing Group, developed in conjunction with the European Association of Echocardiography, a branch of the European Society of Cardiology. J Am Soc Echocardiogr. 2005 Dec;18(12):1440–63.

220. Burns AT, La Gerche A, Prior DL, Macisaac AI. Left Ventricular Untwisting Is an Important Determinant of Early Diastolic Function. JACC Cardiovasc Imaging. 2009 Jun 1;2(6):709–16.

221. Castillo S, Mattila I, Miettinen J, Oresic M, Hyötyläinen T. Data analysis tool for comprehensive two-dimensional gas chromatography/time-of-flight mass spectrometry. Anal Chem. 2011 Apr 15;83(8):3058–67.

222. Nygren H, Seppänen-Laakso T, Castillo S, Hyötyläinen T, Oresic M. Liquid chromatography-mass spectrometry (LC-MS)-based lipidomics for studies of body fluids and tissues. Methods Mol Biol. 2011;708:247–57.

223. Pluskal T, Castillo S, Villar-Briones A, Oresic M. MZmine 2: modular framework for processing, visualizing, and analyzing mass spectrometry-based molecular profile data. BMC Bioinformatics. 2010 Jul 23;11:395.

224. Fraley C, Raftery A. Model-based Methods of Classification: Using the mclust Software in Chemometrics. J Stat Softw. 2007 Jan 30;18(6):1–13.

225. Robin X, Turck N, Hainard A, Tiberti N, Lisacek F, Sanchez J-C, et al. pROC: an open-source package for R and S+ to analyze and compare ROC curves. BMC Bioinformatics. 2011;12:77.

226. Kampstra P. Beanplot: A boxplot alternative for visual comparison of distributions. J Stat Softw. 2008;28.

227. Correia E, Rodrigues B, Santos LF, Moreira D, Gama P, Cabral C, et al. Longitudinal Left Ventricular Strain in Hypertrophic Cardiomyopathy: Correlation with Nonsustained Ventricular Tachycardia. Echocardiography. 2011 May 12;28(7):709–14.

228. D'Andrea A. Prognostic value of intra-left ventricular electromechanical asynchrony in patients with hypertrophic cardiomyopathy. Eur Heart J. 2006 Mar 16;27(11):1311–8.

229. Sarvari SI, Haugaa KH, Anfinsen O-G, Leren TP, Smiseth OA, Kongsgaard E, et al. Right ventricular mechanical dispersion is related to malignant arrhythmias: a study of patients with arrhythmogenic right ventricular cardiomyopathy and subclinical right ventricular dysfunction. Eur Heart J. 2011 May;32(9):1089–96.

230. Haugaa KH, Grenne BL, Eek CH, Ersbøll M, Valeur N, Svendsen JH, et al. Strain echocardiography improves risk prediction of ventricular arrhythmias after myocardial infarction. JACC Cardiovasc Imaging. 2013 Aug;6(8):841–50.

231. Alexander D, Lombardi R, Rodriguez G, Mitchell MM, Marian AJ. Metabolomic distinction and insights into the pathogenesis of human primary dilated cardiomyopathy. Eur J Clin Invest. 2011 May;41(5):527–38.

232. Wang J, Li Z, Chen J, Zhao H, Luo L, Chen C, et al. Metabolomic identification of diagnostic plasma biomarkers in humans with chronic heart failure. Mol Biosyst. 2013 Nov;9(11):2618–26.

233. Sansbury BE, DeMartino AM, Xie Z, Brooks AC, Brainard RE, Watson LJ, et al. Metabolomic analysis of pressure-overloaded and infarcted mouse hearts. Circ Heart Fail. 2014 Jul;7(4):634–42.

234. Lu G, Ren S, Korge P, Choi J, Dong Y, Weiss J, et al. A novel mitochondrial matrix serine/threonine protein phosphatase regulates the mitochondria permeability transition pore and is essential for cellular survival and development. Genes Dev. 2007 Apr 1;21(7):784–96.

235. Huang Y, Zhou M, Sun H, Wang Y. Branched-chain amino acid metabolism in heart disease: an epiphenomenon or a real culprit? Cardiovasc Res. 2011 May 1;90(2):220–3.

236. Lopes LR, Rahman MS, Elliott PM. A systematic review and meta-analysis of genotype-phenotype associations in patients with hypertrophic cardiomyopathy caused by sarcomeric protein mutations. Heart. 2013 Dec;99(24):1800–11.

237. Sakamoto N, Kawamura Y, Sato N, Nimura A, Matsuki M, Yamauchi A, et al. Late gadolinium enhancement on cardiac magnetic resonance represents the depolarizing and repolarizing electrically damaged foci causing malignant ventricular arrhythmia in hypertrophic cardiomyopathy. Heart Rhythm. 2015 Jun;12(6):1276–84.